Paleoenvironmental changes in Southern Patagonia during late Quaternary inferred from lake sediments of Laguna Potrok Aike, Argentina

Von der Fakultät für Georessourcen und Materialtechnik
der Rheinisch-Westfälischen Technischen Hochschule Aachen

zur Erlangung des akademischen Grades eines

Doktors der Naturwissenschaften

genehmigte Dissertation

vorgelegt von **Dipl.-Geograph**

Jiayun Zhu

aus Shanghai, China

Berichter: Univ.-Prof. Dr. rer. nat. Frank Lehmkuhl
Prof. Dr. Frank Schäbitz

Tag der mündlichen Prüfung: 16. Oktober 2014

Diese Dissertation ist auf den Internetseiten der Hochschulbibliothek online verfügbar

Acknowledgements

I would like to express my great thanks to Andreas Lücke who gave me the opportunity to work on the PASADO project and brought me into the field of isotope analyses of aquatic mosses. There were many helpful suggestions, remarks and comments over the past three and a half years and I learned to see things from different angles.

I am deeply indebted to my Doktorvater, Frank Lehmkuhl, for supervising my doctorate at the RWTH Aachen University. I would like to thank Frank Schäbitz for the time devoted to review this thesis.

For the great technical supports and helpful discussions, I am very grateful to Holger Wissel. My sincere thanks to other colleagues of the PASADO project (Christoph Mayr, Bernd Zolitschka, Christian Ohlendorf, Dirk Enters and others) for the discussions and valuable criticism of the manuscripts.

I would also like to thank Heinz Vogt for the help of statistical analyses and colleagues of IBG-2 at the Forschungszentrum Jülich for allowing me to take microscopical pictures of aquatic mosses in their lab.

Finally, I would like to express my great appreciation to my parents, Le Ziping and Zhu Zhongming, and to my wife, Jiang Weijian. This PhD thesis is dedicated to them.

Contents

List of figures

List of tables

1 Introduction 1

1.1 Motivation of research 1

1.2 Study site 3

1.3 Materials and methods 6

1.4 Objectives and organization of manuscripts 7

2 The last Glacial – Interglacial transition in Patagonia, Argentina: the stable isotope record of bulk sedimentary organic matter from Laguna Potrok Aike 9

2.1 Introduction 11

2.2 Site description 12

2.3 Material and methods 13

2.4 Results 15

2.4.1 Geochemistry 15

2.4.2 Cluster analysis 16

2.5 Discussion and Interpretation 23

2.5.1 Nitrogen proxies and inorganically bound nitrogen 23

2.5.2 Phase 1 (26,075 – 17,300 cal. BP) 25

2.5.3 Phase 2 (17,300 – 13,000 cal. BP) 26

2.5.4 Phase 3 (13,000 – 10,970 cal. BP) 30

2.5.5 Phase 4 (10,970 – 8400 cal. BP) 31

2.5.6 Inter-phase relations 31

2.5.7 Regional and global context 32

2.6 Conclusions 32

3 Characterizing oxygen isotope variability and host water relation of modern and subfossil aquatic mosses 34

3.1 Introduction 36

3.2 Study sites 37

3.3 Materials and methods 40

3.3.1 Materials 40

3.3.1.1 Modern samples 40

3.3.1.2 Sediment samples 40

3.3.2 Cellulose extraction 43

3.3.3 Stable isotope measurements 44

3.4 Results and discussion . . . 45
3.4.1 Correlation of aquatic mosses and host-water $\delta^{18}O$ values . . . 45
3.4.2 Isotope composition of cellulose and organic matter of aquatic moss . . . 49
3.4.3 Isotope composition of aquatic moss and aquatic vascular plant . . . 52
3.4.4 Species- and tissue-specific offsets . . . 53
3.4.5 Post-depositional change of subfossil moss material . . . 55
3.5 Application for paleolimnological reconstruction . . . 57
3.6 Conclusions . . . 59
4 Climate history of the Southern Hemisphere Westerlies belt during the last glacial-interglacial transition revealed from lake water oxygen isotope reconstruction of Laguna Potrok Aike (52°S, Argentina) . . . 62
4.1 Introduction . . . 64
4.2 Regional setting . . . 66
4.3 Material and methods . . . 69
4.3.1 Material . . . 69
4.3.2 Age-depth model . . . 70
4.3.3 Laboratory Methods . . . 73
4.3.4 Reconstructed lake water $\delta^{18}O$ values . . . 75
4.4 Results . . . 76
4.5 Discussion . . . 80
4.5.1 Factors controlling lake water $\delta^{18}O$ of Laguna Potrok Aike . . . 80
4.5.2 $\delta^{18}O_{lw\text{-}corr}$ of the full Glacial (26,000 – 21,000 cal. BP) . . . 81
4.5.3 Evolution of $\delta^{18}O_{lw\text{-}corr}$ and deglaciation history since 21,000 cal. BP . . . 86
4.6 Conclusions . . . 89
5 Synthesis . . . 91

References . . . 96

List of figures

Figure 1.1 Location of Laguna Potrok Aike 4
Figure 1.2 Mean near-surface (1000 mb) zonal wind (m/s) in Southern Hemisphere 4
Figure 2.1 Location of Laguna Potrok Aike 12
Figure 2.2 Downcore changes in TOC and TN contents, $\delta^{13}C_{TOC}$ and $\delta^{15}N_{TN}$, and TOC/TN ratios 17
Figure 2.3 Proportion of four grain-size sieving fractions and its isotopic and elementary values 18
Figure 2.4 Three phases in proxy parameters based on CONISS cluster analysis 19
Figure 2.5 Cross-plots of proxy parameters for the four main phases 20
Figure 2.6 Proposed four main phases of proxy parameters during the investigated period 21
Figure 3.1 Sampling location in southern Patagonia 38
Figure 3.2 Subfossil plant remains in sediment samples from Laguna Potrok Aike 41
Figure 3.3 Work flow for the preparation of subfossil samples 41
Figure 3.4 Correlation between $\delta^{18}O$ of aquatic moss and host waters 45
Figure 3.5 Relationship between $\delta^{18}O$ and $\delta^{13}C$ of modern and subfossil aquatic mosses 50
Figure 3.6 Comparison of $\delta^{18}O$ and $\delta^{13}C$ of aquatic mosses and aquatic vascular plants 53
Figure 3.7 Relation between amount of moss fragments and cellulose yield 56
Figure 3.8 Lake-water $\delta^{18}O$ inferred from three fractions 57
Figure 4.1 Location of Laguna Potrok Aike 67
Figure 4.2 Mean near-surface (1000 mb) zonal wind (m/s) in Southern Hemisphere 67
Figure 4.3 Relationship between air temperature and $\delta^{18}O$ of precipitation at Punta Arenas 69
Figure 4.4 Improved age-depth model 71
Figure 4.5 Weighed dry mass of handpicked aquatic moss remains 77
Figure 4.6 $\delta^{18}O$ values of all measured samples for the investigated period 78
Figure 4.7 Relationship between moss dry mass and $\delta^{18}O$ values of moss organic matter 79
Figure 4.8 Reconstructed lake-water $\delta^{18}O$ from moss and residue fractions 79
Figure 4.9 Isotopic record of reconstructed lake-water $\delta^{18}O$ 80
Figure 4.10 Reconstructed lake-water $\delta^{18}O$ in comparison to global proxy records 85
Figure 5.1 Proxy records of Laguna Potrok Aike in comparison with Antarctic records 94

List of tables

Table 3.1 Isotopic parameters of modern aquatic mosses and host waters 39
Table 3.2 $\delta^{13}C$ and $\delta^{18}O$ of modern plant samples from Laguna Potrok Aike 43
Table 3.3 Linear regression parameters between $\delta^{18}O$ of aquatic cellulose and host waters 48
Table 3.4 Lake-water $\delta^{18}O$ reconstructed from subfossil aquatic mosses 51
Table 3.5 $\delta^{13}C$ and $\delta^{18}O$ of subfossil plant organic matter from Laguna Potrok Aike 54
Table 4.1 AMS ^{14}C ages for the modeled sediment depth range 72

Chapter 1

Introduction

1.1. Motivation of research

Studying the climate evolution from the last Glacial towards the current Interglacial enables us to better understand the response of the climate system to external and internal forcing without anthropogenic impact. Compared to the northern hemisphere, high-resolution paleoclimate studies from the high latitudes of the southern hemisphere are still rare, though the proxy records from this part of the world are of great importance to understand regional impacts of global climate changes.

A key region in the southern hemisphere for conducting paleoclimate reconstructions is undoubtedly southern Patagonia (particularly the part south of 49°S), because it is the only continental mass intersecting the Southern Hemisphere westerly winds (SHW), which controls large-scale ocean ventilation and carbon cycling and could have played an important role in driving the global deglacial warming during the last glacial termination (Toggweiler et al., 2006; Anderson et al., 2009; Denton et al., 2010). The proxy records in southern Patagonia reconstructing the evolution of the SHW provide then valuable terrestrial evidences that can be compared to those from the Southern Ocean.

The possibilities for reconstructing paleoenvironmental conditions in southern Patagonia and the evolution of the SHW during the last glacial-interglacial transition period are, however, limited, because the Andean part of southern Patagonia was covered by the immense Patagonian Ice Sheet during the last Glacial and suitable paleoclimatic archives in extra-Andean Patagonia are largely absent. The available proxy records are mostly restricted to the periods of the late Glacial and, especially, the Holocene (cf. Kilian and Lamy, 2012). The evidences for the climatic changes in southern Patagonia throughout the last glacial-interglacial transition are mainly derived from glacial geologic records (e.g. McCulloch et al., 2005; Kaplan et al., 2008; Sagredo et al., 2011), low-resolution pollen records (e.g. Mancini et al., 2008) as well as highly discontinuous lake level records (e.g. Stine and Stine, 1990).

Under these circumstances, the lacustrine sediment archive of Laguna Potrok Aike, a deep maar lake located in southern extra-Andean Patagonia (52°S; Fig. 1.1), is highly unique. The previous project "South Argentinean Lake Sediment Archives and modeling" (SALSA) has investigated the modern sedimentological and hydrological processes of Laguna Potrok Aike (e.g. Mayr et al., 2007a; Kastner et al., 2010) and employed geochemical and palynological approaches (e.g. Haberzettl et al., 2007; Wille et al., 2007; Mayr et al., 2009) to analyze Laguna Potrok Aike sediments for the last 16,000 years. In 2008, within the framework of the ICDP deep drilling project "Potrok Aike maar lake sediment archive drilling project" (PASADO) (for details of the project cf. Zolitschka et al., 2013), seven holes at two pelagic sites in Laguna Potrok Aike were drilled. The resulting sedimentary composite profile for site 2 reaches back more than 50,000 years (Ohlendorf et al., 2011; Kliem et al., 2013b).

Stable isotope analysis of organic material preserved in lake sediments is a powerful tool to reconstruct paleoenvironmental conditions. Changes in primary productivity and nutrient loading in the lake can be reflected by stratigraphic variations in carbon and nitrogen isotope composition of sedimentary organic matter (e.g. Meyers and Lallier-Vergès, 1999; Meyers, 2003; Lücke and Brauer, 2004). In addition, the oxygen isotope composition of authigenic carbonates and biogenic material (e.g. ostracodes, molluscs, biogenic silica) is commonly used as paleoclimate proxy for temperature and the oxygen isotope composition of lake water ($\delta^{18}O_{lw}$) (Leng and Marshall, 2004). However, the above mentioned $\delta^{18}O$ proxy material is hardly available in the Laguna Potrok Aike sediment section of the last glacial-interglacial transition. The well preserved remains of submerged aquatic mosses in the sediments of Laguna Potrok Aike provide, thus, a useful alternative for $\delta^{18}O$ proxy investigations. Based on the highly significant linear correlation between $\delta^{18}O$ of aquatic moss cellulose and their host waters verified by the results from laboratory (Sauer et al., 2001) and field studies (Mayr et al., 2013), past changes in $\delta^{18}O_{lw}$ can be well traced by analyzing $\delta^{18}O$ of submerged aquatic moss remains. Since the modern $\delta^{18}O_{lw}$ of Laguna Potrok Aike largely reflect the magnitude of evaporative ^{18}O enrichment of lake water, which is closely related to the westerly wind intensity, the reconstruction of $\delta^{18}O_{lw}$ throughout the last glacial-interglacial transition can provide valuable views into the evolution of the SHW and the steppe climate in southern Patagonia.

1.2. Study site

Laguna Potrok Aike is located on the leeward side of the southern Andes in the Pali Aike Volcanic Field near the Argentina-Chile border in southern Patagonia, Argentina (51°58'S, 70°23'W; 113 m a.s.l.; Fig. 1.1a). Several non-permanent, dry or ephemeral lakes are visible on satellite images from this region (Ohlendorf et al., 2013). Laguna Potrok Aike is the larger and deeper one of the two permanent lakes. Groundwater throughflow play an important role in the hydrological regime of the lake (Mayr et al., 2007a).

The near circular maar lake originates from a phreatomagmatic eruption with a $^{40}Ar/^{39}Ar$ age of 770 ± 240 ka BP and has a diameter of almost 3.5 km (Zolitschka et al., 2006). The crater itself has a diameter of approximately 5 km. The maximum water depth is about 100 m. The lake's bathymetry reveals an almost flat and pot-shaped morphology of the lake floor. The lake basin has a funnel-shaped structure of the surrounding soft bedrock filled by up to 370 m thick lacustrine sediments overlying probably volcanoclastic sediments of unknown thickness (Gebhardt et al., 2011).

Under modern conditions, Laguna Potrok Aike is a phosphorous-rich and subsaline lake (conductivity of >3000 µS cm^{-1}). The lake water body circulates constantly under the prevailing strong west-wind conditions, which inhibits the development of any pronounced summer stratification in the water column. The present lake has no surface outflow and only episodic surface inflows from snow melt through gullies and canyons. Its catchment area is of about 200 km^2 with predominantly flat topography and extends far south into Chile (Ohlendorf et al., 2013).

Subaerial and submerged terraces around and in the lake indicate pronounced lake-level fluctuations resulting from past hydrological changes (Zolitschka et al., 2006; Haberzettl et al., 2008; Anselmetti et al., 2009; Gebhardt et al., 2012; Kliem et al., 2013b). These findings evidence lake-level fluctuations in the order of 50 m during the Holocene. A maximum lake level rise of up to 200 m from a desiccation of the lake probably during Marine Isotope Stage 4 to the highstand during the last glacial period has also been inferred by seismic refraction profiles (Gebhardt et al., 2012).

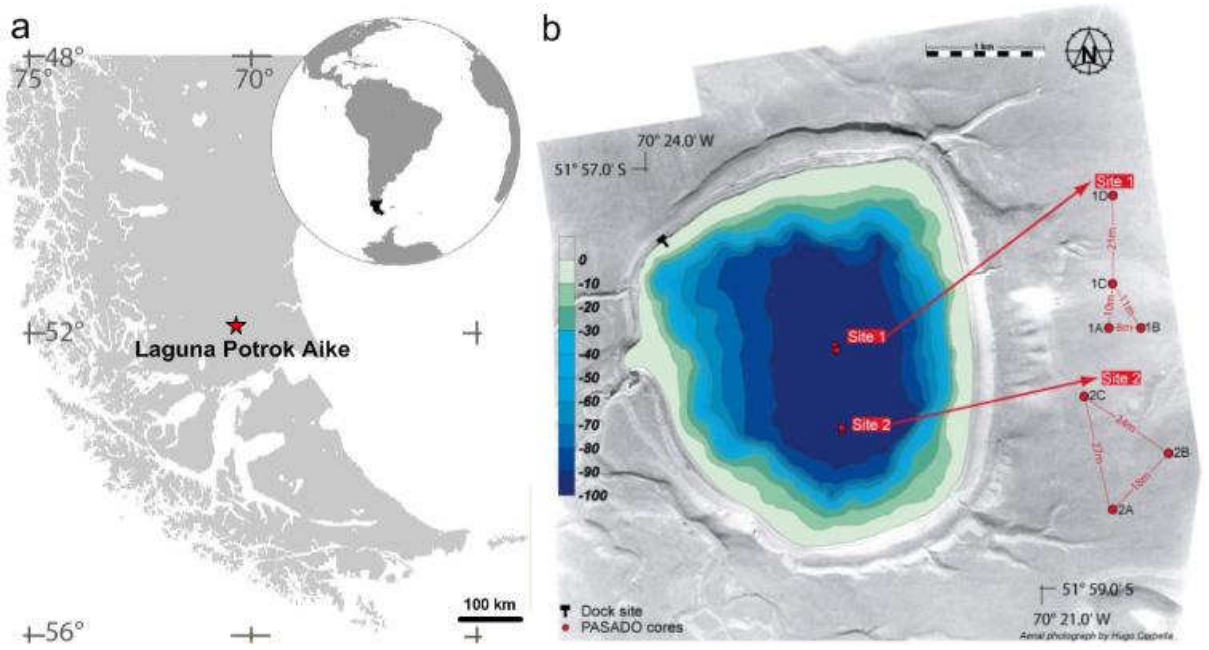


Figure 1.1. a) Location of Laguna Potrok Aike (red star) in southern Patagonia indicated as a black area on the inserted map. **b)** Sediment cores were taken in 2008 within the framework of PASADO at two drilling sites shown on the bathymetric map of Laguna Potrok Aike inserted into an aerial photography (provided by Hugo Corbella). The figures are provided by Ohlendorf et al. (2013).

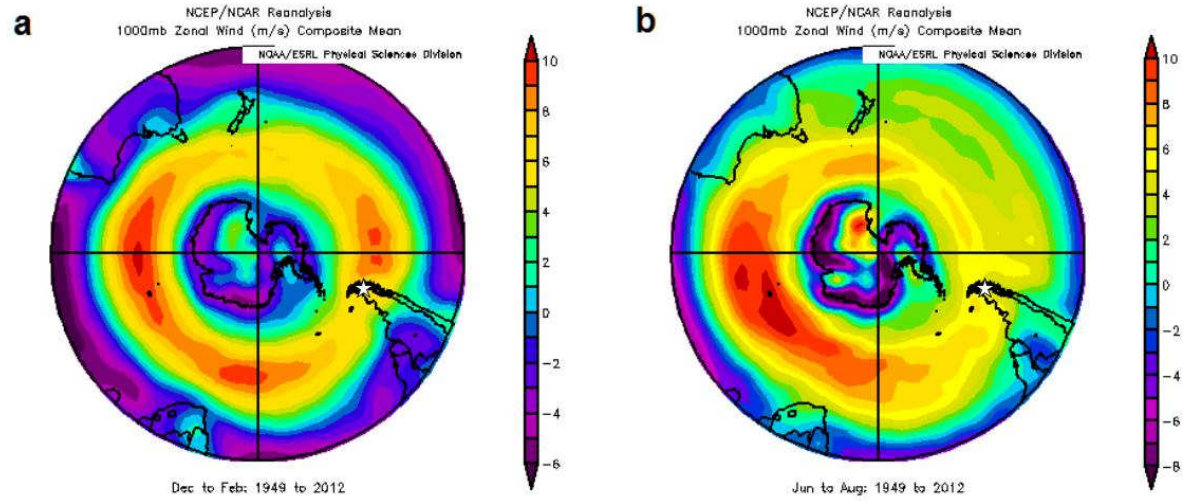


Figure 1.2. Mean near-surface (1000 mb) zonal wind (m/s) in Southern Hemisphere for austral summer **(a)** and winter months **(b)** based on NCEP/NCAR Reanalysis. Location of Laguna Potrok Aike is indicated as white stars. Data source: http://www.esrl.noaa.gov/psd/cgi-bin/data/composites/printpage.pl, accessed on 06 Feb. 2014.

The bedrock of the Laguna Potrok Aike area is dominated by hundred meters thick continental sedimentary rocks of the Miocene Santa Cruz Formation, which consists mainly of fine-grained molasse–type fluvial sediments (Zolitschka et al., 2006; Coronato et al., 2013). The nearly flat

and broad surface is mainly overlain by degraded late Miocene and early Pleistocene basaltic lava flow field/tableland and early Pleistocene fluvioglacial deposits (Coronato et al., 2013). After the middle Pleistocene the landforms in the Laguna Potrok Aike area have experienced little modification because neither glacial advances nor major volcanic activities occurred in this area since 800 ka (Coronato et al., 2013; Zolitschka et al., 2013). Glaciers of the last Glacial cycle were restricted to the western Río Gallegos valley and to the southern Strait of Magellan (McCulloch et al., 2005) and did not reach the Laguna Potrok Aike area.

The climate of southern Patagonia is temperate to cold and semiarid. Its small landmass does not warm up during austral summers, mainly due to the relative proximity of the Antarctic continent and cold ocean currents along the South American coasts (Weischet, 1996; Zolitschka et al., 2006). Mean temperatures of austral summer (DJF) and winter (JJA) recorded at the local weather station at Laguna Potrok Aike are around 13 °C and 2 °C, respectively, resulting in an annual mean temperature of about 7.5 °C (Ohlendorf et al., 2013). Because of the location on the leeward side of the southern Andes and in the core of the Southern Hemisphere Westerlies belt (Fig. 1.2a and b), the regional climate is characterized by a low precipitation to evaporation ratio and predominant strong westerly winds reaching more than 10 m/s during austral summers (Kilian and Lamy, 2012; Garreaud et al., 2013; Ohlendorf et al., 2013). Wind direction is primarily from the west, shifting occasionally to NW and SW (Weischet, 1996; Baruth et al., 1998). The westerly winds bring humid air from the Pacific to the Andes. The annual precipitation on the windward side can be more than 7000 mm and is strongly positively correlated with westerly wind intensity, whereas on the leeward side it can be less than 300 mm owing to the rain shadow effects and more precipitation moisture originates from the Atlantic (Baruth et al., 1998; Schneider et al., 2003; Mayr et al., 2007b). Mean annual precipitation at Laguna Potrok Aike is around 200 mm during the period from 2000 to 2011, being nearly 300 mm in wet years and only some 150 mm in dry years (Ohlendorf et al., 2013). By comparison, evaporation rates from the surface of the lake can be more than 1200 mm per year and show clear seasonal variations with high rates during austral summers and low rates during austral winters (Ohlendorf et al., 2013). This seasonal pattern results from seasonal variation of relative humidity with high values (up to 85%) during austral winters and low values (down to 30%) during austral summers (Ohlendorf et al., 2013).

The Laguna Potrok Aike area is covered by a dry type of the Magellanic steppe with *Festuca gracillima* as the dominant species (Wille et al., 2007). An inventory of the flora around Laguna Potrok Aike was published by Masco et al. (2005). In the lake, several meter thick

forest-like cover of subaquatic vegetation grows on the lake floor down to a water depth of 15 to 20 m (Anselmetti et al., 2009), which consists mainly of *Potamogeton pectinatus* and *Myriophyllum cf. quitense* (Wille et al., 2007). Aquatic mosses (*Drepanocladus perplicatus*) and *Ruppia* sp. were also observed in the littoral zone during snorkeling explorations.

1.3. Materials and methods

A total of 533 m of sediment was recovered from two drilling sites in Laguna Potrok Aike in 2008 in the framework of the PASADO project (Zolitschka et al., 2009; Ohlendorf et al., 2011; Fig. 1.1b). Sediment samples used in this thesis are from the composite profile 5022-2CP of site 2 which has a composite depth (cd) of 106 m, consisting of undisturbed pelagic sediments, volcanic tephra layers and mass movement sediments that resulted from lake internal sediment redistribution. The composite profile is divided into five lithological units based on the prevailing sedimentary structures and frequency of deposits of mass movement (Kliem et al., 2013b). Mass movement deposits and tephra layers were removed from the composite profile resulting in an event-corrected composite depth profile (cd-ec) of 45.8 m (Kliem et al., 2013b). The sediment section investigated in this thesis ranges between ca. 10 and 30 m (cd) or between 9.6 and 21.4 m (cd-ec) and consists of lithological unit B and C-1 (Kliem et al., 2013b). Both unit B and C-1 mainly comprise pelagic laminated silts intercalated with thin fine sand and coarse silt layers originating from mass movement deposits. Pelagic silts are poorly laminated in unit C-1 which has a greenish and bluish gray color spectrum compared to dark and light gray laminations of unit B (Kliem et al., 2013b).

The age-depth model version 3 constructed for the entire composite profile 5022-2CP (Kliem et al., 2013b) is used in Chapter 2. This model is based on AMS radiocarbon dates of undisturbed pelagic sediments and developed using the mixed-effect regression approach of Heegaard et al. (2005). To improve the chronology in the investigated sediment section, additional 22 samples of bulk aquatic moss material or other organic material were selected from the undisturbed pelagic sediment sections for AMS ^{14}C determination. With these new datings, a constrained age-depth model is constructed for the time period of interest here with the software *clam 2.2* (Blaauw 2010), using the SHCal13 calibration curve (Hogg et al., 2013) and smoothed spline interpolation with a smoothing level of 0.5. This improved model has been used in Chapter 4. The main difference between these two models can be found in the depth range between 12 and 15 m (cd-ec). More details are given in Chapter 4. According to both age-depth models, the

investigated sediment section spans roughly from 26,000 to 8500 cal. BP, ranging from the Last Glacial Maximum towards early Holocene.

In general, freeze-dried samples were cautiously homogenized and sieved at 200 µm to partition the fine-grained fraction from the coarse organic debris. The former is used for the carbon and nitrogen isotope analysis of bulk sedimentary organic matter. From the latter, plant fragments (remains of aquatic mosses and of aquatic vascular plants) were carefully handpicked under a binocular. More details regarding pretreatment of material, preparation of subfossil moss samples, cellulose extraction and isotopic analysis can be found in the following chapters.

1.4. Objectives and organization of manuscripts

The overall goal of this thesis is to reconstruct primary productivity, nutrient supply and lake water balance of Laguna Potrok Aike based on stable isotope analyses (carbon, nitrogen and oxygen) of sedimentary organic material, to interpret the data in the context of global and regional climatic changes throughout the last glacial-interglacial transition and to provide paleoenvironmental evidences for the development of the SHW and the southern Patagonian climate. The highlight of the thesis is to develop a unique isotopic proxy tool which uses subfossil submerged aquatic mosses to reconstruct the past $\delta^{18}O_{lw}$. The strongly significant correlation between $\delta^{18}O$ of submerged aquatic mosses and their host waters and the good availability of well preserved subfossil moss material enables a high-resolution $\delta^{18}O_{lw}$ record of Laguna Potrok Aike to identify past changes in lake water balance.

The main body of this thesis is formed by three discrete manuscripts that are either published or submitted, presented in Chapter 2, 3 and 4. **Manuscript 1 (Chapter 2)** analyzes elemental parameters (total organic carbon (TOC) content, total nitrogen (TN) content and TOC/TN ratio) and stable carbon and nitrogen isotope compositions ($\delta^{13}C_{TOC}$, $\delta^{15}N_{TN}$) of fine-grained (<200 µm) sedimentary bulk organic matter for the investigated period. This chapter provides insights into past changes in primary productivity and nutrient supply in the lake as well as associated environmental conditions in southern Patagonia. **Manuscript 2 (Chapter 3)** explores the relation between oxygen isotope compositions of aquatic plants (mosses and vascular plants) and host waters. The aim of this chapter is to establish a reliable proxy approach to reconstruct the past $\delta^{18}O_{lw}$ based on stable oxygen isotope analysis of purified organic matter and extracted cellulose of subfossil aquatic moss remains. **Manuscript 3 (Chapter 4)** applies the approach

developed in Chapter 3 to generate a high-resolution $\delta^{18}O_{lw}$ record of Laguna Potrok Aike for the investigated period. The interpretation of the record focuses on the factors affecting the changes in $\delta^{18}O_{lw}$ and lake water balance as well as the role of the SHW. The climate history of the SHW and southern Patagonia is also discussed.

Chapter 2

The last Glacial – Interglacial transition in Patagonia, Argentina: the stable isotope record of bulk sedimentary organic matter from Laguna Potrok Aike

Jiayun Zhu[1], Andreas Lücke[1], Holger Wissel[1], Daniela Müller[1], Christoph Mayr[2,3], Christian Ohlendorf[4], Bernd Zolitschka[4] and the PASADO science team[5]

[1]Institute of Bio- and Geosciences, IBG-3: Agrosphere, Research Center Jülich, D-52428 Jülich, Germany,

[2]Institute of Geography, University of Erlangen-Nürnberg, D-91054 Erlangen, Germany,

[3]GeoBio-Center and Dept. of Earth and Environmental Sciences, University of Munich, D-80333 Munich, Germany,

[4]GEOPOLAR, Institute of Geography, University of Bremen, D-28359 Bremen, Germany,

[5]The PASADO science team as listed at http://www-icdp.icdp-online.org/front_content.php?idcat=1494

This chapter is originally published as:

Zhu J., Lücke A., Wissel H., Müller D., Mayr C., Ohlendorf C., Zolitschka B. and the PASADO Science Team (2013) The last Glacial-Interglacial transition in Patagonia, Argentina: the stable isotope record of bulk sedimentary organic matter from Laguna Potrok Aike. *Quaternary Science Reviews* 71, 205-218, doi: 10.1016/j.quascirev.2012.05.025.

Abstract

An investigation of stable isotope ($\delta^{13}C_{TOC}$ and $\delta^{15}N_{TN}$) and elemental parameters (TOC, TN contents and TOC/TN ratios) of bulk organic matter (<200 µm) from sediment cores recovered from the Patagonian lake Laguna Potrok Aike (Argentina) in the framework of the ICDP deep drilling project PASADO provided insights into past changes in lake primary productivity and environmental conditions in South Patagonia throughout the last Glacial – Interglacial transition. Stratigraphically constrained cluster analyses of all proxy parameters suggest four main phases. From ca. 26,100 to 17,300 cal. years BP, lacustrine phytoplankton was presumably the predominant organic matter source in an aquatic environment with low primary productivity rates. At around 17,300 cal. years BP, abrupt and distinct shifts of isotopic and elemental values indicate that the lacustrine system underwent a rapid reorganization. Lake primary productivity (phytoplankton and aquatic macrophytes) shows higher levels albeit with large variations during most of the deglaciation until 13,000 cal. years BP. The main causes for this development can be seen in improved growing conditions for primary producers because of deglacial warming in combination with expedient availability of nutrients and likely calm wind conditions. After 13,000 cal. years BP, decreased $\delta^{13}C_{TOC}$ values, TOC, TN contents and TOC/TN ratios indicate that the lake approached a new state with reduced primary productivity probably induced by unfavorable growing conditions for primary producers like strengthened winds and reduced nutrient availability. The steady increase in $\delta^{15}N_{TN}$ values presumably suggests limitation of nitrate supply for growth of primary producers resulting from a nutrient shortage after the preceding phase with high productivity. Nitrate limitation and consequent decreased lacustrine primary productivity continued into the early Holocene (10,970 – 8400 cal. years BP) as reflected by isotopic and elemental values.

2.1. Introduction

Stable isotope analysis of bulk organic matter has been widely used in ecological research (e.g. Fry, 2006; Michener and Lajtha, 2007). However, these variables not only provide present day environmental information, but the isotopic composition of e.g. sedimentary organic matter preserves also evidence of past environmental changes (Meyers, 1994). Stratigraphic changes in carbon and nitrogen isotope composition of organic matter contained in lake sediments thus help trace histories of environmental and climate change (e.g. Meyers and Lallier-Vergès, 1999; Meyers, 2003; Lücke and Brauer, 2004).

Although several lacustrine isotope records have provided evidence for climate changes during the last deglaciation in the northern hemisphere (e.g. Yu and Eicher, 1998; von Grafenstein et al., 1999; Lücke et al., 2003; Parplies et al., 2008) and in the mid-latitudes of the southern hemisphere (e.g. Valero-Garcés et al., 2005; Bertrand et al., 2010), understanding of late Quaternary climate changes in the southern hemisphere higher latitudes is still incomplete because of the lack of long, continuous and high-resolution terrestrial records. Hence, due to its unique geographic location, records from southernmost Patagonia can offer new palaeoclimatic insights and an important linkage with marine records from southern oceans and ice core records from Antarctica. The sediment archive of Laguna Potrok Aike, further developed by the Potrok Aike maar lake sediment archive drilling project (PASADO) within the framework of the International Continental Scientific Drilling Program (ICDP), has initiated interdisciplinary multiproxy investigations to advance the understanding of past environmental and climatic changes in South Patagonia throughout the last Glacial – Interglacial cycle (e.g. Recasens et al., 2012; Hahn et al., 2013). Here we report on the results of high-resolution carbon and nitrogen isotope analyses of bulk sedimentary organic matter from Laguna Potrok Aike for a time window from 26,075 to 8,400 cal. years BP, including the Last Glacial Maximum (LGM) and the glacial-interglacial transition period, and discuss their paleoenvironmental significance. Our investigation builds on the earlier studies of surface and older sediments as well as core catcher samples (Mayr et al., 2009; Kastner et al., 2010; Lücke et al., 2010) and expands their scope with respect to temporal resolution and depositional history.

2.2. Site description

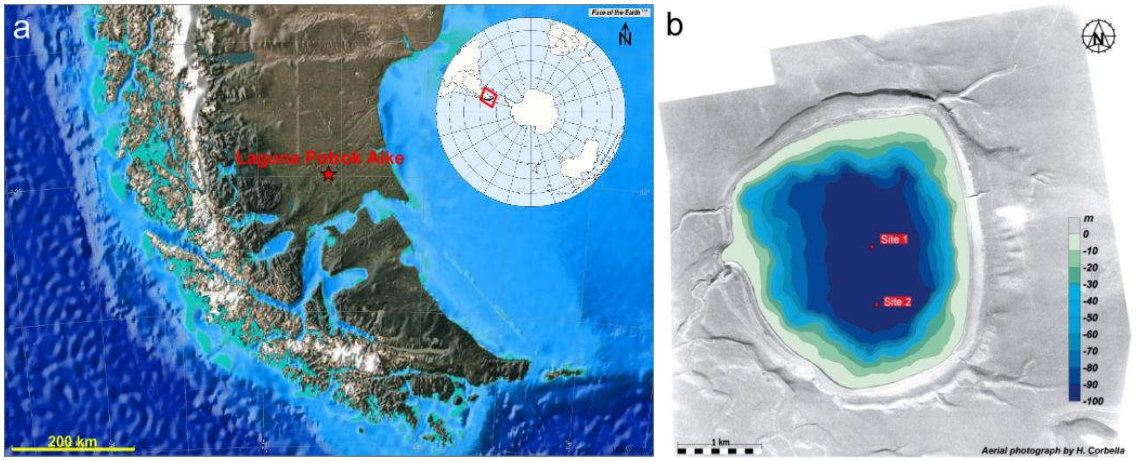


Figure 2.1. a) Location of Laguna Potrok Aike (red star) in South Patagonia in the relief map modified from http://jules.unavco.org/voyager/EarthScope. Red frame marked in the inserted map (source: Sean Baker/Wikipedia) shows the location of South Patagonia on the Southern Hemisphere. **b)** Drilling sites in 2008 in the aerial photography of Laguna Potrok Aike with bathymetry.

Laguna Potrok Aike is located at 113 m above sea level in the Pali Aike Volcanic Field in southern Patagonia, Argentina (51°58'S, 70°23'W; Fig. 2.1a) and originated from a phreatomagmatic explosion (Zolitschka et al., 2006). A detailed description about geomorphological characters and landscape evolution of the Laguna Potrok Aike area can be found in Coronato et al. (2013). During the last Glacial the catchment of the lake was not covered by the Patagonian glaciers (Zolitschka et al., 2006). Under modern conditions, Laguna Potrok Aike is a polymictic, phosphorous-rich and subsaline lake with a surface area of 7.58 km^2 and a maximum depth of 100 m (further lake characteristics in Zolitschka et al., 2006). The lake has presently only several episodic inflows through gullies and canyons and a catchment area of about 200 km^2. Subaerial and submerged paleoshorelines around and in the lake indicate pronounced lake-level fluctuations resulting from past hydrological changes (Zolitschka et al., 2006; Anselmetti et al., 2008; Gebhardt et al., 2012; Kliem et al., 2013a). The littoral zone of Laguna Potrok Aike is covered by aquatic macrophytes (e.g. *Potamogeton pectinatus* and *Myriophyllum* cf. *quitense*) from a water depth of ca. 1.5 – 15 m (Wille et al., 2007). Phosphate, as an important nutrient, appears to be unlimited in Laguna Potrok Aike (total phosphorus measurements: 1297 to 3609 µg/L), since the total phosphorus concentration is rather high presumably related to the regional geology (Zolitschka et al., 2006). The observed nitrate concentrations in lake water were considerably variable (nitrate measurements: < 0.05 to 3.07 mg/L) and indicate a potential nitrate limitation for primary production (Zolitschka et al., 2006). The climate at Laguna Potrok Aike is influenced by the rain shadow

of the Andes and nowadays characterized by semiarid steppe with a high annual evaporation/precipitation ratio of up to 24 (Wille et al., 2007; Ohlendorf et al., 2013). The modern vegetation in the area around Laguna Potrok Aike is a dry Magellanic steppe with grasses, shrubs, bushes and cushions as a result of overgrazing because of sheep farming during the last 100 years (Aagesen, 2000; Wille et al., 2007).

Laguna Potrok Aike is located at the center of the present-day Southern Hemisphere Westerlies that are characterized by their strong intensity associated with a strong meridional pressure gradient between the semi-permanent high pressure cells located over the subtropical South Pacific and South Atlantic oceans and the subpolar low pressure belt at approximately 60° S (Cerveny, 1998; Paruelo et al., 1998). As topographic barrier for the Westerlies, the Andes play a crucial role in determining the Patagonian precipitation pattern in the lee of the cordillera. Precipitation in the eastern part of South Patagonia is additionally affected by air masses coming from the Atlantic Ocean resulting in a more evenly distributed seasonal precipitation (Paruelo et al., 1998). Meteorological data of Laguna Potrok Aike have also shown the influence of rain-bringing easterly winds on the precipitation in the area (Mayr et al., 2007). A mean annual precipitation of 251 ± 62 mm and a mean annual temperature of 7.4 ± 0.7 °C are recorded at the weather station in Río Gallegos at the Atlantic coast, ca. 90 km east of Laguna Potrok Aike where both mean annual precipitation and temperature are 30-40% lower compared to the coastline (Zolitschka et al., 2006). Mean annual values of wind speed vary between 4 – 6 m/s in the central part of Patagonia (Paruelo et al., 1998) and around 7.4 m/s at Río Gallegos (Baruth et al., 1998). The seasonal distribution of the wind speed, particularly in southern South Patagonia, shows a maximum during austral summers and a minimum during austral winters (Baruth et al., 1998; Garreaud et al., 2009).

2.3. Material and methods

A total of 533 m of sediment cores was recovered from two drilling sites in Laguna Potrok Aike in 2008 in the framework of the ICDP deep drilling project PASADO (Zolitschka et al., 2009; Ohlendorf et al., 2011; Fig. 2.1b). In this study, we used the samples collected from the 106 m long Site 2 composite profile 5022-2CP (Ohlendorf et al., 2011) that covers the last 51,000 years according to the age-depth model (version 3) of Kliem et al. (2013b). The profile consists of undisturbed pelagic sediments, tephra layers and mass movement sediments that result from lake internal sediment redistribution. The mass movement deposits are characterized by ball and pillow structures, normally graded beds, structureless sand and fine

gravel layers, matrix supported layers and one folded sediment structure (Kliem et al., 2013b). Mass movement deposits and tephra layers were removed from the composite profile resulting in an event-corrected composite depth profile (m cd-ec) of 45.80 m to establish the age model. The age-depth model is based on radiocarbon dates of undisturbed pelagic sediments and was developed using the mixed-effect regression approach of Heegaard et al. (2005). For our analysis we chose the composite depth (cd) from 30.03 to 10.03 m (21.56 - 9.57 m cd-ec) covering the period between ca. 26,100 – 8,400 cal. years BP including the LGM and the last glacial-interglacial transition. The age–model for this sediment section relies on nine radiocarbon dates. A lithostratigraphic description for the composite profile has been given by Kliem et al. (2013b). Accordingly, our investigated sediment depths cover the parts of lithostratigraphic units B (8.82-18.72 m cd) and C-1 (18.72-40.23 m cd). Unit B consists mainly of pelagic laminated silts varying between dark grey (in the upper part) and brownish and light grey (in the lower part) intercalated with thin fine sand and coarse silt layers. Unit C-1 is also dominated by pelagic laminated silts which are greenish, bluish grey and have poor lamination compared with unit B. More mass movement deposits are found in unit C-1. Around 600 samples with 2 cm spatial resolution from sections with undisturbed pelagic sediments defined by Kliem et al. (2013b) were measured contiguously with an average temporal resolution of 28 years. In addition, about 100 samples from sections with re-deposited sediments were measured at 8 cm intervals (every 4^{th}) for carbon and at 16 cm intervals (every 8^{th}) for nitrogen isotope analyses, respectively.

Freeze-dried samples were cautiously homogenized and sieved at 200 µm to remove coarse organic debris. An aliquot (< 200 µm) for carbon isotope analysis was pre-treated with HCl (5 %) in a water bath (50°C) for two hours to remove carbonates and rinsed with distilled water three times to remove reagents. The samples were weighed before and after treatment to estimate HCl-insoluble content in weight percentage. Nitrogen isotope analysis was performed on the untreated freeze-dried samples of the same sediment fraction (< 200 µm). For isotope analyses, samples were weighed into tin capsules to provide approx. 100 µg of carbon and 80 µg of nitrogen, respectively, for analyses. Isotope ratios were measured using a continuous flow system that comprises an elemental analyzer (Flash 2000, Thermo Scientific for carbon and Euro EA 3000, Eurovector for nitrogen) directly attached to an isotope ratio mass spectrometer (IRMS; Delta V Advantage, Thermo Scientific for carbon and IsoPrime, Micromass for nitrogen). The samples were combusted in a He atmosphere with an excess of oxygen in the elemental analyzer and the analytical gases were transported into the IRMS in a continuous He flow through a series of traps and a GC column for purification and isolation of

the target analyte. Isotope ratios are expressed as δ-values in per mil (‰), where $\delta = (R_{sample}/R_{standard} - 1) * 1000$, with R_{sample} and $R_{standard}$ as isotope ratios ($^{13}C/^{12}C$ and $^{15}N/^{14}N$) of samples and international standards. For carbon and nitrogen, results are reported against the Vienna PeeDee Belemnite (VPDB) and atmospheric nitrogen (AIR), respectively. Laboratory standard materials were inserted between samples to monitor the working conditions of the instrument. Analytical precision (one standard deviation) was ±0.10‰ for carbon and ±0.15‰ for nitrogen isotope ratios.

Carbon and nitrogen contents were calculated according to the amounts of CO_2 and N_2 after sample combustion in the elemental analyzer. The obtained carbon content values and HCl-insoluble contents were used to estimate the total organic carbon (TOC) contents expressed in weight percentage (wt. %). Total nitrogen (TN) content (wt. %) was obtained directly from the nitrogen contents measured. The TOC/TN mass ratio is multiplied by 1.167 (the ratio of atomic weights of nitrogen and carbon) to yield the TOC/TN molar ratio (Meyers and Teranes, 2001), which is used in this study.

Stratigraphically constrained cluster analyses of all proxy parameters were performed by the CONISS program (Grimm, 1987) to identify the stratigraphical boundaries for the period investigated.

To further elaborate on the composition of the grain-size fractions and their isotope compositions, 11 HCl-untreated samples were selected from the total profile to be further sieved into four size fractions (< 10 µm, 10 – 63 µm, 63 – 125 µm and 125 – 200 µm) by wet sieving. These fractions were analysed separately with the above described methods to obtain the $\delta^{13}C_{TOC}$, $\delta^{15}N_{TN}$ values for each fraction.

2.4. Results

2.4.1. Geochemistry

For all measured samples, TOC contents range from 0.02 to 9.87% (mean 1.00%, *n* = 737) and TN contents from 0.01 to 0.66% (mean 0.12%, *n* = 700) (Fig. 2.2). TOC/TN ratios range between 1.73 and 29.44 (mean 7.33, *n* = 696). Carbon and nitrogen isotope compositions vary from -28.1 to -22.3‰ (mean -25.6‰, *n* = 741) and 1.3 to 7.6‰ (mean 3.4‰, *n* = 685), respectively. Below 18.73 m (cd) most samples show comparably low and stable values of TOC and TN contents and TOC/TN ratios. $\delta^{13}C_{TOC}$ values here are almost all lower than -

25.5‰ and $\delta^{15}N_{TN}$ values vary between 2.0 and 4.0‰. In terms of measured variables, there is no clear difference between undisturbed pelagic and re-deposited mass movement sediments in this depth range. The majority of samples with high TOC, TN contents, TOC/TN ratios, $\delta^{13}C_{TOC}$ values and low $\delta^{15}N_{TN}$ values in the total profile can be found between 18.60 and 13.00 m (cd). Except nitrogen isotope compositions, all variables exhibit high variability with e.g. 9% range for TOC contents and 5‰ range for carbon isotope compositions. By comparison with pelagic sediments, re-deposited sediments present here a different character with generally low TOC, TN contents, highly variable TOC/TN ratios and carbon isotope compositions. Above 13.00 m, most samples display low TOC, TN contents and TOC/TN ratios as well as decreased $\delta^{13}C_{TOC}$ values and increased $\delta^{15}N_{TN}$ values.

The samples below 20 m (cd) from lithostratigraphic unit C-1 have a generally high proportion of the finest sediment fraction (<10 µm) and a low proportion of the coarsest fraction (125-200 µm) in the bulk sediment (< 200 µm) compared to the samples from the upper part of the profile of lithostratigraphic unit B (Fig. 2.3a). The coarsest fraction found in the samples between 14 and 19 m (cd) is usually composed of visible organic material, such as remains of aquatic vascular plants and mosses. Three samples at 18.49, 21.17 and 23.21 m (cd) show highly various TOC/TN ratios in the sieve fractions with higher ratios in the coarser fractions and lower ratios in the fine fractions. Other samples exhibit a general small range of TOC/TN ratios with highest ratios in the coarsest fraction (Fig. 2.3b). The differences in $\delta^{13}C_{TOC}$ values between the coarsest and the finest fraction range from 0.08 to 3.36‰ (mean 1.47‰, n = 11) whereby the samples between 15 and 19 m (cd) show the largest differences. The coarsest fraction is always most depleted in ^{13}C (Fig. 2.3b). Nitrogen isotope compositions of sieve fractions show a trend in the samples below 20 m (cd) of least ^{15}N enriched values associated with the finest fraction. Both carbon and nitrogen isotope compositions of bulk sediments smaller than 200 µm show a pattern similar to that of the sieve fraction between 10 and 63 µm.

2.4.2. Cluster analysis

The CONISS cluster analysis included all proxy parameters from undisturbed pelagic samples. Three main clusters with highest dispersion and two main boundaries at around 17,300 and 13,000 cal. years BP were determined (Fig. 2.4a). Analyses without the outliers have confirmed that the absence or presence of outliers has no substantial influence on the division of the main clusters.

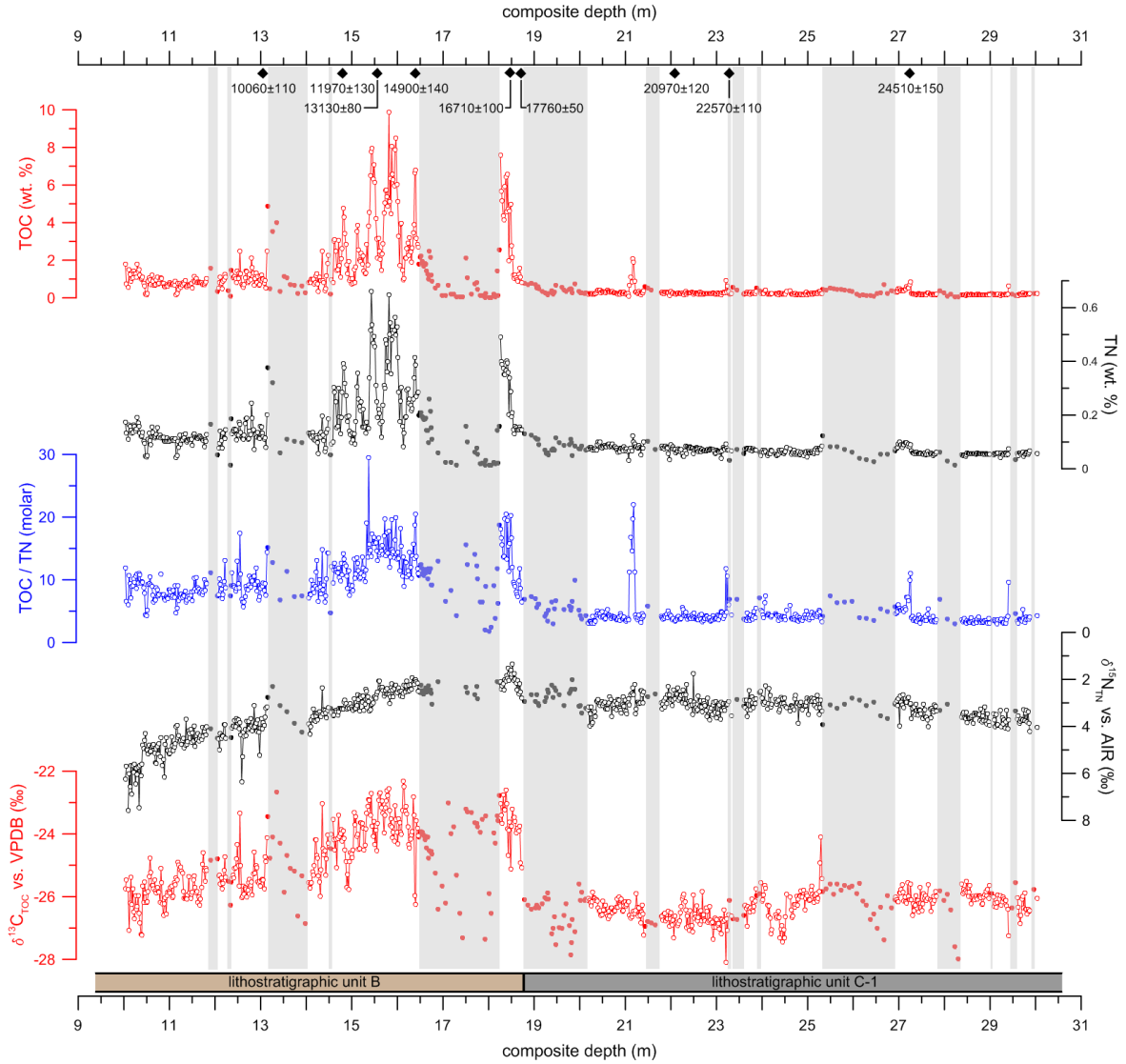


Figure 2.2. Downcore changes in carbon and nitrogen isotope compositions, TOC and TN contents (wt. %) and TOC/TN ratios during the investigated period (ca. 10–30 m cd) for core 5022-2CP from Laguna Potrok Aike. Measured samples from sections with undisturbed pelagic sediments as well as from disturbed and re-deposited sediments are plotted. Composite depths of sections with re-deposited sediments like mass movement and tephra deposits (Kliem et al., 2013b) are marked by grey bars. Lithostratigraphic units B and C-1 are described in Kliem et al. (2013b). Note inverse scale of $\delta^{15}N_{TN}$ values. Black diamonds with numbers on the upper depth scale show the depths of AMS radiocarbon ages (cal. years BP) with error (1σ) given by Kliem et al. (2013b).

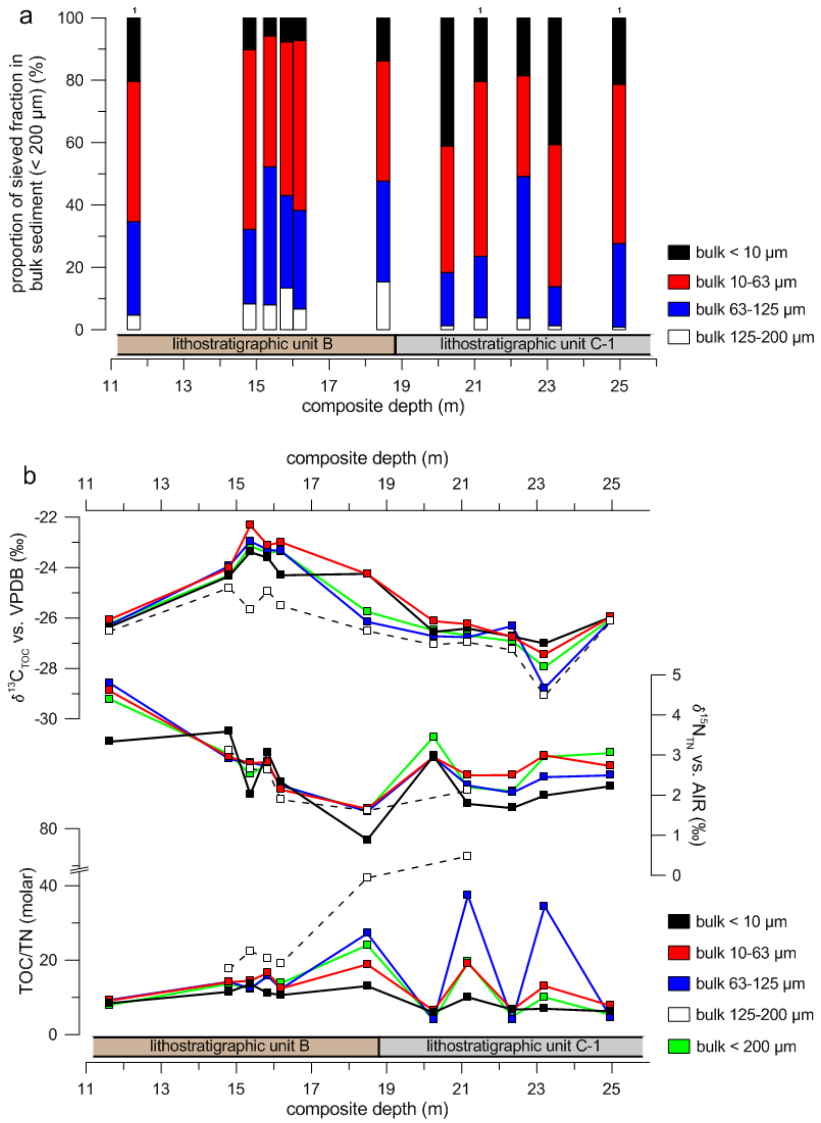


Figure 2.3. Proportion of four grain-size sieving fractions (< 10 µm, 10–63 µm, 63–125 µm and 125–200 µm) and its isotopic and elementary values of samples of core 5022-2CP from Laguna Potrok Aike. **a)** proportion of four sieving fractions in percentage. [1]small proportion loss of the fraction smaller than 10 µm due to tube breakage during centrifuge. **b)** Carbon and nitrogen isotope compositions and TOC/TN ratios of bulk sediments (< 200 µm) and four sieving fractions. Samples from the composite depth between 11 and 19 m correspond to the early Holocene and late Glacial time interval (lithostratigraphic unit B), whereas sediments at 19–25 m composite depth (lithostratigraphic unit C-1) were deposited prior to 17,300 cal. years BP (cf. Kliem et al., 2013b for age-depth model).

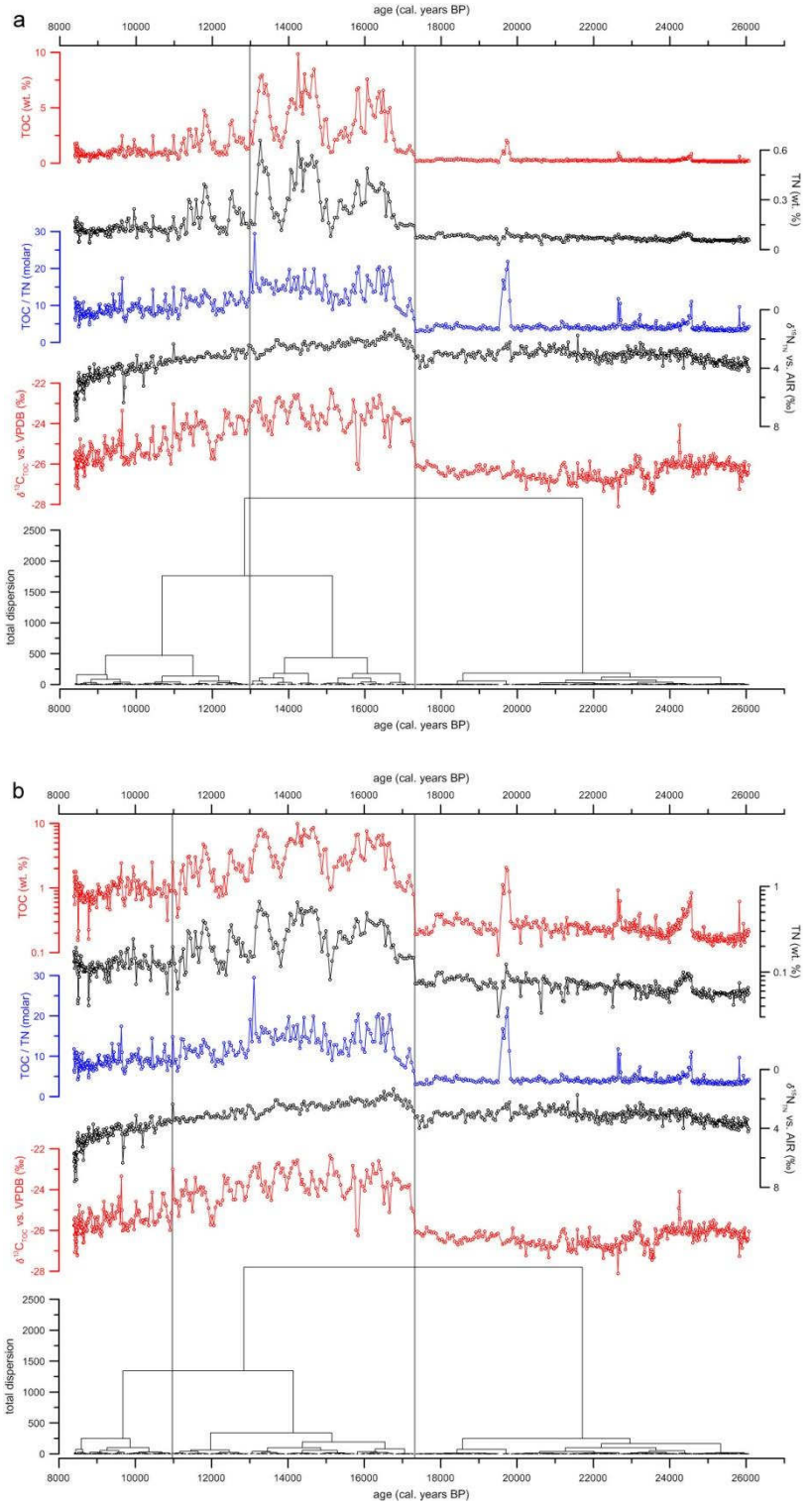


Figure 2.4. Three main phases with boundaries (grey lines) in measured proxy parameters during the last glacial-interglacial transition for core 5022-2CP from Laguna Potrok Aike suggested by cluster analysis (CONISS program by Grimm, 1987). Samples from sections of re-deposited sediments are excluded for the analysis. **a**) TOC and TN used on the linear scale. **b)** TOC and TN values logarithmized for the cluster analysis and used on the log scale. For details refer to the text. Note inverse scale of $\delta^{15}N_{TN}$ values.

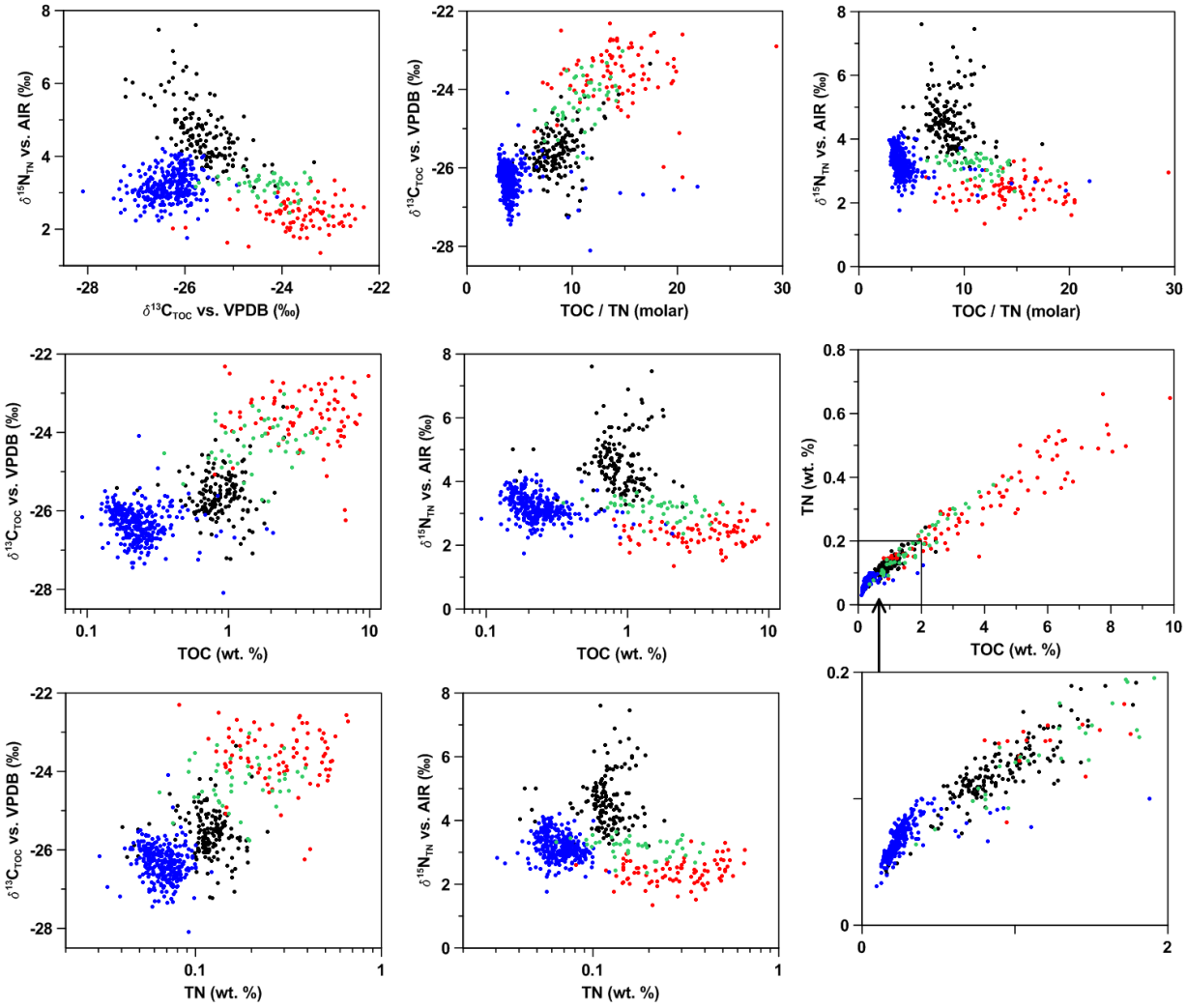


Figure 2.5. Cross-plots of the measured proxy parameters for the four main phases (blue: phase 1, 26,075 – 17,300 cal. years BP; red: phase 2, 17,300 – 13,000 cal. years BP; green: phase 3, 13,000 – 10,970 cal. years BP; black: phase 4, 10,970 – 8400 cal. years BP). Samples from sections of re-deposited sediments are excluded. The cross-plot of TOC and TN is enlarged in the lower right. Low correlations on the intra-phase scale can be observed, however there are visible inter-phase relationships among the proxy parameters.

Considering the data structure of single variables it is evident that the distribution function of total organic carbon and total nitrogen follows more a logarithmic than a linear law (Fig. 2.5, lower right). Accounting for this difference by using logarithmic TOC and TN data for the cluster analysis indeed changes the outcome. The basic structure of three main clusters remains and the older boundary at around 17,300 cal. years BP (18.73 m cd) is confirmed but the younger boundary is shifted from 13,000 to 10,970 cal. years BP (Fig. 2.4b). While the boundary at around 17,300 cal. years BP matches with the transition from lithostratigraphic unit B to unit C-1 (Kliem et al., 2013b), no lithostratigraphic change is described for either of the younger boundaries. Justification for the demarcation of clusters can be found in the data for both linear and log-scaled element contents. Whereas a change in variance of TOC and TN

seems to determine the classification in the latter case (Fig. 2.4b), the development of absolute values seems to be more important in the former case (Fig. 2.4a). As there are no lithostratigraphic criteria to decide the case and the data justify both scenarios, we suggest respecting both divisions. Because after 10,970 cal. years BP the elemental contents of organic carbon and nitrogen in the sediments of Laguna Potrok Aike remain on one and the same reduced level with minimal variance, we are inclined to assign higher palaeoenvironmental importance to this than to the boundary of 13,000 cal. years BP. The period between around 13,000 and 10,970 cal. years BP seems to be a transition from high to low TOC and TN values with smaller variability but still overall similarity to the period between around 17,300 – 13,000 cal. years BP (Fig. 2.4a).

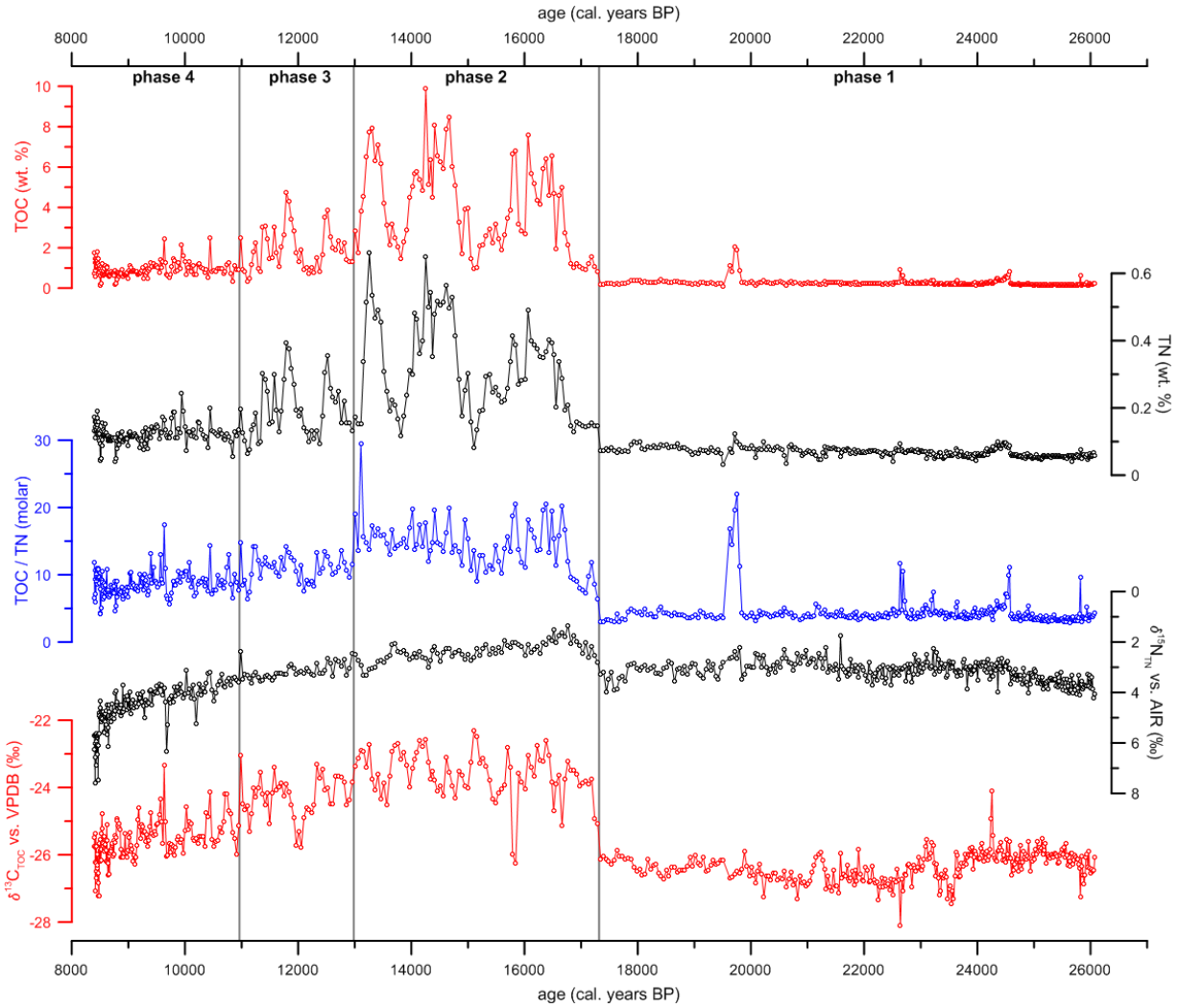


Figure 2.6. Proposed four main phases of measured proxy parameters during the investigated last glacial-interglacial transition for core 5022-2CP from Laguna Potrok Aike determined by assemblage of two approaches of stratigraphically constrained CONISS cluster analyses (Fig. 2.4). Grey lines mark the boundaries of the proposed stages. Note inverse scale of $\delta^{15}N_{TN}$ values.

Considering the points outlined above we propose to structure the investigated time window of the Laguna Potrok Aike profile into four characteristic phases (Fig. 2.6):

Phase 1 (26,075 - 17,300 cal. years BP):

TOC and TN contents have very low values, mean 0.26 and 0.07% (n = 323) for TOC and TN, respectively. Except for several outlier samples, both TOC and TN contents stay more or less on a constant level during this phase. TOC/TN ratios are usually lower than 5 (mean 4.31, *n* = 322). Only several outlier samples show extreme high TOC/TN ratios up to 19. $\delta^{13}C_{TOC}$ values vary in a small range with the mean value of -26.3‰ (*n* = 324). Most $\delta^{15}N_{TN}$ values have a range between 2‰ and 4‰ with a mean value of 3.2‰ (*n* = 323). Generally there is no clear correlation between all proxy parameters in this phase, apart from the relation of TOC and TN which has, however, a steeper slope compared with the later phases.

Phase 2 (17,300 – 13,000 cal. years BP):

Around 17,300 cal. years BP, an abrupt und marked shift occurs for all proxy parameters. TOC and TN contents rise to the highest values within the total profile investigated. TOC contents range from 0.80 to 9.87% (mean 4.00%, *n* = 85) and TN contents from 0.08 to 0.66% (mean 0.31%, *n* = 85) in the whole phase. A two step increase at the transition from phase 1 to 2 can be observed in both variables. The first rise of smaller extent within a short time (from 0.20 to 1.50% for TOC, from 0.07 to 0.15% for TN) is followed by a second larger increase (from 1.5 to more than 6% for TOC, from 0.15 to more than 0.4% for TN). TOC/TN ratios also display a two step increase and rise to a mean value of 14.34 (*n* = 85). In comparison to the changes in TOC, the increase in $\delta^{13}C_{TOC}$ values by up to 2.5‰ occurs in just one step. During the whole phase the $\delta^{13}C_{TOC}$ values have a high mean value of -23.6‰ (*n* = 85). By contrast with other proxy parameters, the $\delta^{15}N_{TN}$ values decrease at first with about 2.0‰ at the transition from phase 1 to 2. About five hundred years later, the $\delta^{15}N_{TN}$ values begin to rise slightly into the next phase. TOC, TN contents, TOC/TN ratios and $\delta^{13}C_{TOC}$ values exhibit here the highest variability in the total profile investigated.

Phase 3 (13,000 – 10,970 cal. years BP):

TOC and TN contents decline with reduced variability, ranging from 0.35 to 4.75% (mean 1.89%, *n* = 46) for TOC and from 0.06 to 0.39% (mean 0.19%, *n* = 46) for TN. TOC/TN ratios drops to a mean value of 10.99 (*n* = 46). A decrease in $\delta^{13}C_{TOC}$ values can also be observed

having a mean value of -24.3‰ (n = 46). The slow and slight increase in the $\delta^{15}N_{TN}$ values continues with little variability like the former phases. This phase can be considered as a transition from phase 2 to 4.

Phase 4 (10,970 – 8400 cal. years BP):

After 10,970 cal. years BP, both TOC and TN contents decrease to a low level that is nevertheless still higher than in the phase 1. TOC has a range from 0.15 to 2.47% (mean 0.91%, n = 153) and TN from 0.04 to 0.24% (mean 0.12%, n = 153). TOC/TN ratios decrease down to a mean value of 8.56 (n = 152). The $\delta^{13}C_{TOC}$ values with a mean of -25.6‰ (n = 154) drop towards the level of the phase 1 with a still higher variability. The $\delta^{15}N_{TN}$ values proceed to rise reaching more than 7.0‰ at the end of this phase. Cross plots reveal a negative correlation between $\delta^{13}C_{TOC}$ and $\delta^{15}N_{TN}$ values (r = -0.6, $p < 0.0001$) in this phase.

There are no obvious correlations among the proxy parameters, except for the TOC and TN relation (Fig. 2.5). This behavior could be seen as an indication of a variety of independent control factors determining the elemental and isotopic values of bulk organic matter looking at the intra-phase scale. However, an inter-phase relation can be found for several parameters (Fig. 2.5). Phase 1 distinguishes itself from other phases by low values of all proxy parameters and their narrow range of variability. From phases 2 to 4, carbon isotope compositions decrease with the rise of nitrogen isotope compositions, thus showing an overall negative correlation. This trend is accompanied by a reduction in TOC, TN contents and TOC/TN ratios correlating positively with carbon isotope compositions.

2.5. Discussion and Interpretation

2.5.1. Nitrogen proxies and inorganically bound nitrogen

One of the geochemical proxies frequently used in environmental studies is the nitrogen content, for example to determine the carbon to nitrogen ratio. Nitrogen in aquatic sediments is a constituent of organic matter as well as bound to inorganic matter, mainly clay minerals (Müller, 1977). Normally, their carbon to nitrogen ratio is expressed as the TOC to TN ratio due to difficulties in the separation between the organic and the inorganic fraction of total nitrogen. However, especially in sediments with low organic matter concentrations (TOC < 0.3%), TOC/TN ratios could be reduced due to an elevated proportion of inorganic nitrogen

(Meyers, 2003) thus being a poor estimator of the carbon to nitrogen ratio in sedimentary organic matter.

For Laguna Potrok Aike a gross estimation of the portion of inorganic nitrogen (IN) in TN (e.g. Talbot, 2001; Lücke and Brauer, 2004) seems insufficient, as no simple linear relation exists between TOC and TN (Fig. 2.5, lower right) thus excluding a straightforward estimation of IN. Comparably low TOC/TN ratios as in phase 1 of Laguna Potrok Aike have been observed in modern sediments of Lake Ohrid (Vogel et al., 2010) and were also reported by Melles et al. (2007) for Lake El'gygytgyn and by Watanabe et al. (2004) for Lake Baikal. The steeper slope of the TOC versus TN regression line of phase 1 compared to those of phases 2-4 (Fig. 2.5, lower right) and TOC/TN ratios below 5 might be interpreted as contribution of IN downward of 20.18 m (cd). However, there are several other factors including soil or source rock organic matter input, organic matter decomposition/degradation or grain size distribution that might cause low sedimentary TOC/TN ratios beside inorganically bound nitrogen. This issue is of broader importance as it also affects the interpretation of stable nitrogen isotopes as well as their relation to the respective stable carbon isotope signature.

Measurements reported by Mayr et al. (2009) for recent soils from the catchment of Laguna Potrok Aike cannot explain the very low glacial TOC/TN ratios of the record. A summary of carbon and nitrogen content of soils by Batjes (1996) shows that TOC/TN ratios generally range around 10 and do not fall below 7. Nevertheless a decline of TOC/TN ratios with depth and age, i.e. in the course of decomposition of soil humus was detectable (Batjes, 1996) - a process that might reduce the TOC/TN ratios of fossil soils further than observed in modern soils. Low TOC/TN ratios at around 3 were also found in the samples of rocks beneath soils in the catchment of Lake Holzmaar (Lücke et al., unpublished data). The TOC/TN ratios of such organic matter incorporated into rocks are dependent on the origin of its source rocks. Low sedimentary TOC/TN ratios might be influenced by source rock organic matter originating from the catchment of Laguna Potrok Aike.

Decomposition experiments describe an initial increase in TOC/TN followed by a less significant reduction under oxic conditions (Lehmann et al., 2002). Successive decomposition within a 50 cm long marine core was also found to cause a gradual reduction of TOC/TN ratios in a study by Freudenthal et al. (2001) where the IN content was determined explicitly. The authors attribute this to an increasing importance of inorganically bound nitrogen as decomposition of organic matter proceeds in oligotrophic, organic matter poor sediments. As the $\delta^{15}N$ of IN is depleted in ^{15}N compared to organic nitrogen (Freudenthal et al., 2001;

Kienast et al., 2005), a higher portion of IN to TN in the sediments of Laguna Potrok Aike below 20.18 m (cd) would lead to an underestimation of the $\delta^{15}N$ signature of organic nitrogen by the respective bulk nitrogen isotope signature. Kienast et al. (2005) has reported considerable differences of 1‰ to 2‰ in the $\delta^{15}N$ of bulk sediment separated into different size fractions. In their study heavier isotope values seem to be associated with the finer sediment fractions whereas coarser fractions seem to become increasingly isotopically lighter. However, our elemental and $\delta^{15}N$ data of size fractions do not indicate such a dependence on grain size distribution for both lithostratigraphic units (Fig. 2.3).

In short, the issue of IN and its likely influence on TOC/TN and $\delta^{15}N_{TN}$ values in the glacial sediments of Laguna Potrok Aike cannot be decided on the available data. The low TOC/TN ratios of phase 1 sediments seem to imply an overestimation of IN, while the potential bias of IN during phases 2-4 is strongly restricted due to the high organic matter content.

2.5.2 Phase 1 (26,075 – 17,300 cal. years BP)

Studies on Patagonian glacier fluctuations have shown that full glacial conditions should dominate the climate in southern South Patagonia prior to around 17,500 cal. years BP (e.g. McCulloch et al., 2005; Sugden et al., 2005; Kaplan et al., 2008). A study of glacial moraines from Kilian et al. (2007) has suggested the start of deglaciation at Gran Campo Nevado, located about 200 km southwestern from Laguna Potrok Aike, at around 18,000 cal. years BP.

These dates coincide well with the end of phase 1 as inferred from our organic geochemical dataset (Fig. 2.6). During phase 1, the origin of low TOC/TN ratios around 4, as discussed in the section 2.5.1, remains unclear but could imply that sedimentary organic matter predominantly stemmed from phytoplankton production as the algae produce organic matter which has lower TOC/TN ratios of 4-10 than those from mosses and vascular-plants with 20 and greater (Meyers et al., 2003). The samples with distinct spikes of high TOC/TN ratios contain usually high amounts of aquatic moss debris that could affect the analyzed bulk fraction (<200 µm), as suggested by the TOC/TN ratios of sieve fractions (Fig. 2.3b).

Simulation models of Hulton et al. (2002) suggest a decline in temperature of 6°C compared to the present values during the LGM in southern South Patagonia. At that time the area of Laguna Potrok Aike was climatically more continental than it is now because of the sea level lowering of up to 150 m below present on the Argentine Shelf (Guilderson et al., 2000).

Under such cold and dry climatic conditions, a tundra-like vegetation and thin soil layers with low nitrogen mineralization rate can be expected in the lake catchment. During the long winter period the lake was likely ice covered with little snow and stratified. Algal production can be maintained under the lake ice cover as reported by many studies (e.g. Spaulding et al., 1993; McKnight et al., 2000). Low air and water temperatures could, however, induce low lake algal productivity as suggested by the low TOC, TN contents and by low $\delta^{13}C_{TOC}$ values (Fig. 2.6). Although respiration and decomposition would be low due to the low primary production, dissolved CO_2 from internal respiration in the lake could be a main carbon source for algal assimilation during periods with ice cover. This re-utilized CO_2 is depleted in ^{13}C and could contribute to the low $\delta^{13}C$ values. Sediments with low organic carbon contents are characteristic of glacial-age lake sediments in temperate climate zones (Meyers and Lallier-Vergès, 1999). The narrow range of changes in total nitrogen isotope composition may reflect little changes in the lacustrine nitrogen cycle during that time.

2.5.3 Phase 2 (17,300 – 13,000 cal. years BP)

The abrupt increase in $\delta^{13}C_{TOC}$ values around 17,300 cal. years BP is interpreted as a fast and persistent increase in lake primary productivity triggered by deglacial warming which caused extended growing seasons, high growth rates and consequent fast consumption and probably lowering of dissolved CO_2 concentrations. Photosynthetic processes use preferentially ^{12}C and lead to organic matter production enriched in ^{12}C and dissolved inorganic carbon (DIC) of surface waters enriched in ^{13}C. Progressively, newly produced organic matter then becomes enriched in ^{13}C by assimilation of isotopically heavier DIC. This effect can also be intensified by a depletion of the dissolved CO_2 concentration as the result of high primary productivity, because a low CO_2 concentration in the photic zone diminishes discrimination against ^{13}C during photosynthesis (O'Leary, 1988; Hollander and McKenzie, 1991). These processes of isotopic fractionation are especially active during phases of lake stratification in the often productive summer season with high carbon demand for photosynthesis but low carbon replenishment from the hypolimnion. Isotopically heavier organic matter can also be produced by increased growth rate of phytoplankton because of declined isotopic fractionation (Laws et al., 1995; Burkhardt et al., 1999). An influence of atmospheric pCO_2 and carbon isotope composition of atmospheric CO_2 can be ruled out (Leuenberger et al., 1992; Monnin et al., 2001), because the small variation observed in ice cores around that time cannot account for the abrupt change in $\delta^{13}C_{TOC}$ values within 150 years in Laguna Potrok Aike. Nevertheless,

increased carbon replenishment from the atmospheric CO_2 due to the extended ice-free summer season should be taken into account as an additional more ^{13}C enriched carbon source compared to the re-utilized CO_2 derived by respiration.

The positive shift in $\delta^{13}C_{TOC}$ values of bulk sediment could have been caused, however, also by an increased contribution of aquatic macrophytes which are able to use HCO_3^- as inorganic carbon source thus showing high $\delta^{13}C_{TOC}$ values of about -13‰ to -15‰ (Mayr et al., 2009; Zhu et al., unpublished data). This argument is supported by the massive occurrence of pollen from the aquatic macrophyte *Myriophyllum* in Laguna Potrok Aike within this time window (Wille et al., 2007). A simultaneous drastic rise in TOC/TN above 15 also adds to the argument of a massive increase in organic matter sources from aquatic macrophytes. The abundance of aquatic macrophytes in the lake could be favored by calm wind conditions during that period, because strong wind-induced currents and waves would strongly hamper or even destroy macrophytes growing in the littoral zone. Comparably calm or absent winds would, in combination with the warming, also permit thermal stratification of the lake during summer months favoring not only macrophyte but also phytoplankton growth. According to Talbot and Lærdal (2000), TOC/TN data would also react on restrictions in the availability of dissolved nitrogen for photosynthesis. It could thus not be ruled out that nitrogen deficiency might partly cause the high TOC/TN ratios of algal organic matter (Healey and Hendzel, 1980), considering nitrate as the probable limiting factor in present Laguna Potrok Aike (Zolitschka et al., 2006).

Compared to the large one-step increase in $\delta^{13}C_{TOC}$ values at around 17,300 cal. years BP, TOC as well as TN contents responded to deglacial warming in two steps. The first steep rise occurs concurrent with the $\delta^{13}C_{TOC}$ increase, however, after about 500 years, at around 16,800 cal. years BP, a second steep rise in TOC and TN values took place. In view of the relatively smooth changes in sedimentation rates during the transition from phase 1 to phase 2 indicated by the applied age-depth model (Kliem et al., 2013b), the shift in TOC and TN contents should be mainly controlled by the amount of deposited and preserved organic matter itself. The $\delta^{13}C_{TOC}$ values record the immediate response of lake primary productivity to the improvement of growth conditions in the lake which however may not simultaneously generate a proportional high amount of buried sedimentary organic matter. Lehmann et al. (2004a) have shown that $\delta^{13}C_{TOC}$ values are more coupled with lake primary productivity per water volume and not necessarily correlate with total primary production. According to that, increased algal productivity and accompanying more biomass per water volume can result in a thinning of the trophogenic zone due to a reduction in light penetration. Thus, there could be a still relatively

low level of total algal production during this time. After several hundred years, continuous lake algal production combined with increased contribution of aquatic macrophytes could cause increased organic matter accumulation and cause the high sedimentary TOC and TN contents.

The declined $\delta^{15}N_{TN}$ values on the onset of phase 2 appear to contrast with enhanced lake primary productivity and accompanying high nitrate utilization with progressively enrichment of ^{15}N in the organic matter (Teranes and Bernasconi, 2000). However, Hodell and Schelske (1998) have reported that on the seasonal scale a decrease in $\delta^{15}N$ values is associated with phytoplankton blooms and coincides with an increase in $\delta^{13}C_{TOC}$ values. Furthermore, nitrogen isotope composition of bulk organic matter in lake sediments is also controlled by other factors like $\delta^{15}N$ values of dissolved inorganic nitrogen (internal and external source), change in algal assemblages and selective preservation of isotopically distinct fractions of organic matter (Talbot and Lærdal, 2000; Talbot, 2001; Lehmann et al., 2004b). A depletion of ^{15}N observed for anaerobic incubations has been attributed to the selective loss of ^{15}N-enriched organic matter and possible addition from ^{15}N-depleted bacterial biomass (Lehmann et al., 2002). However, a geomicrobiological study of Laguna Potrok Aike sediments shows that such microbial processes have mainly secondary effects without distorting paleoenvironmental signals contained in organic proxies of bulk sediments (Vuillemin et al., 2013). Abruptly increased lake productivity since around 17,300 cal. years BP could cause anaerobic hypolimnic conditions in the deep basin for several months, while the extensive wind-generated circulation might still be absent due to ice cover. The increased assimilation of isotopically light ammonium (NH_4^+) derived from organic matter degradation can be another reason for the reduction in the nitrogen isotope composition of bulk organic matter at the beginning of phase 2. Since 16,800 cal. years BP bulk organic matter became slowly enriched in ^{15}N indicating probably declined assimilation of isotopically light nitrogen and/or better preservation of ^{15}N-enriched organic matter.

A previous study of Laguna Potrok Aike sediments based on an isotopic mixing model has inferred that at a depth comparable to the onset of phase 2 cyanobacteria were dominant in bulk sediment organic matter with about 52% (Mayr et al., 2009). Regarding this interpretation, the decrease in $\delta^{15}N$ values, increase in $\delta^{13}C_{TOC}$ values and, in particular, the still relatively low TOC/TN ratios between 17,300 and 16,800 cal. years BP could also be explained by cyanobacterial organic matter which shows a mean carbon and nitrogen isotope composition of -21.8‰ and -0.3‰, respectively, in recent samples (Mayr et al., 2009). The dominance of cyanobacteria can be attributed to the ability to fix molecular nitrogen (nitrogen-fixing species)

in lakes with nitrogen limitation and the competitive ability to uptake ammonium-nitrogen (non-nitrogen-fixing species) in lakes with nitrate depletion (Blomqvist et al., 1994). Since phosphorous supply might be unlimited in Laguna Potrok Aike due to the characteristics of the regional geology (Zolitschka et al., 2006), the high phosphorous concentration in lake water could favor the occurrence of cyanobacteria (Downing et al., 2001; Wagner and Adrian, 2009). Probably decreased nitrate availability being concurrent with abruptly increased primary productivity might then promote cyanobacteria species using ammonium-nitrogen. Considering our present isotopic data and TOC/TN ratios, however, the proportion of cyanobacterial organic matter with about 52% estimated by the isotopic mixing model in Mayr et al. (2009) appears to be high. Because the factors causing the dominance of cyanobacteria in lakes can be diverse and depend also on the respective environment and the species involved (Dokulil and Teubner, 2000), a better understanding of cyanobacteria development in Laguna Potrok Aike needs further investigations.

Beginning with a shift of all proxy parameters, the lake reached a new state with the warming-induced increase in lacustrine primary productivity. However, the water of Laguna Potrok Aike in the late Glacial was still cool, clear and fresh, as inferred by the microfossil record showing the abundance of the diatom *Cyclostephanos patagonicus* and the chlorophyte *Pediastrum kawraiskyi* (Wille et al., 2007; Massaferro et al., 2013). Although additional nutrient supply may be low due to the still sparse vegetation cover in the catchment, a lake with long-term low primary productivity under full glacial conditions could retain a certain nutrient reservoir being probably sufficient for such warming-induced blooms of algae with low nutrient demand. It is, however, unclear, if the general high algal productivity during phase 2 is linked to the improved nutrient supply from the catchment (increased terrestrial productivity and nutrients leaching through soil columns because of permafrost thawing) and/or to enhanced recycling in the lake (shortened ice cover period).

Besides two samples at around 15,800 cal. years BP that may contain moss debris, TOC, TN contents and TOC/TN ratios tend to decrease from 16,000 to 15,000 cal. years BP. The onset of this shift is simultaneous with the occurrence of an about 1.5 m thick Reclús tephra layer. It is well known that a strong volcanic eruption event has climatic impact on an annual scale (Litt et al., 2003). Considering the decadal resolution of the samples and the duration of the decrease (about 1000 years), it is unlikely that the Reclús eruption caused this development. A similar large reduction in TOC and TN contents also occurs within the period from 14,200 to 13,500 cal. years BP, however, without an obvious decline in TOC/TN ratios. Because of the

independent change in carbon isotope compositions (Fig. 2.6), both large reductions in TOC and TN contents may not be mainly caused by changes in lacustrine primary productivity, but could be controlled by variations in redox and preservation conditions in bottom waters (e.g. Melles et al., 2007). Nevertheless, it seems to be unlikely that the large TOC variation of up to 8% is only derived from a shift in the oxic-anoxic conditions. The concentration of organic matter in lake sediments is also determined by the proportion of the clastic fraction which can dilute the organic fraction in weight percentage (e.g. Veres et al., 2009). During the periods from 16,000 to 15,000 cal. years BP and from 14,200 to 13,500 cal. years BP such a dilution effect may be the case. XRF data by Jouve et al. (2013) show relatively high Si contents (kcps), interpreted as an indicator of detrital input, in both periods, but low Si values in the adjacent periods with high concentrations of organic matter.

2.5.4 Phase 3 (13,000 – 10,970 cal. years BP)

Decreasing TOC/TN ratios in phase 3 are likely caused by a reduced proportion of aquatic macrophyte organic matter probably suggesting increasing wind-induced waves on the lake. The progressive decline in $\delta^{13}C_{TOC}$ values could give another indication of the resulting decrease in gross lake algal productivity. However, strong waves in the lake can decrease resistance of CO_2 diffusion and encourage discrimination against ^{13}C in aquatic plants which in turn would lead to organic matter more depleted in ^{13}C than during calm phases (Osmond et al., 1981; O'Leary, 1988; Keeley and Sandquist, 1992). In addition, strong mixing and continuous upwelling of ^{13}C depleted CO_2 to the photic zone can replenish the DIC pool of surface water and prevent enrichment in ^{13}C of lacustrine produced organic matter. Similar effects would be induced by increasing the input of dissolved remineralized ^{13}C depleted soil carbon dioxide, as respiration processes in the catchment intensify due to increased terrestrial productivity over the course of deglaciation warming. The hypothesis about the decrease in lake primary productivity of both algae and aquatic macrophytes can be partly supported by the decline in TOC and TN contents, although a dilution effect by clastic material can still be effective as inferred from contemporaneously elevated Si contents (kcps) (Jouve et al., 2013).

Based on the tendency and variation range of TOC, TN, TOC/TN and $\delta^{13}C_{TOC}$ values, similarities with phase 2 are high and phase 3 may be merely seen as a prolonged transition to the next phase 4, when the lake reaches a reduced nutrient level after the maximum of lacustrine productivity in the early phase of the late Glacial.

2.5.5 Phase 4 (10,970 – 8400 cal. years BP)

Lower TOC/TN ratios below 10 may reflect predominant organic matter origin from algae. The absence of the signature of aquatic macrophytes can suggest the persistence of strong wind conditions since phase 3. Lower $\delta^{13}C_{TOC}$ values could be induced by the rapid and continuous replenishment of the DIC pool due to strong mixing of the whole water column preventing enrichment in ^{13}C of algal organic matter. Accompanied by the low TOC and TN contents, ^{13}C depleted algal organic matter could indicate low primary productivity of the lake during this phase. Strong mixing occurring in the whole water column can also give rise to fast degradation of organic matter resulting in the low concentration of organic fraction in sediments. Increased $\delta^{15}N_{TN}$ values since the last phase could be caused by limitations in nitrate availability (Hodell and Schelske, 1998; Jones et al., 2004) which might have been exhausted during the early bloom phase of the lake. Extremely high $\delta^{15}N_{TN}$ values at round 8,400 years BP can be the consequence from the high input of ^{15}N enriched soil organic matter during a period with a very low lake level (Haberzettl et al., 2007; Mayr et al., 2009; Kliem et al., 2013a).

2.5.6 Inter-phase relations

Phase 1 with low productivity under LGM conditions is clearly distinct from the later phases with high and variable productivity (Fig. 2.5). Deglacial warming and improved growth conditions led to a distinct and large shift of lake productivity of both algae and aquatic macrophytes from phase 1 to phase 2 as there was possibly a relatively sufficient nutrient reserve in Laguna Potrok Aike directly after the glacial phase with little consumption. The primary productivity in Laguna Potrok Aike reached its maximum at around 14,000 cal. years BP during phase 2 (Fig. 2.6). Simultaneously, nutrient availability, particularly nitrate, could likely start to become reduced with persistent enhancement in the primary productivity. After phase 2, lake primary productivity declined progressively documented by the overall positive relation between $\delta^{13}C_{TOC}$ values and elemental parameters like TOC, TN contents and TOC/TN ratios (Fig. 2.5). Under conditions of nitrate limitation, diminished discrimination against ^{15}N by algal assimilation can result in ^{15}N enriched algal organic matter. This factor may explain the negative relation between carbon and nitrogen isotope compositions over the course of the late Glacial and the early Holocene (Fig. 2.5 upper left).

2.5.7 Regional and global context

The timing of the onset of the last deglacial warming in the southern hemisphere is illustrated in Antarctic ice cores and Southern Ocean sediments at around 17,000 – 19,000 cal. years BP (Sachs et al., 2001; EPICA, 2006; Jouzel et al., 2007; Lamy et al., 2007). Moraine records (e.g. McCulloch et al., 2005; Sugden et al., 2005; Kilian et al., 2007; Kaplan et al., 2008) and palynological evidences from peat bog records in South Patagonia (e.g. McCulloch and Davies, 2001; Markgraf and Huber, 2010) have confirmed the terrestrial response to the initial warming signal that also caused an increase in bio-productivity and the shift from phase 1 to phase 2 in Laguna Potrok Aike. McCulloch et al. (2000) suggested two steps of deglacial warming influencing southern South America at 17,600 and 11,400 cal. years BP. Since in southern Patagonia temperature changes primarily control effective moisture (Markgraf and Huber, 2010), which has in turn large impact on the lake-system, both steps can be associated with changes in primary productivity in Laguna Potrok Aike at the onset of phase 2 and phase 4, respectively. A warming induced poleward shift of the southern westerlies could take several thousand years to reach their latitudes of the present day centered on 50° S (McCulloch et al., 2000), thus causing the windier conditions since 13,000 cal. years BP in the Laguna Potrok Aike area. The Antarctic Cold Reversal that is well recorded in Antarctic ice cores (e.g. Stenni et al., 2011) is not evident in our lake sediment geochemical archive. The algal productivity in late-glacial Laguna Potrok Aike appears to be mainly controlled by nutrient availability as long as temperature was not low enough to influence the primary producers substantially. However, more investigations particularly comparisons with other proxies in Laguna Potrok Aike are needed to gain a better understanding, especially of the connection between the lake response and the Antarctic signal.

2.6. Conclusions

Based on high-resolution measurements of the TOC, TN contents, TOC/TN ratios, $\delta^{13}C_{TOC}$ and $\delta^{15}N_{TN}$ values from bulk sediments (<200 µm) of Laguna Potrok Aike, insights into the paleoenvironment in southern Patagonia during the last Glacial-Interglacial transition are provided. Under full glacial conditions, from ca. 26,000 to 17,300 cal. years BP, the lake had a very low primary productivity with a dominant organic matter source from lake algae. At around 17,300 cal. years BP, the lake underwent a rapid reorganization and lacustrine primary productivity increased and remained high during most of the deglaciation until 13,000 cal.

years BP as the nutrient supply was still high. The main causes for this development were interpreted as improved growing conditions for primary producers in the lake because of deglacial warming and possible calm wind conditions that might have led to partial thermal summer stratification of Laguna Potrok Aike. This favored the growth and production of aquatic macrophytes that would have made an important contribution to the sedimentary organic matter. The variations of most proxy parameters are obviously larger during deglaciation than in the LGM suggesting lake and environment instability during this transitional period. Since around 13,000 cal. years BP, the lake appeared to approach a new state with deteriorated growing conditions for all primary producers. This development was likely caused by windier conditions and insufficient nutrient (nitrate) availability probably due to the low regeneration of nutrients in the lake after its exhaustion during the early phase with high primary productivity. This tendency continued into the early Holocene and primary productivity was comparably low but remained on a stable level until around 8400 cal. years BP.

Acknowledgement

We thank H. Vos (Research Center Jülich) for providing the software of CONISS cluster analysis und for helpful discussions. We thank D. Dumitrescu for support in sample preparation in the laboratory. This research used samples provided by the International Continental Scientific Drilling Program (ICDP) in the framework of the Potrok Aike Maar Lake Sediment Archive Drilling Project (PASADO). Funding for drilling was provided by the ICDP, the German Science Foundation (DFG), the Swiss National Funds (SNF), the Natural Sciences and Engineering Research Council of Canada (NSERC), the Swedish Vetenskapsrådet (VR) and the University of Bremen, Germany. Finally, we would like to thank Philip Meyers and an anonymous reviewer for their valuable comments on the manuscript.

Chapter 3

Characterizing oxygen isotope variability and host water relation of modern and subfossil aquatic mosses

Jiayun Zhu[1], Andreas Lücke[1], Holger Wissel[1], Christoph Mayr[2,3], Christian Ohlendorf[4], Bernd Zolitschka[4]

[1]Institute of Bio- and Geosciences, IBG-3: Agrosphere, Research Center Jülich, D-52428 Jülich, Germany

[2]Institute of Geography, University of Erlangen-Nürnberg, D-91054 Erlangen, Germany

[3]GeoBio-Center, Dept. of Earth and Environmental Sciences, University of Munich, D-80333 Munich, Germany

[4]GEOPOLAR, Institute of Geography, University of Bremen, D-28359 Bremen, Germany

This chapter is originally published as:

Zhu J., Lücke A., Wissel H., Mayr C., Ohlendorf C. and Zolitschka B. (2014) Characterizing oxygen isotope variability and host water relation of modern and subfossil aquatic mosses. *Geochimica et Cosmochimica Acta* 130, 212-228, doi: 10.1016/j.gca.2014.01.013.

Abstract

A field survey in southern Patagonia has shown a highly significant linear correlation between $\delta^{18}O$ values of cellulose extracted from modern submerged aquatic mosses and their respective host-waters. The amount of aquatic moss remains preserved in lake sediments is, however, often not sufficient for cellulose extraction for oxygen isotope analysis. By comparison, the $\delta^{18}O$ analysis of bulk organic matter of aquatic mosses requires much less material, but further pretreatment due to inorganic contamination is needed. In this study we extend the cellulose $\delta^{18}O$ approach to aquatic moss organic matter and aquatic vascular plants in order to explore the relation between $\delta^{18}O$ values of aquatic plants and host waters. Furthermore, we focus on a comparison between cellulose and pretreated organic matter of subfossil aquatic mosses and vascular plants with regard to their $\delta^{18}O$ and $\delta^{13}C$ values from Laguna Potrok Aike, a southern Patagonian maar lake. Subfossil remains of two representative submerged aquatic moss species and different moss parts (branches and leaves) are handpicked and an investigation on moss organic matter, moss cellulose and cellulose from coarse plant debris is performed in pairs within a moss-rich sediment section. Our results show that, similar to moss cellulose, a significant linear correlation exists between $\delta^{18}O$ values of purified moss organic matter and their respective host waters. Past lake water $\delta^{18}O$ values can thus be inferred from moss cellulose as well as from purified moss organic matter with comparable precision. Only a marginal ^{18}O enrichment (ca. 1‰) is observed for $\delta^{18}O$ values of cellulose from aquatic vascular plants compared to that of aquatic mosses, whereas $\delta^{13}C$ values of aquatic vascular plant cellulose show a pronounced ^{13}C enrichment (ca. 20‰) relative to aquatic mosses. Noticeable differences in $\delta^{18}O$ values of organic matter from different moss species suggest a monospecific analysis for the reconstruction of lake water $\delta^{18}O$ values based on moss organic matter. Separation of different submerged aquatic moss parts (branches and leaves) is, however, not necessary due to their indistinguishable $\delta^{18}O$ values. The paired investigation demonstrates a consistent variation of lake water $\delta^{18}O$ values inferred from moss organic matter, moss cellulose and, within limitations, cellulose from coarse plant debris. This offers the potential for combining results from different moss organic fractions (cellulose, purified OM) into a composite lake water $\delta^{18}O$ record to achieve high-resolution paleoenvironmental reconstructions. Despite several open issues, the approach could be successfully applied to other lakes worldwide where aquatic moss remains are preserved.

3.1. Introduction

Early studies pointed out that isotope differences between different biochemical components in plants can mask the isotopic ratios determined by effects of climate change (Epstein et al., 1976). Therefore, analysis of a single biochemical component, like cellulose, is traditionally used to eliminate issues associated with the isotopic heterogeneity of plant biochemical compounds. Moreover, it has been shown that the relationship between stable oxygen isotope ratios ($\delta^{18}O$) of cellulose and the water used for its synthesis is constant with an enrichment factor of about 27‰, however, with an uncertainty of ±4‰ (Epstein et al., 1977; DeNiro and Epstein, 1981; Sternberg, 2009). Based on this constant fractionation factor, stable oxygen isotope analysis of fine-grained lake sediment cellulose has been widely used to infer lake water $\delta^{18}O$ values for the reconstruction of past hydrological conditions (e.g. Edwards and McAndrews, 1989; MacDonald et al., 1993; Beuning et al., 2002; Wolfe et al., 2007; Heikkilä et al., 2010). A fundamental assumption for interpreting these data is the predominant aquatic origin of the investigated bulk fine-grained sediment cellulose (Wolfe et al., 2001). However, this assumption is invalid for lake sediments containing a significant contribution of cellulose with a terrestrial origin (Sauer et al., 2001). Even aquatic cellulose can originate from different plant types like vascular and nonvascular plants with potentially different $\delta^{18}O$ values (Cooper and DeNiro, 1989). Species-dependent variability in overall oxygen isotope fractionation during cellulose synthesis has also been suggested (Sternberg et al., 2006). Such uncertainties can be avoided by analyzing cellulose extracted from submerged aquatic mosses identified to the species level. Mosses are valuable for isotopic studies because their leaf anatomy and physiology are rather simple (Sauer et al., 2001; Glime, 2007). As aquatic moss leaves are not subjected to evapotranspiration, $\delta^{18}O$ values of cellulose extracted from submerged aquatic mosses are predominantly influenced by the host-water isotopic composition as revealed by laboratory (Sauer et al., 2001) as well as by field studies (Mayr et al., 2013), demonstrating the high potential for analyzing oxygen isotopic compositions of aquatic moss cellulose to reconstruct changes in lake-water balances.

Mosses can be a major component of lake and peat deposits and, thus, are frequently used for paleoenvironmental reconstruction (e.g. Dickson, 1986; Janssens, 1990; Jonsgard and Birks, 1995; Van der Putten et al., 2004). The published stable oxygen and carbon isotope records of moss cellulose are, however, often confined to *Sphagnum* mosses from peat bogs (e.g. White et al., 1994; Ménot-Combes et al., 2002; Daley et al., 2010; Moschen et al., 2011; El Bilali and Patterson, 2012). Permanently submerged mosses in lakes are characteristic especially for polar

regions (e.g. Light and Heywood, 1973; Longton, 1988; Sand-Jensen et al., 1999; Imura et al., 2003; Wagner and Seppelt, 2006; Li et al., 2009), indicating the possibility to perform isotope analyses of submerged mosses preserved in the lake sediments especially at high latitudes. Cellulose extracted from aquatic moss remains can therefore be a powerful tool to infer past lake water $\delta^{18}O$ values and changes in lake water balance.

An investigation of submerged aquatic mosses collected from different sites in southern Patagonia has displayed a highly significant linear correlation between the $\delta^{18}O$ values of aquatic moss cellulose and their respective host-waters (Mayr et al., 2013). The analysis of cellulose from aquatic moss requires, however, large quantities of moss tissues for cellulose extraction, which restricts high-resolution stratigraphic studies. Compared to cellulose, isotopic measurements of aquatic moss bulk organic matter (OM) need much less moss tissues and can potentially improve the temporal resolution of isotopic records based on the moss cellulose alone. However, oxygen isotope measurements on moss organic matter must overcome the problem of inorganic contamination (e.g. by an acid pretreatment with HCl-HF) to avoid any minerogenic bias in the measured $\delta^{18}O$ values.

In this study we first examined the correlation between the $\delta^{18}O$ values of pretreated aquatic moss OM and their respective host waters and compared this to measurements of moss cellulose by Mayr et al. (2013). The relationship between $\delta^{18}O$ values of modern aquatic mosses (OM and cellulose) and host waters was used as a calibration to infer past lake water $\delta^{18}O$ values from subfossil aquatic mosses. Moreover, in order to verify the necessity of analyzing OM within a functional group or even at a monospecific level, $\delta^{18}O$ and $\delta^{13}C$ values of OM from two plant groups (aquatic vascular plants and aquatic mosses) and two representative submerged moss species and their different parts (branches and leaves) have been measured. Finally, we compared $\delta^{18}O$ and $\delta^{13}C$ values of moss OM, moss cellulose and cellulose from coarse plant debris within a moss-rich Late Glacial sediment core section from Laguna Potrok Aike, and proposed an approach to evaluate uncertainties of the application of moss OM and coarse plant debris cellulose for reconstructing past lake water $\delta^{18}O$ values.

3.2. Study sites

Laguna Potrok Aike is located in southern Patagonia, Argentina (51°58'S, 70°23'W; 113 m asl.; Fig. 3.1a) and has a surface area of 7.58 km^2 and a maximum depth of 100 m (further lake characteristics in Zolitschka et al., 2006). The present lake has no outflows and only episodic

inflows through gullies and canyons and a catchment area of about 200 km^2. The lake water body circulates constantly under the prevailing strong west-wind conditions. Oxygen isotope composition of the lake water shows constant values along a depth gradient and low inter-annual and intra-annual isotopic variations with a range between -3.4‰ and -3.9‰ during a three year monitoring interval (Mayr et al., 2007). The littoral zone of Laguna Potrok Aike is partly covered by aquatic vascular plants (e.g. *Potamogeton pectinatus* and *Myriophyllum* cf. *quitense*) between water depths of ca. 1.5–15 m (Wille et al., 2007). A detailed survey of the recent habitat of aquatic mosses has, however, so far not been conducted due to the difficult access in this remote area.

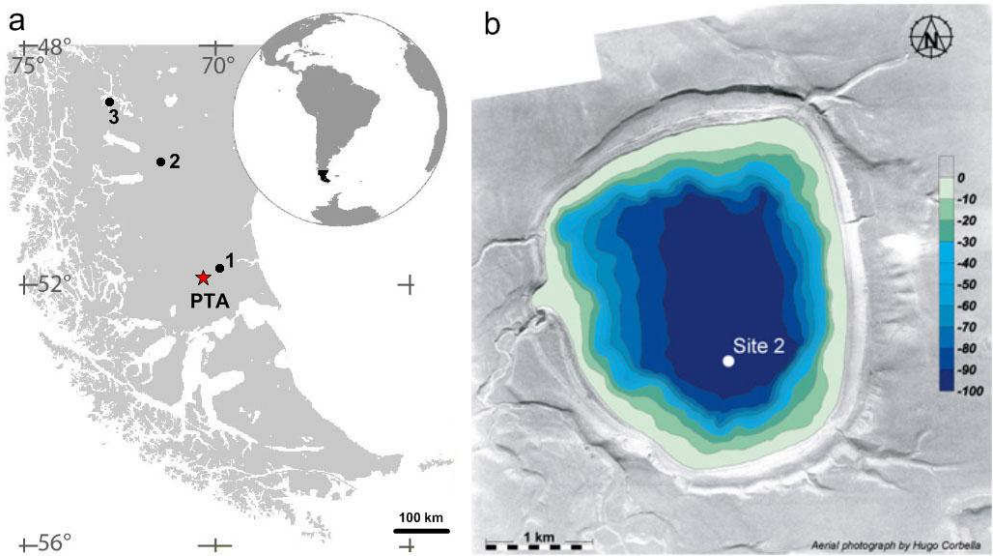


Figure 3.1. a) Sampling location in southern Patagonia indicated as a black area on the inserted map. Red star: Laguna Potrok Aike (PTA); 1: Spring at Ea. La Carolina; 2: Laguna Cháltel; 3: Lago del Desierto. Two German sites are not shown. Details about sampling location and material are given in Table 3.1. **b)** Sediments used in this study derive from the drilling site 2 shown on the bathymetric map of Laguna Potrok Aike inserted into an aerial photography (provided by Hugo Corbella).

In addition to Laguna Potrok Aike, modern aquatic mosses were also collected at other field sites (Fig. 3.1a). These sites include a spring at Estancia La Carolina, Laguna Cháltel and Lago del Desierto in southern Patagonia for the calibration study and the brooks in Kirnitzschtal and Wennigsen in Germany for analyzing moss cellulose and moss OM (for detailed location information: cf. Table 3.1).

Table 3.1. C/O ratio, $\delta^{13}C$ and $\delta^{18}O$ values of organic matter and extracted cellulose from modern aquatic moss samples and $\delta^{18}O$ values of respective host-waters from different field sites in South Patagonia and Germany. $\delta^{18}O$ values of moss cellulose (except PAIS-102g and PAIS-102b) and host-waters are from Mayr et al. (2013).

			Moss organic matter (OM)			Moss cellulose			Host-water	Enrichment in $\delta^{18}O$		Fractionation factor	
Sample ID	Sampling location	Material	C/O	$\delta^{13}C$	$\delta^{18}O$	C/O	$\delta^{13}C$	$\delta^{18}O$	$\delta^{18}O$	$\varepsilon_{OM\text{-}water}$	$\varepsilon_{cell\text{-}water}$	$\alpha_{OM\text{-}water}$	$\alpha_{cell\text{-}water}$
PAIS-102g*†	Laguna Potrok Aike, E shore (51°58'S. 70°23'W)	*Drepanocladus perplicatus* with chlorophyll (shore)	1.13	-32.9	24.2	0.88	-31.7	25.7	-3.8	28.0	29.5	1.0281	1.0296
PAIS-102b*†	Laguna Potrok Aike, E shore (51°58'S. 70°23'W)	*Drepanocladus perplicatus* without chlorophyll (shore)	1.09	-32.2	24.7	0.88	-30.9	25.7	-3.8	28.5	29.5	1.0286	1.0296
PAIS-173*	Laguna Potrok Aike, W shore (51°58'S. 70°23'W)	*Drepanocladus perplicatus* (3-4 m depth)	1.20	-33.4	24.9	0.89	-32.1	26.3	-3.8	28.7	30.0	1.0288	1.0301
PAIS-84	Laguna Potrok Aike (51°58'S. 70°23'W)	*Drepanocladus perplicatus*. outcrop at shore	1.14	-30.7	24.0	0.89	-29.7	25.0	–	–	–	–	–
PAIS-95*	Spring at Ea. La Carolina (51°50'S. 70°14'W)	recent moss	1.13	-36.5	18.4	0.89	-35.9	18.8	-11.2	29.6	30.0	1.0299	1.0303
PAIS-175*	Laguna Cháltel, E shore (49°58'S. 71°7'W)	*Drepanocladus perplicatus*	1.17	-32.1	23.1	0.89	-31.4	24.5	-5.3	28.4	29.7	1.0285	1.0299
PAIS-178*	Laguna Cháltel, inflow (49°58'S. 71°7'W)	*Vittia sp.*	1.18	-36.6	15.8	0.91	-35.4	15.9	-14.3	30.1	30.2	1.0305	1.0306
Lago del Desierto*	Lago del Desierto (49°05'S. 72°53'W)	recent moss	1.13	-36.9	15.1	0.89	-36.2	15.5	-14.3	29.4	29.8	1.0298	1.0302
Fontinalis I	Kirnitzschtal, brook (50°57'N. 14°15'O)	*Fontinalis antipyretica*	1.35	-39.7	18.7	0.88	-37.8	19.7	–	–	–	–	–
Fontinalis II	Wennigsen, brook (52°16'N. 9°34'O)	*Fontinalis antipyretica*	1.21	-42.2	19.9	0.87	-41.2	21.1	–	–	–	–	–
	mean		**1.17**	**-35.3**	**20.9**	**0.89**	**-34.2**	**21.8**	**-8.1**	**28.9**	**29.8**	**1.0292**	**1.0301**

* Samples which are used to calibrate the relation between $\delta^{18}O$ values of aquatic mosses and respective host-waters in Fig. 3.4.

† Samples are aliquots of material extracted for moss cellulose with the $\delta^{18}O$ value of 26.1‰ reported in Mayr et al. (2013). These two aliquots are newly analyzed in this study and have replaced the old value, thus enabling the direct comparison of moss OM and cellulose.

3.3. Materials and methods

3.3.1. Materials

3.3.1.1. Modern samples

Modern samples of aquatic vascular plants and aquatic mosses from Laguna Potrok Aike and aquatic mosses from other field sites in southern Patagonia and Germany were used to analyze $\delta^{18}O$ and $\delta^{13}C$ values of plant OM and extracted cellulose. Plant material was collected in the field, immediately dried at temperatures below 40°C or brought directly to the laboratory. Type and location of samples are summarized in Table 3.1 and 3.2. Plant material was initially cleaned through washing in deionized water, ultrasonic treatment and handpicking and separated into two aliquots for isotope measurement of plant OM and cellulose (for cellulose extraction: cf. 3.3.2, for isotope measurement: cf. 3.3.3). To avoid inorganic contamination of plant OM, OM samples were treated with a mixture of HCl and HF (10% respectively) and left for 16 h at room temperature to completely remove attached carbonates and other minerogenic components. Treated samples were rinsed with deionized water three times to remove reagents and remaining clastic matter. Samples were then freeze-dried and homogenized using ball milling at room temperature for 30-60s. The other aliquot was used for cellulose extraction without further pretreatment. Host-water samples of different sites in southern Patagonia were collected as well and analyzed for their $\delta^{18}O$ values (Mayr et al., 2007, 2013).

3.3.1.2. Sediment samples

Sediment samples from Laguna Potrok Aike used in this study derive from the cores of the composite profile 5022-2CP of site 2 drilled in 2008 (Fig. 3.1b; Ohlendorf et al., 2011).

Moss fragments are frequently occurring in the sediment samples. There are mainly three species: *Drepanocladus perplicatus* (Amblystegiaceae) (Fig. 3.2a), *Blindia inundata* (Seligeriaceae) (Fig. 3.2b) and *Vittia pachyloma* (Amblystegiaceae). These moss species are all reported as submerged aquatic species (Ochyra and Lightowlers, 1988; Hedenäs, 1997; Frahm, 2001). Fragments of *D. perplicatus* are dominant in many sediment samples. Mainly branches and individual leaves are found in the sediments (Fig. 3.2). In the case of *D. perplicatus*, stems and branches are morphologically similar tissues and they all have similar leaves (Hedenäs, 1997). Due to the different degree of preservation, some branches bear leaves and some do not.

The leaf laminae were frequently eroded before sedimentation and in these cases only costae remain on the branches (Fig. 3.2a and b).



Figure 3.2. Subfossil plant remains in sediment samples from Laguna Potrok Aike. **a)** Branches of *Drepanocladus perplicatus*. **b)** Branches of *Blindia inundata*. **c)** Remains of aquatic vascular plants. **d)** Leaves of *Drepanocladus perplicatus* and *Blindia inundata*.

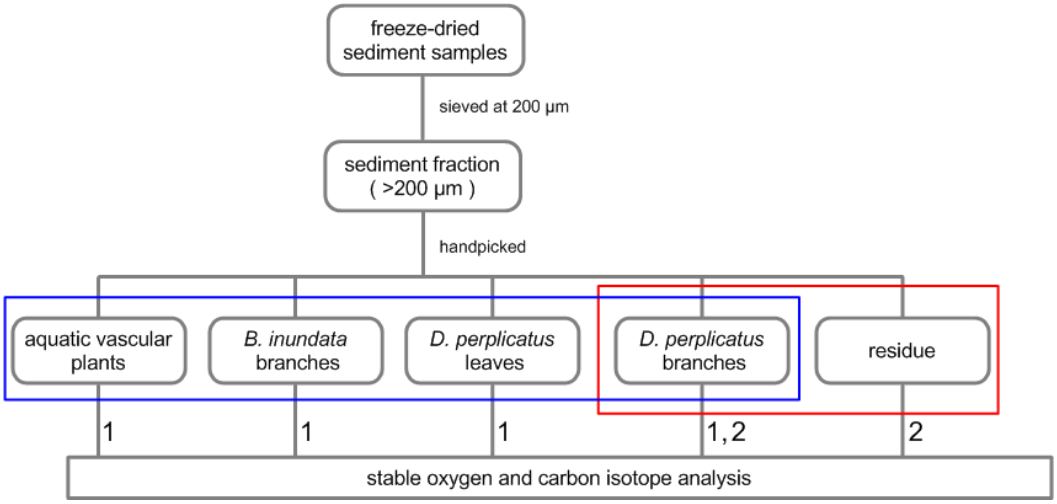


Figure 3.3. Work flow for the preparation of subfossil samples. Fractions in the red frame are separated from 23 moss-rich Late Glacial sediment samples and used for the paired investigation, while fractions in the blue frame are separated from additional samples of a larger depth range used for the comparison between them. *B. inundata* for *Blindia inundata* and *D. perplicatus* for *Drepanocladus perplicatus.* 1: HCl-HF (10%) treated and homogenized. Samples of *Drepanocladus perplicatus* branches used for the paired investigation were pretreated by HCl-HF (10%) for measurement of moss organic matter prior to chemical bleaching and cellulose extraction. 2: chemical bleaching and cellulose extraction (CUAM protocol).

From the composite depth range between 15 and 19 m, corresponding to the Late Glacial time period (Kliem et al., 2013b), 23 moss-rich bulk sediment samples of undisturbed pelagic sediments were selected for the paired investigation of subfossil material with regard to their $\delta^{18}O$ and $\delta^{13}C$ values. From the composite depth range between 13 and 30 m, 24 additional bulk sediment samples, in which adequate amounts of aquatic vascular plants and different species of aquatic mosses (*D. perplicatus* and *B. inundata*) coexisted (Fig. 3.2), were selected for isotopic analyses. Branches of *B. inundata* were easily distinguishable from those of *D. perplicatus* (Fig. 3.2a and b). But this is not the case for *V. pachyloma*. Due to the frequent lack of identifiable leaves, branches of *V. pachyloma* were not easily differentiated from those of *D. perplicatus* and, therefore, were not analyzed separately.

Each freeze-dried bulk sediment sample was first placed on a magnetic stirrer with deionized water and stirred for 2 h to disaggregate it. Subsequently, the sample was carefully wet sieved on a 200 µm sieve to obtain the coarse plant debris fraction. The sieve fraction (>200 µm) consists mainly of plant fragments such as branches and leaves of mosses and remains of vascular plants. Plant fragments were handpicked from the >200 µm fraction under a binocular (Fig. 3.3). For samples used in the paired investigation, subfossil moss branches were picked in sufficient amounts for OM and cellulose analyses. To obtain monospecific moss samples, we tried to pick only subfossil branches of *D. perplicatus*. However, some branches without leaves were not identifiable. Therefore, an admixture of such moss fragments (like *V. pachyloma*) to the monospecific *D. perplicatus* samples cannot be ruled out. The remaining plant material in this coarse sieve fraction (>200 µm) containing fragments of *B. inundata*, *V. pachyloma* and other unidentifiable mosses and individual leaves of *D. perplicatus* as well as remains of aquatic vascular plants is termed as 'residue fraction' hereafter. For the additional sediment samples from the larger depth range, three additional fractions of plant fragments were picked: individual leaves of *D. perplicatus*, branches of *B. inundata* and remains of aquatic vascular plants.

Like the modern samples, each of these subsamples was HCl-HF treated prior to isotope analyses (for treatment details: cf. 3.3.1.1). The cleaned and freeze-dried samples were homogenized by cutting the coarse plant fragments into fine segments with scissors which avoids the loss of fine moss material compared to milling. For samples of the stratigraphic study, moss OM was first analysed for $\delta^{18}O$ and $\delta^{13}C$ values (not for the residue fraction) before cellulose extraction was conducted. HCl-HF treatment of moss tissue prior to cellulose extraction has no distinguishable effect on the $\delta^{13}C$ and $\delta^{18}O$ values of cellulose (cf.

supplemental table for results of HCl-HF treated and untreated modern as well as subfossil moss samples). The gain of plant material from additional sediment samples was not sufficient to allow cellulose extraction.

Table 3.2. $\delta^{13}C$ and $\delta^{18}O$ values of plant organic matter and extracted cellulose from modern plant samples (dead remains and fresh material) from Laguna Potrok Aike.

		Plant organic matter		Cellulose	
Sample type	Sample ID	$\delta^{13}C$ (‰)	$\delta^{18}O$ (‰)	$\delta^{13}C$ (‰)	$\delta^{18}O$ (‰)
Aquatic vascluar plants					
remains from shoreline sample	PTA 08-3	-12.8	20.2	-11.4	26.5
remains from shoreline sample	PTA 08-7	-13.5	20.2	-	-
remains from shoreline sample	PTA 08-15	-12.9	20.1	-11.6	26.3
remains from shoreline sample	PTA 08-31	-14.0	19.9	-11.7	25.6
remains from shoreline sample	PTA 08-37	-13.9	20.9	-13.4	26.3
mean		**-13.4**	**20.3**	**-12.0**	**26.2**
Myriophyllum sp. (fresh material, shore)	PAIS-96	-10.9	24.2	-9.3	26.4
Potamogeton sp. (fresh material, shore)	PAIS-97	-11.5	24.9	-11.3	27.5
Potamogeton sp. (fresh material, 3-4 m depth)	PAIS-174	-12.3	23.8	-10.2	27.0
mean		**-11.6**	**24.3**	**-10.3**	**27.0**
Aquatic mosses					
remains from shoreline sample	PTA 08-3	-32.4	24.7	-30.6	25.3
remains from shoreline sample	PTA 08-7	-32.8	24.7	-31.3	25.5
remains from shoreline sample	PTA 08-31	-33.0	25.0	-31.5	25.5
remains from shoreline sample	PTA 08-37	-32.6	24.9	-30.8	25.6
mean		**-32.7**	**24.8**	**-31.0**	**25.5**
Drepanocladus perplicatus (with chlorophyll, shore)	PAIS-102g	-32.9	24.2	-31.7	25.7
Drepanocladus perplicatus (without chlorophyll, shore)	PAIS-102b	-32.2	24.7	-30.9	25.7
Drepanocladus perplicatus (fresh material, 3-4 m depth)	PAIS-173	-33.4	24.9	-32.1	26.3
mean		**-32.8**	**24.6**	**-31.6**	**25.9**

3.3.2. Cellulose extraction

Cellulose was extracted from modern and subfossil plant material using the Cuprammonium solution (CUAM) protocol that has shown high reliability in yielding clean and pure cellulose from aquatic plants and freshwater sediments (Wissel et al., 2008). According to this protocol, samples were first bleached with $NaClO_2$ (7%) acidified to pH 4-5 with concentrated acetic acid (96%) in a water bath for 10 h at 60 °C. The residue was washed two times with hot deionized water (~70 °C) to remove the reagents and freeze-dried. The dry sample was mixed with ca. 30 ml CUAM solution (15 g/L) while placed in a dark room and stirred on a magnetic

stirrer for 6 h and left for further 10 h at room temperature to completely dissolve the cellulose. Subsequently, the cellulose solution was carefully decanted into a centrifuge tube and treated with 3 ml H_2SO_4 (20%) for cellulose precipitation. The white precipitate (cellulose) was then rinsed three times with deionized water and freeze-dried. Compared to other methods this extraction achieves pure cellulose by dissolving and reprecipitating cellulose from whole plant material. Before and after cellulose extraction, samples were weighed to determine the cellulose yield for subfossil mosses.

3.3.3. Stable isotope measurements

For carbon isotope analyses, an amount of plant OM or cellulose equivalent to 100 µg of carbon was weighed into tin capsules. Samples were combusted at 1020 °C using an elemental analyser (Thermo Scientific Flash 2000) interfaced on-line with an isotope ratio mass spectrometer (Thermo Scientific Delta V Advantage). Carbon content was determined by peak integration of mass-to-charge ratio (m/z) 44, 45 and 46, and calibrated against elemental standards. For oxygen isotope analyses, an amount of plant OM or cellulose providing 125 µg of oxygen was weighed into silver capsules. Immediately prior to oxygen isotope analysis, samples were placed overnight (16 h) in a vacuum drier at 100 °C to avoid analytical bias by adsorbed air moisture. Vacuum-dried samples were then pyrolysed at 1450 °C in a high temperature pyrolysis analyzer (HTO, HEKAtech) and measured on-line with a coupled isotope ratio mass spectrometer (Micromass IsoPrime). Oxygen content was determined by peak integration of m/z 28, 29 and 30, and calibrated against elemental standards. Each sample was measured at least 2 times as long as material was available. Isotope ratios are expressed as δ-values in per mil (‰), where

$$\delta = (R_{sample}/R_{standard} - 1) \cdot 1000$$

with R_{sample} and $R_{standard}$ as isotope ratios ($^{13}C/^{12}C$ and $^{18}O/^{16}O$) of samples and standards, respectively. Isotope values are reported on the VPDB scale for carbon and on the VSMOW scale for oxygen. Laboratory standards were inserted between samples to monitor the performance of the instrument. To calibrate laboratory standards, reference materials USGS24 (-16.05‰), IAEA-CH-6 (-10.45‰) and IAEA-CH-7 (-32.15‰) were used for carbon isotope ratios (Coplen et al., 2006). The benzoic acid standards IAEA-601 (23.14 ±0.19‰) and IAEA-602 (71.28 ±0.36‰) (Brand et al., 2009) were used for oxygen isotope ratios. The overall precision of replicate analyses was better than ±0.1‰ for carbon and ±0.3‰ for oxygen isotope

ratios. Ratios of carbon and oxygen content (C/O) of moss OM and cellulose were calculated on a weight base. The fractionation factor between cellulose and water respectively OM and water is defined as $\alpha_{cell\text{-}water} = (\delta^{18}O_{cell} + 1000) / (\delta^{18}O_{water} + 1000)$ and $\alpha_{OM\text{-}water} = (\delta^{18}O_{OM} + 1000) / (\delta^{18}O_{water} + 1000)$.

3.4. Results and discussion

3.4.1. Correlation of aquatic mosses and host-water $\delta^{18}O$ values

OM from modern aquatic mosses collected in southern Patagonia span a range of $\delta^{18}O$ values between 15.1‰ and 24.9‰ (Table 3.1). $\delta^{18}O$ values of the respective host-waters vary between -14.3‰ and -3.8‰. This reveals a strong linear correlation between $\delta^{18}O$ values of moss OM and host-waters explaining 99.5% ($R^2 = 0.995$, $n = 7$) of their variance (Fig. 3.4). The linear regression is given as

$$\delta^{18}O_{OM} = 0.861\ (\pm 0.027)\ \delta^{18}O_{host\text{-}water} + 27.8\ (\pm\ 0.3)‰ \qquad (3.1)$$

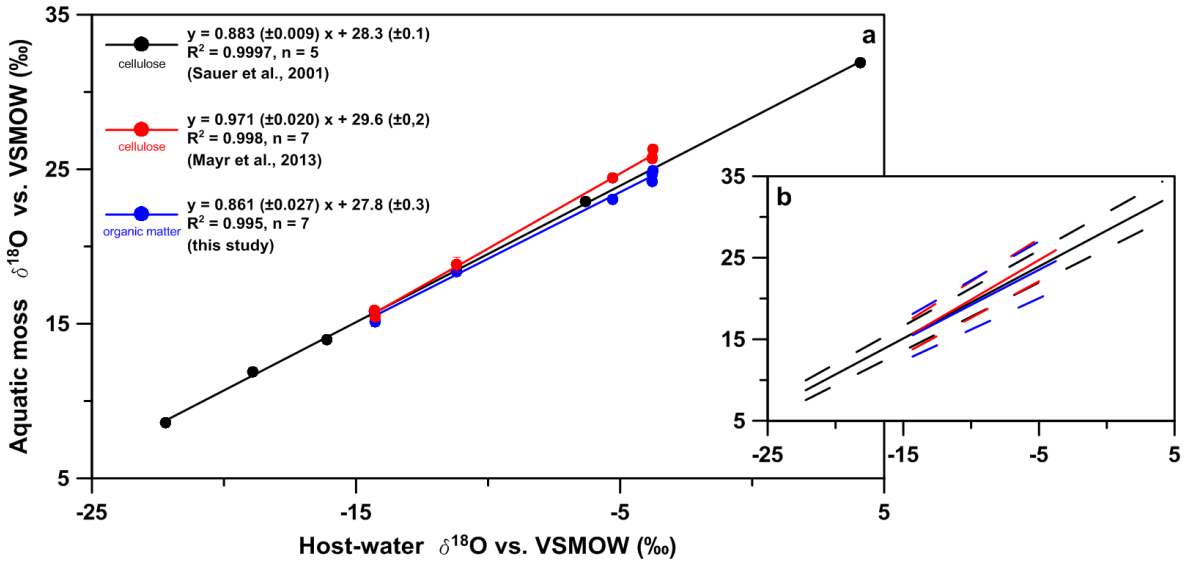


Figure 3.4. a) Correlation between $\delta^{18}O$ values of aquatic moss organic matter and host waters from Southern Patagonia (this study; blue) compared with correlation between cellulose of cultured aquatic mosses and aquarium waters (Sauer et al., 2001; black) and between aquatic moss cellulose and host waters from Southern Patagonia (Mayr et al., 2013; red). Regression equations and coefficient of determination (R^2) are shown for each regression line. Note that two aliquots of one sample from Laguna Potrok Aike used in Mayr et al. (2013) were re-analyzed and the linear regression was re-calculated (cf. Table 3.1). Locations of sites are given in Table 3.1. **b)** Regression lines with dashed lines representing 99% confidence intervals in the same colors used in a).

with $\delta^{18}O$ values of moss OM ($\delta^{18}O_{OM}$) and $\delta^{18}O$ values of host-water ($\delta^{18}O_{host\text{-}water}$). This relation is as significant as the correlation between $\delta^{18}O$ values of aquatic moss cellulose ($\delta^{18}O_{cell}$) and host waters (R^2 = 0.998, n = 7) for the same sample set (Table 3.1) reported by Mayr et al. (2013) with the linear regression

$$\delta^{18}O_{cell} = 0.971\ (\pm 0.020)\ \delta^{18}O_{host\text{-}water} + 29.6\ (\pm\ 0.2)‰. \quad (3.2)$$

The uncertainty of the calibration (standard error of the regression) is slightly larger for OM vs. host-water (±0.3‰) than for cellulose vs. host-water (±0.2‰). However, the degree of explained variance is similar for both regressions. The intercept of the OM regression is about 1.8‰ lower, which can be explained by the stronger oxygen isotopic enrichment of cellulose compared to other plant organic compounds (Schmidt et al., 2001).

A calibration between aquarium water and aquatic moss cellulose cultured under controlled conditions in the laboratory performed by Sauer et al. (2001) resulted in a linear regression of

$$\delta^{18}O_{cell} = 0.883\ (\pm 0.009)\ \delta^{18}O_{aquarium\ water} + 28.3\ (\pm\ 0.1) \quad (3.3)$$

with 99.97% of explained variance (R^2 = 0.9997, n = 5) and a standard error of the regression of ±0.1‰.

Moreover, for a compilation of data from various field studies Cooper and DeNiro (1989) reported a relationship between cellulose of submerged aquatic plants and ambient water defined by the regression

$$\delta^{18}O_{cell} = 0.78\ (\pm 0.04)\ \delta^{18}O_{ambient\ water} + 26.2 \quad (3.4)$$

explaining about 88% of common variance (R^2 = 0.88, n = 56).

The host-water relationship of aquatic moss cellulose $\delta^{18}O$ values determined in laboratory experiments has intermediate values compared with host-water field calibrations for aquatic moss cellulose and aquatic moss OM (Fig. 3.4), while an early field calibration has lower slope and intercept values (Cooper and DeNiro, 1989). With respect to uncertainty margins, the calibration equation determined under laboratory conditions obviously performs best while the field calibration of aquatic moss OM shows the largest error of estimation. However, this observation is not unexpected since field samples are inherently less well defined, e.g. regarding temporal integration of the sample value. Also, additional influences can impact on their isotopic composition compared to controlled laboratory conditions.

For submerged aquatic plants current models of oxygen isotope fractionation suggest a nearly constant enrichment factor of 27‰ for $\delta^{18}O$ values of cellulose relative to host water (Epstein et al., 1977; DeNiro and Epstein, 1981; Cooper and DeNiro, 1989; Sternberg, 2009). In the absence of evapotranspiration, the $\delta^{18}O$ signature of ambient water during primary carbohydrate synthesis (sucrose) and cellulose synthesis, where post-photosynthetic isotopic exchange between oxygen in carbohydrates and stem water occurs, is almost the same (Sternberg, 2009). Thus, the $\delta^{18}O$ values of cellulose versus those of lake water are expected to plot on a line with slope of 1 for submerged aquatic mosses (Sauer et al., 2001). This relationship holds true provided that (i) biochemical oxygen isotope fractionation is constant and independent of temperature (DeNiro and Epstein, 1981) and (ii) cellulose synthesis does not involve storage tissue formed under deviant ambient water oxygen isotopic composition (Cooper and DeNiro, 1989). Condition (i) has recently been challenged by Sternberg and Ellsworth (2011) who propose a temperature effect on cellulose oxygen isotopic enrichment relative to source water especially at temperatures below 20 °C. This is contrary to DeNiro and Epstein (1981) who found no temperature effect on the oxygen isotopic fractionation between cellulose and water. In the modern calibration data set there is also no apparent effect of host-water temperature on $\alpha_{cell\text{-}water}$ (Mayr et al., 2013). For submerged aquatic mosses growing in non-stratified lakes, like Laguna Potrok Aike, condition (ii) would apply as stored carbohydrates will always have $\delta^{18}O$ values related to lake water values varying in a narrow amplitude (Mayr et al., 2007) and as the relative contribution of storage tissue to total annual biomass/cellulose formation can be considered insignificant for mosses (Glime, 2007; Goffinet et al., 2008).

Despite these considerations, neither the well-controlled laboratory study (Sauer et al., 2001) nor the field studies (Cooper and DeNiro, 1989; Mayr et al., 2013) could find a one-to-one relationship between $\delta^{18}O$ values of moss cellulose and host-water (Table 3.3). Even if Mayr et al. (2013) found a slope of almost one, representing a constant biogeochemical oxygen isotope fractionation factor and a constant oxygen exchange rate with ambient water during cellulose synthesis, the difference to the laboratory study of Sauer et al. (2001) needs to be explained. A further evaluation of this issue, however, remains difficult because the reasons for such diverging observations could be related to the different methods for cellulose extraction (CUAM extraction vs. traditional cellulose extraction technique) as well as analytical techniques (off-line pyrolysis vs. high temperature pyrolysis) used in the two studies. Different cellulose extraction techniques may indeed yield cellulose fractions of varying ‘purity’, e.g. by

incomplete removal of hemicellulose and consequentially lead to biased $\delta^{18}O$ values of cellulose (Wissel et al., 2008). Various slopes of the relationship within experiments using the same plant species have also been assigned to the different analytical techniques applied (Sternberg et al., 2006). As shown by Boettger et al. (2007) and Chapligin et al. (2011) another source for considerable deviations in reported results for the analyses of $\delta^{18}O$ ratios of organic/biogenic material is the use of different and not inter-compared calibration and reference standards. Therefore, a detailed discussion of oxygen isotope fractionation between aquatic moss cellulose and host water should be postponed until more data derived under comparable analytical conditions are available including rigorous calibration with common standards and calibration techniques. Certainly, more experiments on the effect of temperature on oxygen isotope fractionation of aquatic moss cellulose are needed.

Table 3.3. Linear regression parameters between $\delta^{18}O$ of cellulose and host waters from the studies discussed in section 3.4.1.

	This study	Mayr et al. (2013)*	Sauer et al. (2001)	Cooper and DeNiro (1989)
Material	Aquatic moss organic matter from field samples	Aquatic moss cellulose from field samples	Aquatic moss cellulose from cultured samples	Aquatic plant cellulose from field samples
n	7	7	5	56
Slope	0.861±0.027	0.971±0.020	0.883±0.009	0.78±0.04
Intercept	27.8±0.3	29.6±0.2	28.3±0.1	26.2
R^2	0.995	0.998	0.9997	0.88
P	< 0.001	< 0.001	< 0.001	< 0.001

* We newly analyzed two aliquots of one sample from Laguna Potrok Aike used in Mayr et al. (2013) and the linear regression parameters have been re-calculated accordingly. The differences in the parameters of the regression are minor.

The data for moss OM and those presented by Mayr et al. (2013) for moss cellulose can be directly compared because they were gained under identical analytical conditions. Compared to the slope of the cellulose-water relation of 0.971, a lower slope of 0.861 is observed in the present study for the relation between $\delta^{18}O$ of moss OM and host-water from the same sample set (Table 3.1 and 3.3). Accordingly, the fractionation factor (α) is apparently constant for cellulose within the analytical uncertainty with a mean value of $\alpha_{cell\text{-}water} = 1.0301$. This is different for OM, which has a smaller mean value of $\alpha_{OM\text{-}water} = 1.0292$ but varies between 1.0281 and 1.0305. Reasons for the different slopes and the variable fractionation factor (α) for OM are not yet fully understood, but can probably be attributed to the mixture of organic compounds with different (lower) oxygen isotope signatures than coexisting cellulose in total moss OM (Schmidt et al., 2001). The data also imply a dependence of the observed ^{18}O enrichment between OM and water on the growth habitat, because samples from hydrologically

open habitats (spring/brook/lake) reveal somewhat lower enrichment compared to closed lakes (Table 3.1). This could be an effect of different moss species and their biochemical composition, but an extended data set from lacustrine habitats is clearly necessary to further resolve this issue. Such a data set would further refine the host-water relationship of $\delta^{18}O$ values of aquatic moss OM, but is not expected to lead to fundamentally different conclusions.

We will use the direct field calibrations (Eqs. (3.1) and (3.2)) determined under identical laboratory and analytical conditions for our further considerations. The significance of both calibrations allows an estimation of past lake-water $\delta^{18}O$ values ($\delta^{18}O_{lw}$) which can thus be inferred from $\delta^{18}O$ values of moss OM and cellulose using the equations:

$$\delta^{18}O_{lw} = 1.156\ (\pm 0.036)\ \delta^{18}O_{OM} - 32.2\ (\pm 0.8); \qquad (R^2 = 0.995,\ n = 7) \qquad (3.5)$$

$$\delta^{18}O_{lw} = 1.028\ (\pm 0.021)\ \delta^{18}O_{cell} - 30.4\ (\pm 0.5). \qquad (R^2 = 0.998,\ n = 7) \qquad (3.6)$$

The uncertainty of the prediction (standard error of the regression) is ±0.4‰ for Eq. (3.5) and ±0.3‰ for Eq. (3.6), respectively. Although the uncertainty of the prediction is larger than the uncertainty of the calibration, the inference is valid within these limitations.

Certainly, such a reconstruction of past lake water $\delta^{18}O$ values postulates that the principle of actualism is applicable, that post-depositional effects on the oxygen isotope composition of moss OM are negligible and that admixture of OM from other sources with different isotope signatures is avoided.

3.4.2. Isotope composition of cellulose and organic matter of aquatic moss

The $\delta^{18}O$ and $\delta^{13}C$ values of cellulose from modern aquatic mosses from a variety of sites are slightly enriched compared to those of moss OM (Table 3.1). The mean isotopic offset in $\delta^{18}O$ is 0.9‰ and in $\delta^{13}C$ 1.1‰, respectively. For modern and subfossil moss fragments from Laguna Potrok Aike, similar isotopic offsets between cellulose and OM are also observed in the range between from 0.9 to 2.0‰ for both $\delta^{18}O$ and $\delta^{13}C$ (Table 3.2 and 3.4). The relation of $\delta^{18}O$ and $\delta^{13}C$ values, respectively, of moss cellulose versus moss OM from both modern and subfossil samples is described by a highly significant positive correlation (Fig. 3.5a and b). According to Turetsky et al. (2008), the bulk organic matter of peat mosses consists mainly of biochemical components like soluble non-polars (fats, oils and waxes), hot water-soluble carbohydrates, water-soluble phenolics, acid-insoluble material (mixture of tannins and

lignins), hemicellulose and cellulose. Other than lignin, polyphenols have also been suggested for the composition of cell wall material of mosses (Erickson and Miksche, 1974). $\delta^{18}O$ values of organic compounds in plants vary due to the different origin of oxygen atoms and biosynthetic reactions affecting isotopic effects. Higher $\delta^{18}O$ values are usually found in cellulose than in other organic compounds (Schmidt et al., 2001) accounting for the higher $\delta^{18}O$ values of moss cellulose compared to those of moss OM. Similarly, because cellulose is ^{13}C-enriched compared to other biochemical components of plants (Benner et al., 1987), moss cellulose is expected to be enriched in ^{13}C in comparison to moss OM.

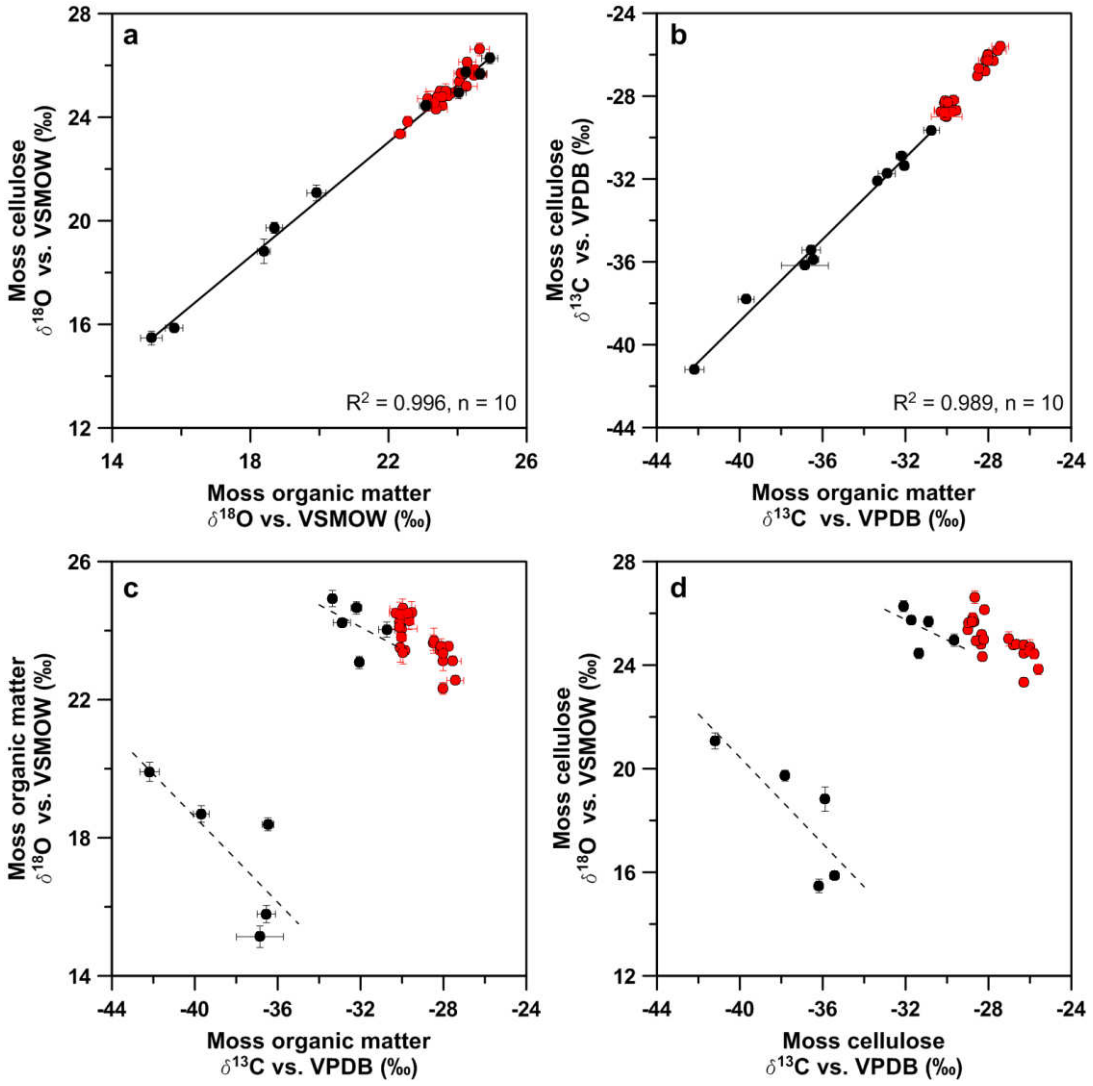


Figure 3.5. Relationship between **a)** $\delta^{18}O$ values and **b)** $\delta^{13}C$ values of organic matter and cellulose from modern aquatic moss samples (black circles) collected from different sites in South Patagonia and Germany and the respective $\delta^{18}O$ - $\delta^{13}C$ relations of **c)** organic matter and **d)** cellulose (standard deviations in bars). Dashed lines in c) and d) indicate directions of regression lines for two subgroups of data (cf. text and Table 3.1 for further details). Cellulose $\delta^{18}O$ data from modern aquatic moss samples are from Mayr et al. (2013). In comparison, data of cellulose and organic matter from subfossil branches of *Drepanocladus perplicatus* from Late Glacial sediment samples of Laguna Potrok Aike (red circles) are also shown (standard deviations in bars).

Table 3.4. C/O and isotope ratios as well as inferred lake water $\delta^{18}O$ values ($\delta^{18}O_{lw}$) from organic matter and cellulose of subfossil moss branches and cellulose of residue fraction (>200 µm) sieved from Late Glacial sediment samples of Laguna Potrok Aike. For moss cellulose, organic matter amount for cellulose extraction and yield are also given.

		Moss organic matter (OM)				Moss cellulose						Residue (>200 µm) cellulose			
Sample ID	Composite depth (m)	C/O	$\delta^{13}C$ (‰)	$\delta^{18}O$ (‰)	$\delta^{18}O_{lw}$ (‰)	OM amount (mg)	Yield (%)	C/O	$\delta^{13}C$ (‰)	$\delta^{18}O$ (‰)	$\delta^{18}O_{lw}$ (‰)	C/O	$\delta^{13}C$ (‰)	$\delta^{18}O$ (‰)	$\delta^{18}O_{lw}$ (‰)
743	15.05	1.13	-27.7	23.6	-5.0	23.6	18.8	0.87	-26.3	24.4	-5.3	0.87	-25.0	25.2	-4.5
758	15.35	1.11	-30.0	24.1	-4.4	3.1	7.9	0.87	-29.0	25.4	-4.4	0.88	-27.2	25.7	-4.0
763	15.45	1.17	-30.0	24.6	-3.7	4.6	12.6	0.88	-28.7	26.6	-3.1	0.92	-26.8	26.4	-3.2
770	15.59	1.16	-29.8	23.4	-5.1	6.2	8.3	0.90	-28.4	24.8	-4.9	0.90	-26.3	24.9	-4.8
772	15.63	1.15	-30.1	24.3	-4.2	7.6	12.6	0.88	-28.3	25.2	-4.5	0.90	-27.1	25.3	-4.5
774	15.67	1.15	-30.0	23.8	-4.7	5.5	9.0	0.92	-28.6	24.9	-4.8	0.88	-27.2	25.3	-4.5
776	15.71	1.16	-30.1	23.5	-5.0	4.9	7.8	0.89	-28.2	25.0	-4.7	0.89	-26.6	25.5	-4.2
780	15.77	1.13	-29.5	24.5	-3.9	9.2	10.6	0.87	-28.7	25.7	-4.0	0.89	-27.3	25.7	-4.0
782	15.81	1.10	-29.7	24.3	-4.1	44.1	19.1	0.87	-28.2	26.1	-3.6	0.88	-27.1	26.0	-3.7
785	15.86	1.12	-30.3	24.5	-3.9	17.9	9.9	0.85	-28.8	25.7	-4.1	0.90	-28.3	26.0	-3.7
787	15.89	1.08	-30.1	24.5	-3.9	41.8	20.8	0.88	-29.0	25.6	-4.1	0.89	-28.6	26.0	-3.7
790	15.95	1.25	-29.7	24.5	-3.9	22.2	16.2	0.88	-28.8	25.8	-3.9	0.89	-27.2	25.9	-3.8
797	16.09	1.18	-30.1	24.1	-4.3	4.6	9.2	0.91	-28.8	25.7	-4.0	0.88	-26.8	25.5	-4.2
812	16.38	1.17	-30.0	23.4	-5.2	27.1	18.1	0.92	-28.3	24.3	-5.4	0.88	-28.7	24.4	-5.4
907	18.26	1.11	-28.2	23.4	-5.1	54.0	22.0	0.88	-26.8	24.8	-5.0	0.91	-26.2	24.9	-4.8
909	18.30	1.19	-28.5	23.7	-4.9	8.0	11.9	0.89	-27.0	25.0	-4.7	0.90	-25.4	25.1	-4.6
911	18.34	1.26	-28.5	23.7	-4.8	8.4	8.2	0.88	-26.7	24.8	-4.9	0.91	-25.5	24.7	-5.0
913	18.38	1.14	-28.1	23.6	-5.0	18.4	20.2	0.88	-26.3	24.8	-4.9	0.88	-25.9	24.8	-4.9
915	18.42	1.15	-28.0	23.1	-5.5	66.5	23.2	0.89	-26.0	24.7	-5.0	0.88	-25.8	24.8	-5.0
917	18.45	1.17	-28.0	23.3	-5.2	4.4	11.5	0.86	-26.0	24.5	-5.2	0.90	-25.5	24.5	-5.3
919	18.49	1.16	-27.6	23.1	-5.5	57.4	21.2	0.91	-25.8	24.4	-5.3	0.89	-25.9	24.4	-5.3
921	18.53	1.20	-27.4	22.6	-6.1	47.6	24.3	0.89	-25.6	23.8	-5.9	0.88	-25.5	23.8	-6.0
929	18.69	1.18	-28.0	22.3	-6.4	13.6	16.1	0.89	-26.3	23.3	-6.4	0.90	-25.3	23.7	-6.0
mean		**1.16**	**-29.1**	**23.7**	**-4.8**	**21.8**	**14.8**	**0.88**	**-27.6**	**25.0**	**-4.7**	**0.89**	**-26.6**	**25.2**	**-4.6**

The scatter plot of $\delta^{18}O$ versus $\delta^{13}C$ values reveals two groups of scattered data for modern aquatic moss samples (Fig. 3.5c and d). The cause for this pattern remains unexplained due to the restricted sample set. However, the upper right 'enriched' cluster is formed by samples from comparably closed lakes, i.e. Laguna Potrok Aike and Laguna Cháltel (sample 'PAIS-175'), whereas the samples scattering in the lower left stem from hydrologically open environments (inflows of lakes, spring as well as brooks, cf. Table 3.1). Within the two clusters negative relations between $\delta^{13}C$ and $\delta^{18}O$ are indicated (dashed lines). Data points of moss OM and moss cellulose from subfossil samples of Laguna Potrok Aike fall into the enriched clusters (Fig. 3.5c and d) and, thus, match with their modern counterpart.

3.4.3. Isotope composition of aquatic moss and aquatic vascular plant

In addition to aquatic mosses, remains of aquatic vascular plants also occur in the residue fraction of Laguna Potrok Aike sediments and may lead to contaminations of the cellulose extracted from the residue fraction. Our modern and subfossil samples from Laguna Potrok Aike show a clear distinction between aquatic vascular plants and aquatic mosses by their $\delta^{13}C$ values (Δ: ~20 ‰), both for OM and cellulose (Fig. 3.6a; Mayr et al., 2009). Submerged aquatic mosses entirely rely on dissolved CO_2 in water and may utilize amounts of respired CO_2 depleted in ^{13}C (Bain and Proctor, 1980; Osmond et al., 1981; Price et al., 1997), while some aquatic vascular plants are capable to assimilate also bicarbonate (HCO_3^-) which has about 9‰ higher $\delta^{13}C$ values compared to dissolved CO_2 (Keeley and Sandquist, 1992). The reason for the predominance of bicarbonate-using aquatic macrophytes in Laguna Potrok Aike is the relatively high pH of its water (8.7 - 9.0) which favors bicarbonate as predominant dissolved inorganic carbon species (Mayr et al., 2009). In contrast to the carbon isotope ratios, the $\delta^{18}O$ values of modern aquatic vascular plants and aquatic mosses are comparably similar (Fig 6a; Table 3.2) testifying their common lacustrine origin. Nevertheless, for cellulose extracted from modern samples a slight enrichment in ^{18}O of ca. 0.9‰ is observed for aquatic vascular plants (mean 26.6‰, n = 7; Table 3.2) compared to aquatic mosses (mean 25.7‰, n = 7; Table 3.2). The $\delta^{18}O_{OM}$ of fresh material is overall ^{18}O-depleted compared to $\delta^{18}O_{cell}$ by a mean of ca. 2.7‰ for aquatic vascular plants and by a mean of ca. 1.3‰ for aquatic mosses (Table 3.2). In addition, relative to tissues sampled alive a clear ^{18}O-depletion of ca. 4‰ in $\delta^{18}O_{OM}$ of dead remains of modern aquatic vascular plants collected on the lake shore indicates a preferential loss of ^{18}O-enriched organic compounds during initial decomposition. Such large ^{18}O-depletion has also been observed for OM from aquatic vascular plants in subfossil samples (Fig. 3.6a; Table 3.5). A less clear indication for such an early loss of enriched compounds may also be drawn from the ca. 2‰ ^{13}C-depletion of dead remains compared to their living counterparts. These data indicate that contaminations of sedimentary moss fractions with aquatic vascular plant debris will only cause a relatively insignificant bias with regard to $\delta^{18}O_{cell}$, whereas the bias can be remarkable for $\delta^{18}O_{OM}$. In any case, the $\delta^{13}C$ values should be an indicator of contamination because of supposedly large $\delta^{13}C$ offset between vascular plants and mosses in alkaline lakes such as Laguna Potrok Aike.

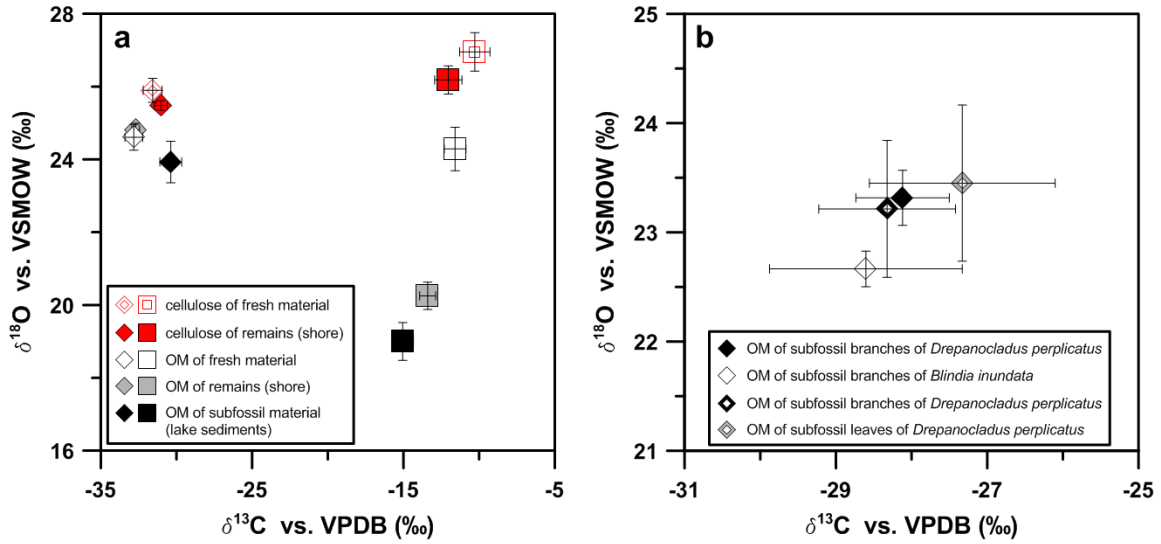


Figure 3.6. a) Comparison of mean $\delta^{18}O$ and $\delta^{13}C$ values of cellulose and organic matter (OM) of aquatic vascular plants (squares) and aquatic mosses (diamonds) from modern and subfossil samples (standard deviation in bars) from Laguna Potrok Aike. **b)** Comparison of mean $\delta^{18}O$ and $\delta^{13}C$ values of moss organic matter for two aquatic moss species and for branches and leaves of *Drepanocladus perplicatus* from sediment core samples (standard deviation in bars). Comparison is in pairs. Detailed data can be found in Table 2 and 5. Note differences in axis scales between a) and b).

3.4.4. Species- and tissue-specific offsets

Independent of possible contamination with aquatic vascular plant debris, certain heterogeneity could be inherent in the isotope composition of different species and parts of aquatic mosses, as reported by previous studies on peat bog plants and *Sphagnum* (e.g. Ménot-Combes et al., 2002; Loader et al., 2007; Moschen et al., 2009). A slight difference in the isotope composition of different moss species is indicated by a comparison of $\delta^{18}O$ and $\delta^{13}C$ values of branches of *D. perplicatus* and *B. inundata* selected from subfossil samples (Fig. 3.6b). Branch OM of *B. inundata* is consistently depleted in $\delta^{18}O$ relative to that of *D. perplicatus* (mean 0.7‰, $n = 10$), whereas for $\delta^{13}C$ the pattern is somewhat ambiguous resulting in a mean depletion of 0.5‰ (Table 3.5). The cause of ^{18}O and ^{13}C enrichment of *D. perplicatus* compared to *B. inundata* remains open but could be affected by individual metabolisms of the different species. Applying Eq. (3.5) on the mean $\delta^{18}O_{OM}$ values of *D. perplicatus* and *B. inundata* would result in a difference of 0.8‰ for inferred lake water $\delta^{18}O$ values (100% of *D. perplicatus*: -5.2‰; 100% of *B. inundata*: -6.0‰). Beside a complete change in species predominance, a mixture of moss OM from both species has, accordingly, a much smaller impact on the inferred lake water $\delta^{18}O$ values (e.g. 50% of *D. perplicatus* and 50% of *B. inundata*: -5.6‰). The slight difference in $\delta^{18}O_{OM}$ between these two moss species indicates, however, an increase in the uncertainty of reconstructed lake water $\delta^{18}O$ values using OM from mixed samples and recommends, where

possible, analysis of $\delta^{18}O_{OM}$ on monospecific aquatic moss samples for paleoclimate studies. Although the $\delta^{18}O_{cell}$ of *B. inundata* has not been measured in parallel to *D. perplicatus* due to restricted availability of material, it can be postulated that their $\delta^{18}O_{cell}$ values should be similar. Even between different submerged plant groups (aquatic vascular and nonvascular plants), probably having different biosynthetic pathways leading to cellulose synthesis, there is only a slight difference of about 1‰ in $\delta^{18}O_{cell}$ (Table 3.2).

Table 3.5. $\delta^{13}C$ and $\delta^{18}O$ values of subfossil plant organic matter of samples from sediment cores taken in Laguna Potrok Aike. *B. inundata* for *Blindia inundata* and *D. perplicatus* for *Drepanocladus perplicatus*.

		Subfossil plant organic matter							
		D. perplicatus (branches)		*D. perplicatus* (leaves)		*B. inundata* (branches)		aquatic vascular plant	
Sample ID	Composite depth (m)	$\delta^{13}C$ (‰)	$\delta^{18}O$ (‰)	$\delta^{13}C$ (‰)	$\delta^{18}O$ (‰)	$\delta^{13}C$ (‰)	$\delta^{18}O$ (‰)	$\delta^{13}C$ (‰)	$\delta^{18}O$ (‰)
790	15.95	-29.6	24.5	-28.7	24.9	_	_	_	_
888	17.90	-28.5	23.8	-27.4	23.9	_	_	_	_
908	18.28	-28.4	23.1	-27.1	23.4	_	_	_	_
916	18.43	-27.1	23.3	-26.6	23.6	_	_	_	_
918	18.47	-27.6	23.0	-27.2	23.1	_	_	_	_
921	18.53	-27.5	22.6	-26.4	22.9	_	_	_	_
929	18.69	-28.0	22.3	-25.7	22.0	_	_	_	_
1166	23.25	-28.6	22.9	-27.9	23.7	_	_	_	_
1200	23.90	-28.3	22.8	-28.6	23.7	_	_	_	_
1309	26.07	-27.9	23.2	-25.7	23.0	_	_	_	_
1481	29.58	-30.1	23.8	-29.4	23.7	_	_	_	_
mean		**-28.3**	**23.2**	**-27.3**	**23.5**	_	_	_	_
1319	26.27	-28.4	23.0	_	_	-29.5	22.7	_	_
1323	26.35	-27.3	23.5	_	_	-27.6	22.5	_	_
1325	26.39	-27.2	23.2	_	_	-28.9	22.8	_	_
1330	26.49	-27.6	23.2	_	_	-25.5	22.4	_	_
1331	26.51	-28.4	23.6	_	_	-29.1	22.8	_	_
1333	26.54	-28.1	23.5	_	_	-29.9	22.8	_	_
1334	26.56	-27.9	23.0	_	_	-29.6	22.9	_	_
1349	26.86	-29.0	23.7	_	_	-28.2	22.7	_	_
1408	28.02	-28.7	23.5	_	_	-28.6	22.7	_	_
1454	29.05	-28.7	23.0	_	_	-29.1	22.4	_	_
mean		**-28.1**	**23.3**	_	_	**-28.6**	**22.7**	_	_
649	13.19	-30.5	24.6	_	_	_	_	-15.6	-
654	13.29	-30.1	23.6	_	_	_	_	-14.5	18.6
657	13.35	-31.7	24.5	_	_	_	_	-16.0	19.1
670	13.60	-29.7	23.9	_	_	_	_	-15.5	-
715	14.49	-30.3	23.1	_	_	_	_	-14.2	19.7
800	16.15	-29.9	23.9	_	_	_	_	-14.7	18.6
mean		**-30.4**	**23.9**					**-15.1**	**19.0**

Branches and leaves of subfossil *D. perplicatus* with mean $\delta^{18}O_{OM}$ values of 23.2‰ and 23.5‰, respectively, are indistinguishable in their oxygen isotope signature (Table 5; Fig. 3.6b). However, the paired comparison of these different tissues indicates a mean deviation of ca. 1‰ for $\delta^{13}C_{OM}$ values (-28.3‰ for branches and -27.3‰ for leaves, n = 11; Table 3.5). Because it is practically impossible to remove leaves from each fragment of branch or stem, the branch fraction contains also a varying amount of leaves. The offset in isotopic values between leaves and leafless branches could therefore be slightly larger than actually observed. Nevertheless, the difference between $\delta^{18}O_{OM}$ as well as estimated $\delta^{18}O_{cell}$ of branches and those of leaves of *D. perplicatus* must be marginal and negligible in terms of inferred lake water $\delta^{18}O$ values, because evaporative isotopic enrichment in leaves is absent for submerged aquatic mosses. The observed depletion in $\delta^{13}C_{OM}$ values of moss branches could be caused by the occurrence of ^{13}C-depleted lipids in these tissues (Park and Epstein, 1961; DeNiro and Epstein, 1977; Goffinet et al., 2008).

3.4.5. Post-depositional change of subfossil moss material

The amount of branches of *D. perplicatus* that was provided from sediment samples for cellulose extraction was highly variable between 3.1 and 66.5 mg (Fig. 3.7 and Table 3.4). This large range expresses the variability of moss burial rate within the sedimentary record which depends on the abundance of moss habitats in the lake, vicinity of these habitats to the coring location, sedimentation rate and redistribution processes by internal currents. The respective cellulose yields range from 7.8% to 24.3% with a mean of 14.8% (n = 23). The relationship between cellulose yield and amount of moss fragments used for cellulose extraction was fit by a logarithmic regression with 82.3% explained variance, where lowest yields were determined for samples providing raw material of <10 mg (Fig. 3.7). We account for this observation by unavoidable processing losses that increase when handling small amounts. This effect leads to an underestimation of yields for small samples. Cellulose yields for larger samples increased to 20% and more reaching values that have been reported for modern aquatic mosses from Laguna Potrok Aike (Wissel et al., 2008). In addition, influences of decomposition on cellulose yields cannot be fully excluded, though microscopic inspection of samples indicates that moss tissues are well preserved.

The C/O ratios of subfossil moss cellulose vary between 0.85 and 0.92 with a mean value of 0.88 (Table 3.4). This is consistent with the stoichiometrically expected C/O ratio of 0.90 for

cellulose and with a mean C/O ratio of 0.89 determined for modern aquatic mosses (Table 3.1). First of all, the C/O ratio is a reliable quality indicator for the cellulose extraction protocol and the purity of extracted cellulose (Wissel et al., 2008), but the absence of obvious deviations from the expected ratio could probably also be taken as an indication for good preservation conditions of moss tissues in the sediments. C/O ratios of residue cellulose (Table 3.4) are indistinguishable from those of moss cellulose and, thus, confirm the extraction of a pure cellulose fraction from this sieve fraction. As expected, C/O ratios of moss OM with a mean value of 1.16 are higher compared to pure cellulose due to the mixed biochemical composition of whole moss tissue (Table 3.4). Again, C/O ratios of moss OM from subfossil samples are similar to those of modern aquatic mosses with a mean value of 1.17 (Table 3.1).

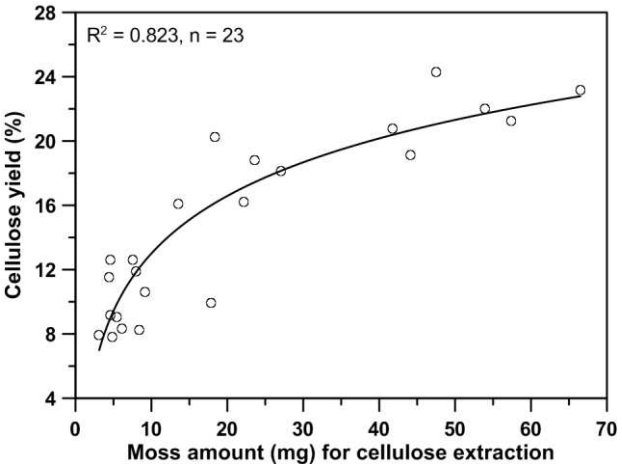


Figure 3.7. Relation between amount of moss fragments extracted and cellulose yield for subfossil aquatic moss material from Late Glacial sediment samples of Laguna Potrok Aike. Best fit is given by a logarithmic expression.

As shown in the section 3.4.2, the mean isotopic offsets between cellulose and OM of fresh ($\delta^{18}O$: 1.3‰, $\delta^{13}C$: 1.3‰, n = 3; Table 3.2) and subfossil aquatic moss samples ($\delta^{18}O$: 1.3‰, $\delta^{13}C$: 1.5‰, n = 23; Table 3.4) from Laguna Potrok Aike are very well comparable. Such isotopic offsets for subfossil samples are fairly constant and no obvious change along with sediment depth is observed (Table 3.4). The strong resemblance of oxygen and carbon isotopic characteristics between modern and subfossil aquatic moss samples also indicates a good preservation of the initial environmental isotopic signal and the absence of a remarkable post-depositional shift in the isotope composition of subfossil moss material.

3.5. Application for paleolimnological reconstruction

As shown in the section 3.4.1, $\delta^{18}O$ values of host waters can be well inferred from both purified aquatic moss OM and aquatic moss cellulose. A reliable stratigraphic study on lake water $\delta^{18}O$ values is, however, mainly determined by the validity of the modern calibration in the past, by the absence of post-depositional effects on the oxygen isotope composition of moss OM and, where possible, by monospecific analysis of moss OM.

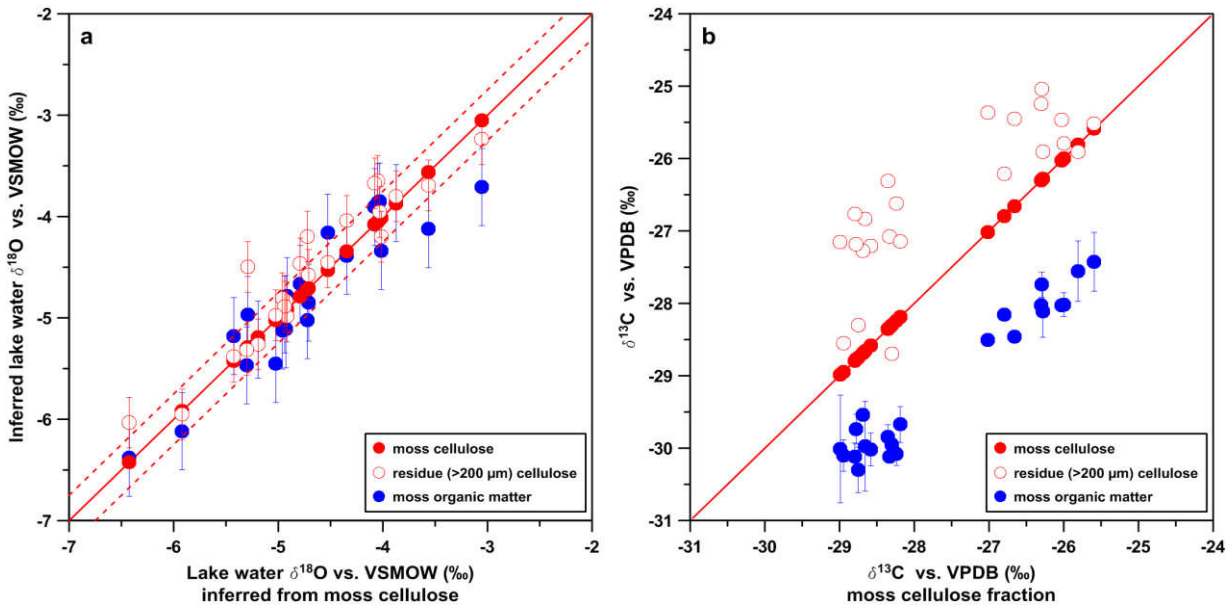


Figure 3.8. a) Lake water $\delta^{18}O$ inferred from moss cellulose, residue cellulose and moss organic matter in relation to moss cellulose inferred lake water $\delta^{18}O$ (cf. Table 3.4 for further details). One-to-one line of moss cellulose inferred lake water $\delta^{18}O$ (red line) and lower as well as upper limit of estimates (dashed lines) according to the standard error of regression for modern moss cellulose (±0.3‰). **b)** Respective representation of $\delta^{13}C$ of moss cellulose, residue cellulose and moss organic matter as potential quality indicator for inferred lake water $\delta^{18}O$ values. One-to-one line of moss cellulose (red line) given as reference. Note that moss cellulose is enriched by ca. 1.3‰ (mean) compared to moss organic matter. Standard deviations are given in bars in a) and b).

Through application of the rearranged calibration Eqs. (3.5) and (3.6), lake water $\delta^{18}O$ values were reconstructed from $\delta^{18}O$ values of moss OM and moss cellulose as well as from residue cellulose between 15 and 19 m composite depth from Laguna Potrok Aike sediments (Table 3.4). These three reconstructed lake water $\delta^{18}O$ records agree within their uncertainties (Fig. 3.8a). This shows that beside aquatic moss cellulose, also moss OM and cellulose from the bulk plant debris fraction (>200 µm) monitors past lake water oxygen isotope variations for Laguna Potrok Aike sediments. However, certain limitations exist that are indicated by $\delta^{13}C$ values of the respective fraction (Fig. 3.8b). Whereas the difference between $\delta^{13}C$ of moss OM and moss

cellulose is characterized by a comparably constant offset, the offset between residue cellulose and moss cellulose varies considerably (Fig. 3.8b). The enriched $\delta^{13}C$ values of residue cellulose compared to moss cellulose can be attributed to the occurrence of vascular plant remains in the residue fraction, that have been observed under the microscope. This certainly limits the application of the bulk coarse fraction without further quality assessment for other lakes.

In general, sediment samples with an adequate amount of moss fragments for cellulose extraction and subsequent isotope measurements can be expected to be much less frequent than samples enabling direct measurements of moss OM or the extraction of residue cellulose. To achieve a high-resolution stratigraphic record, results from different fractions like moss OM and residue cellulose should ideally be combined with moss cellulose data into a composite lake water $\delta^{18}O$ record. Therefore, in addition to quality control of laboratory and analytical techniques (C/O ratio, calibration), measures to control the quality of reconstructions (contamination) are needed. For this purpose, we suggest a straightforward approach by comparing the isotopic relations of moss OM and residue cellulose to moss cellulose with the one-to-one relationship of moss cellulose which is regarded as the 'reference' (Fig. 3.8a, b). Here, we used a limited set of samples (n = 23; Table 3.4) for which the fractions under consideration (cellulose and OM) can be investigated in pairs. In the present case, lake water $\delta^{18}O$ values inferred from moss OM and residue cellulose are located near the one-to-one moss cellulose line and with only a few exceptions within the uncertainty range of the modern moss cellulose to host-water regression (Fig. 3.8a). Larger differences between the fractions than those in $\delta^{18}O$ values are observed for $\delta^{13}C$ values (Fig. 3.8b). Beside the known offset in $\delta^{13}C$ between moss OM and cellulose, additional deviations are evident for several samples. One plausible explanation for these deviations would be the difference in $\delta^{13}C_{OM}$ from moss branches and leaves discussed in 4.3 (Fig. 3.5b; Table 3.4). A varying portion of these tissues within the samples can cause a scatter in the relation between $\delta^{13}C$ values of moss cellulose and moss OM. However, due to their similar $\delta^{18}O$ values this would not cause a considerable offset in $\delta^{18}O$. A clear deviation in $\delta^{18}O_{OM}$ from the one-to-one moss cellulose line observed in several samples (Fig. 3.8a) is more likely to be attributed to contamination with unidentifiable moss fragments which could have biased the $\delta^{18}O_{OM}$ values. Generally, the residue (coarse plant debris) fraction would be the most vulnerable to contamination which could contain remains of aquatic vascular plants and/or terrestrial plants together with moss fragments. Based on the modern samples from Laguna Potrok Aike (Table 3.2), a 5% contribution of aquatic vascular plant remains to the residue fraction would translate into 1‰ enrichment in $\delta^{13}C$

values of residue cellulose. The observed ca. 2‰ enrichment in $\delta^{13}C$ of residue cellulose compared to moss cellulose (Fig. 3.8b) consequently implies 10% contamination with vascular plant cellulose. However, this contamination translates into less than 0.2‰ enrichment in residue cellulose $\delta^{18}O$ values, which is still in the uncertainty range of the measurement of oxygen isotope ratios. Any larger deviations in $\delta^{18}O$ from the one-to-one moss cellulose line can thus be interpreted as potentially larger contamination that needs further inspection and probably leads to exclusion of these data from establishing a lake water $\delta^{18}O$ record.

3.6. Conclusions

This study aims to explore the potential of using isotope analysis of OM from submerged aquatic mosses for paleoenvironmental studies because analyses of OM (cellulose content ca. 15%) need much less material than those of cellulose. In our study OM samples are pretreated with a mixture of HCl and HF (10% respectively) to avoid contamination of the organic $\delta^{18}O$ signal with minerogenic oxygen. We have shown that a highly significant linear correlation exists between $\delta^{18}O$ values of purified OM from modern submerged aquatic mosses and their host-waters. The uncertainty of this calibration is comparable to that of the calibration using moss cellulose (uncertainty of ±0.3‰ versus ±0.2‰) based on the same calibration sample set from southern Patagonia. Both aquatic moss OM and aquatic moss cellulose can thus be used to infer past lake water $\delta^{18}O$ values, potentially in a paired approach to improve the temporal resolution in stratigraphic studies.

$\delta^{18}O_{cell}$ values of modern aquatic vascular plants and aquatic mosses from Laguna Potrok Aike indicate only a marginal difference (ca. 1‰) between fresh material and dead remains collected on the lake shore. $\delta^{18}O_{OM}$ values from fresh material of both aquatic plant types are also similar, whereas dead remains of aquatic vascular plants show depleted $\delta^{18}O_{OM}$ values (ca. 4‰) compared to aquatic moss remains. This indicates the limited impact of post-depositional diagenetic processes on the oxygen isotopic composition of moss OM. The large difference observed in the $\delta^{13}C$ of aquatic vascular plants and aquatic mosses is a good indicator for potential contamination of the investigated moss fraction with vascular plant remains in the investigated lacustrine systems.

Whereas $\delta^{13}C_{OM}$ values of subfossil remains from two investigated aquatic moss species are statistically indistinct, a slight offset (<1‰) in $\delta^{18}O_{OM}$ values between subfossil branches of *D. perplicatus* and *B. inundata* suggests that monospecific aquatic moss isotope analysis should be

preferred for the reconstruction of past lake water $\delta^{18}O$ values, where possible. Indistinguishable $\delta^{18}O_{OM}$ values between branches and leaves of submerged mosses imply that separation of different tissues is not necessary for isotope analysis.

Observed C/O ratios of cellulose extracted from subfossil moss fragments indicate the purity of extracted cellulose and well-preserved moss tissues in the sediments. The absence of a remarkable post-depositional shift in the isotope composition of subfossil moss OM has been confirmed by the strong resemblance of oxygen and carbon isotopic characteristics between modern and subfossil samples.

The investigation of subfossil material from sediment samples has demonstrated a consistent variation of lake water $\delta^{18}O$ values inferred from moss OM, moss cellulose and residue cellulose from Late Glacial sediments of Laguna Potrok Aike. This indicates the possibility for combining these fractions into a composite lake water $\delta^{18}O$ record to achieve a high-resolution reconstruction. However, the coarse plant-debris fraction is most prone to contamination with aquatic and terrestrial plant material. For the necessary assessment of the data quality of inferred lake water $\delta^{18}O$ values, we suggest a straightforward approach to compare the relations of moss OM and residue cellulose to moss cellulose with the one-to-one moss cellulose line which is regarded as the 'reference'. As $\delta^{13}C$ values serve as a reliable indicator of contamination with vascular plants in the investigated residue cellulose from the coarse plant debris fraction, any distinct deviations in inferred lake water $\delta^{18}O$ values from the one-to-one moss cellulose line can be interpreted as potentially high heterogeneity with unidentifiable moss fragments affecting the moss OM fraction.

Remains of submerged aquatic mosses can be a major component of the sediments from lakes at high latitudes. Although handpicking is time-consuming, the isotopic analysis of pure aquatic moss OM and aquatic moss cellulose can indeed provide a reliable tool to infer past lake water $\delta^{18}O$ values and to reconstruct the paleohydrology of lakes. The paired approach of moss OM and cellulose suggested here offers the potential to improve the temporal resolution of such paleorecords and to better assess the uncertainty inherent to the reconstruction. Our approach can be taken to other lakes worldwide taking into account that several issues, e.g. slope of calibration and temperature dependence of fractionation, need further attention and should be verified for each lake system individually.

Acknowledgement

We are indebted to J-P. Frahm and L. Hedenäs for moss identification. This research used samples provided by the International Continental Scientific Drilling Program (ICDP) in the framework of the Potrok Aike Maar Lake Sediment Archive Drilling Project (PASADO). Funding for drilling was provided by the ICDP, the German Science Foundation (DFG), the Swiss National Funds (SNF), the Natural Sciences and Engineering Research Council of Canada (NSERC), the Swedish Vetenskapsrådet (VR) and the University of Bremen, Germany. We acknowledge all scientists of the PASADO science team listed at http://www-icdp.icdp-online.org/front_content.php?idcat=1494. This study was also financed by grants of the DFG (LU786/7-1,2; MA4235/4-1,2) in the framework of the ICDP programme. J. Zhu is grateful to F. Lehmkuhl (RWTH Aachen University, Germany) for co-supervision of his PhD thesis. We kindly acknowledge valuable comments and suggestions from three anonymous reviewers and J. Middelburg that helped to improve the manuscript substantially.

Chapter 4

Climate history of the Southern Hemisphere Westerlies belt during the last glacial-interglacial transition revealed from lake water oxygen isotope reconstruction of Laguna Potrok Aike (52°S, Argentina)

Jiayun Zhu[1], Andreas Lücke[1], Holger Wissel[1], Christoph Mayr[2,3], Dirk Enters[4], Kyeong Ja Kim[5], Christian Ohlendorf [4], Frank Schäbitz[6], Bernd Zolitschka[4]

[1]Institute of Bio- and Geosciences, IBG-3: Agrosphere, Research Center Jülich, D-52428 Jülich, Germany

[2]Institute of Geography, University of Erlangen-Nürnberg, D-91054 Erlangen, Germany

[3]GeoBio-Center and Dept. of Earth and Environmental Sciences, University of Munich, D-80333 Munich, Germany

[4]GEOPOLAR, Institute of Geography, University of Bremen, D-28359 Bremen, Germany

[5]Korea Institute of Geoscience and Mineral Resources, 124 Gwahang-no, Yuseong-gu, Daejeon 305-350, Republic of Korea

[6]Seminar für Geographie und ihre Didaktik, University of Cologne, Gronewaldstr. 2, D-50931 Cologne, Germany

This chapter represents the manuscript published as:

Zhu J., Lücke A., Wissel H., Mayr C., Enters D., Kim K. J., Ohlendorf C., Schäbitz F. and Zolitschka B. (2014) Climate history of the Southern Hemisphere Westerlies belt during the last glacial-interglacial transition revealed from lake water oxygen isotope reconstruction of Laguna Potrok Aike (52° S, Argentina). *Climate of the Past Discussions* 10, 2417-2465, doi:10.5194/cpd-10-2417-2014.

Abstract

The Southern Hemisphere westerly winds (SHW) play a crucial role in the large-scale ocean circulation and global carbon cycling. Accordingly, the reconstruction of its latitudinal position and intensity is essential for understanding global climatic fluctuations during the last glacial cycle. The southernmost part of the South American continent is of great importance for paleoclimate studies as the only continental mass intersecting a large part of the SHW belt. However, continuous proxy records back to the last Glacial are rare in southern Patagonia, owing to the Patagonian Ice Sheets expanding from the Andean area and the scarcity of continuous paleoclimate archives in extra-Andean Patagonia. Here, we present an oxygen isotope record from cellulose and purified bulk organic matter of aquatic moss shoots from the last glacial-interglacial transition preserved in the sediments of Laguna Potrok Aike (52°S, 70°W), a deep maar lake located in semi-arid, extra-Andean Patagonia. The highly significant correlation between oxygen isotope values of aquatic mosses and their host waters and the abundant well-preserved moss remains allow a high-resolution oxygen isotope reconstruction of lake water ($\delta^{18}O_{lw}$) for this lake. Long-term $\delta^{18}O_{lw}$ variations are mainly determined by $\delta^{18}O$ changes of the source water of lake, surface air temperature and evaporative ^{18}O enrichment. Under permafrost conditions during the Glacial, the groundwater may not be recharged by regional precipitation. The isolated groundwater could have had much less negative $\delta^{18}O$ values than glacial precipitation. The less ^{18}O depleted source water and prolonged lake water residence time caused by reduced interchange between in- and outflows could have resulted in the reconstructed glacial $\delta^{18}O_{lw}$ that was only ca. 3‰ lower than modern values. The significant two-step rise in reconstructed $\delta^{18}O_{lw}$ during the last deglaciation demonstrated the response of isotope composition of lake water to fundamental climatic shifts. Rapid deglacial warming is supposed to cause the ^{18}O enrichment of lake water by ca. 2‰ during the first rise between 17,600 and 15,600 cal. BP by increasing temperature-induced evaporation and more ^{18}O enriched precipitation. After a millennial transition period of receding values by up to 0.7‰, the reconstructed $\delta^{18}O_{lw}$ resumed pronounced increase since 14,600 cal. BP. This cumulative enrichment in ^{18}O of lake water could be interpreted as a response to the strengthened wind-driven evaporation, implying the intensification and establishment of the SHW at the latitude of Laguna Potrok Aike (52°S). During the early Holocene the SHW exerted its full influence on the lake water balance, reflected by reconstructed $\delta^{18}O_{lw}$ approaching modern values, indicating a strongly evaporative steppe climate in the Laguna Potrok Aike region.

4.1. Introduction

Studying the climate evolution from the last Glacial towards the current Interglacial enables us to better understand the responses of the climate system to external and internal forcing without anthropogenic impacts. Paleoclimatic sites in southern South America (Patagonia) play an important role for paleoclimate reconstructions, as Patagonia is the only continental mass intersecting the core of the Southern Hemisphere Westerly winds (SHW). The SHW control large-scale ocean ventilation and carbon cycling and could have played a decisive role in driving the global deglacial warming during the last glacial termination (Toggweiler et al., 2006; Anderson et al., 2009; Denton et al., 2010; Mayr et al., 2013). However, reconstructing the position and intensity of the SHW during the last glacial-interglacial transition is limited, because the Andean area of southern Patagonia, where the most paleoclimate sites are located, was covered by the Patagonian Ice Sheets during the Last Glacial Maximum (LGM). The available continuous proxy records in the region south of 45°S are mostly restricted to the periods since the late Glacial and, especially, the Holocene (e.g. Ariztegui et al., 2010; Markgraf and Huber, 2010; Moreno et al., 2010; Moreno et al., 2012; Kilian and Lamy, 2012). The scarcity of long and continuous terrestrial records in these southern latitudes leaves a gap for linking Antarctic ice cores with low southern latitude and Northern Hemispheric records.

A key location to bridge this gap is Laguna Potrok Aike, a deep maar lake located in southern extra-Andean Patagonia (52°S, 70°W). The site was investigated within the framework of the interdisciplinary multiproxy ICDP project "Potrok Aike maar lake sediment archive drilling project" (PASADO) and provided a lake sediment record reaching back more than 50,000 years (Ohlendorf et al., 2011; Kliem et al., 2013b; Zolitschka et al., 2013). Palynological and geochemical studies based on the Laguna Potrok Aike sediments have shown the long-term environmental and climatic changes in southern Patagonia throughout the last glacial-interglacial cycle and shed light on the behavior of the SHW during this transition (e.g. Recasens et al., 2012; Hahn et al., 2013; Mayr et al., 2013; Zhu et al., 2013).

The reconstruction of the intensity of the SHW in southern Patagonia is usually based on the correlation between wind strength and precipitation amount (Kilian and Lamy, 2012). As revealed by Garreaud et al. (2013), the humid western side of the Andes exhibits a significantly positive correlation between precipitation and westerly wind strength, while the semi-arid eastern side of the Andes shows a distinct negative correlation. The significance of the relationship between precipitation and westerly wind intensity on the semi-arid leeward side of

the southern Andes is in fact not as strong as it is on the windward side (Wagner et al., 2007; Garreaud et al., 2013), likely as a consequence of overall low and variable precipitation.

However, the SHW affect water balances of lakes on the leeward side of the Andes not only through their linkage with precipitation amount, but also by evaporative enrichment, which is also controlled by wind intensity. Thus, the modern oxygen isotope composition of Laguna Potrok Aike's lake water ($\delta^{18}O_{lw}$) is mainly controlled by the $\delta^{18}O$ of regional precipitation and evaporative processes (Mayr et al., 2007; Mayr et al., 2013). The former is dependent on air temperature during rainfall events and $\delta^{18}O$ of precipitation of different moisture sources that are in turn associated with the strength of westerly winds. The $\delta^{18}O$ of precipitation brought by easterly winds from the Atlantic is considerably more enriched in ^{18}O than that from the Pacific over the southern Andes (Mayr et al., 2007). Evaporative processes in arid southeastern Patagonia are driven by insolation and westerly winds. Since the processes controlling Laguna Potrok Aike's $\delta^{18}O_{lw}$ are largely related to changes in SHW intensity, a sediment proxy allowing the reconstruction of past $\delta^{18}O_{lw}$ composition provides valuable insights into the SHW evolution at high southern latitudes.

Over recent decades, it has been widely recognized that the oxygen isotope composition of aquatic cellulose ($\delta^{18}O_{cell}$) is a reliable recorder of host water $\delta^{18}O$ values (e.g. Epstein et al., 1977; DeNiro and Epstein, 1981; Sternberg, 1989; Sternberg, 2009). Furthermore, results from laboratory (Sauer et al., 2001) and field studies (Mayr et al., 2013) demonstrate convincingly that $\delta^{18}O$ of cellulose extracted from submerged aquatic mosses are highly correlated to their host waters owing to the absence of uncertainties related to evapotranspiration. However, achieving a high-resolution $\delta^{18}O_{cell}$ record could be impeded, because oxygen isotope analysis of moss cellulose requires large quantities of moss remains for cellulose extraction. An approach to tackle this problem is the isotope analyses of purified bulk organic matter (OM) of preserved aquatic moss shoots, which needs much less material, and can potentially improve the temporal resolution of paleoclimatic reconstructions based on the moss cellulose alone without losing paleoclimatic information (Zhu et al., 2014).

In a previous study, $\delta^{18}O_{cell}$ values of aquatic moss debris were used to infer $\delta^{18}O_{lw}$ of Laguna Potrok Aike over the last deglaciation (Mayr et al., 2013). In the present study, we used handpicked subfossil shoots of a single aquatic moss species from sediment sections covering the last glacial-interglacial transition period to generate a composite record of the $\delta^{18}O_{lw}$ inferred from purified bulk moss OM and extracted cellulose fractions. The aims of the study are: 1) to present a high-resolution $\delta^{18}O_{lw}$ record of Laguna Potrok Aike for the period

containing large global climatic shifts by employing isotope proxies of aquatic mosses, 2) to highlight climatic changes on the southern South American continent during the last glacial-interglacial transition and 3) to evaluate the SHW impact on factors determining the $\delta^{18}O_{lw}$ of Laguna Potrok Aike.

4.2. Regional setting

The maar Laguna Potrok Aike is located on the southern side of the Río Gallegos valley in the Pali Aike Volcanic Field in southern Patagonia, Argentina (51°58' S, 70°23' W, 113 m a.s.l., Fig. 4.1a). The bedrock of the lake area is dominated by fine-grained molasse–type fluvial sediments (Lower Miocene Santa Cruz Formation) that are about 660 m thick in the investigated area (Zolitschka et al., 2006; Coronato et al., 2013). The nearly flat and broad surface is mainly overlain by degraded late Miocene and early Pleistocene basaltic lava flows and tablelands and early Pleistocene fluvioglacial deposits (Coronato et al., 2013). Glaciers of the last Glacial were restricted to the western Río Gallegos valley and to the southern Strait of Magellan and did not reach the Laguna Potrok Aike area (Coronato et al., 2013). The regional vegetation is a dry Magellanic steppe with grasses, dwarf-shrubs and bushes (Wille et al., 2007).

The near circular maar lake originates from a phreatomagmatic eruption with a $^{40}Ar/^{39}Ar$ age of 770 ± 240 ka BP (Zolitschka et al., 2006) and has a flat lake floor (Fig. 4.1b). Under present-day conditions, Laguna Potrok Aike is a phosphorous-rich and subsaline lake with a surface area of 7.58 km^2 and a maximum depth of 100 m (Zolitschka et al., 2006). The lake has only episodic inflows through gullies and canyons from a catchment area of about 200 km^2. According to isotope modeling calculations, about 60% of the water entering groundwater-fed Laguna Potrok Aike evaporates (Mayr et al., 2007). The water body circulates constantly under the prevailing strong west-wind conditions, which inhibits the development of summer stratification in the water column. Subaerial and submerged paleoshorelines indicate pronounced lake-level fluctuations resulting from past hydrological changes (Zolitschka et al., 2006; Haberzettl et al., 2008; Anselmetti et al., 2009; Gebhardt et al., 2012; Kliem et al., 2013a).

Dense aquatic vegetation predominantly formed by *Potamogeton pectinatus* and *Myriophyllum* cf. *quitense* covers the lake floor from a water depth of ca. 1.5 to 15 m (Wille et al., 2007). Aquatic mosses (*Drepanocladus perplicatus*) and *Ruppia* sp. were also observed in the littoral

zone during snorkeling explorations. A detailed survey of the recent limnic habitat has, however, so far not been conducted.

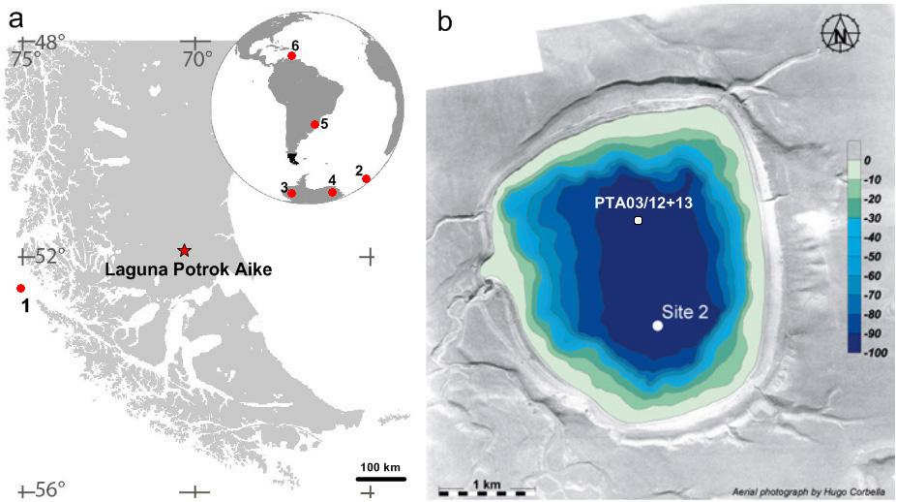


Figure 4.1. a) Location of Laguna Potrok Aike (red star) in southern Patagonia indicated as a black area on the inserted map. Location of sites presented in Fig. 10: 1, MD07-3128 at the Chilean offshore (Caniupán et al., 2011); 2, TN057-13-4PC in the Southern Atlantic (Anderson et al., 2009); 3, WDC in West Antarctica (WAIS Divide Project Members, 2013); 4, EDML of East Antarctica (EPICA Community Members, 2006); 5, Botuverá Cave in Southern Brazil (Wang et al., 2007); 6, Cariaco Basin (Deplazes et al., 2013). **b)** Sediment samples investigated in the present study derive from the drilling site 2 shown on the bathymetric map of Laguna Potrok Aike inserted into an aerial photography (provided by Hugo Corbella). At site 2, hydraulic piston cores were taken in 2008 within the framework of PASADO. The piston core PTA03/12+13 taken in 2003 has been used for the reconstruction of oxygen isotope composition of lake water in Mayr et al. (2013).

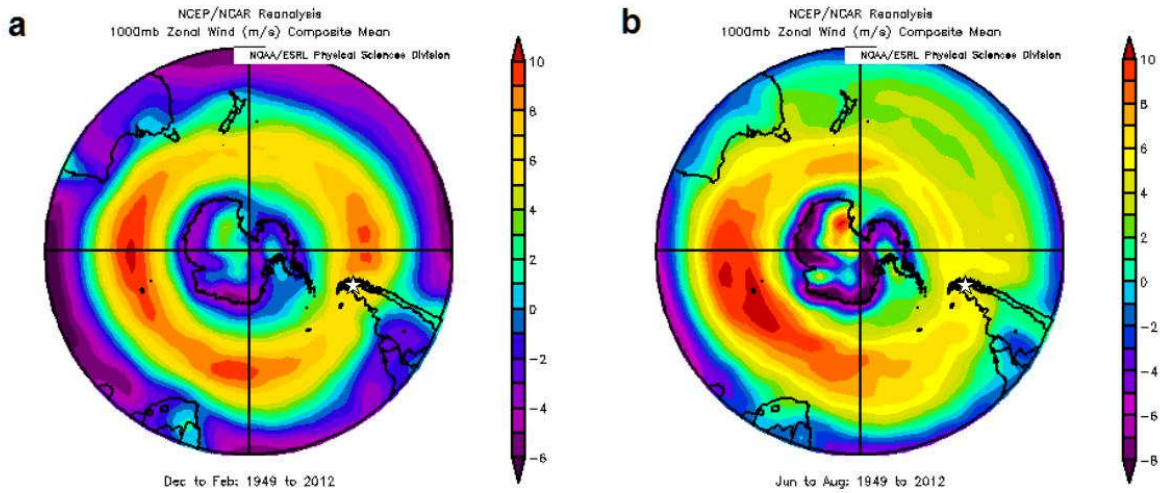


Figure 4.2. Mean near-surface (1000 mb) zonal wind (m/s) in Southern Hemisphere for **a)** austral summer and **b)** winter months based on NCEP/NCAR Reanalysis. Location of Laguna Potrok Aike is indicated as white stars. Data source: http://www.esrl.noaa.gov/psd/cgi-bin/data/composites/printpage.pl, accessed on 06 Feb. 2014.

Laguna Potrok Aike is located on the leeward side of the southern Andes and in the core of the modern SHW (Fig. 4.2). The regional cool and semi-arid climate is characterized by a low precipitation to evaporation ratio and predominant strong westerly wind reaching more than 10 m/s during austral summers (Garreaud et al., 2013; Ohlendorf et al., 2013). Annual precipitation on the leeward side of the southern Andes can be less than 200 mm owing to strong rain-shadow effects. An even seasonal distribution of precipitation in this region was attributed to the influence of relatively humid air masses from the Atlantic (Paruelo et al., 1998; Schneider et al., 2003; Garreaud et al., 2013). Mean annual precipitation at Laguna Potrok Aike is around 200 mm during the period from 2000 to 2011, being nearly 300 mm in wet years and only around 150 mm in dry years (Ohlendorf et al., 2013). By comparison, evaporation rates from the surface of the lake can be more than 1200 mm per year and show clear seasonal variations with high rates during austral summers and low rates during austral winters (Ohlendorf et al., 2013). This seasonal pattern results from seasonal variation of relative humidity with high values (up to 85%) during austral winters and low values (down to 30%) during austral summers (Ohlendorf et al., 2013). Proximity to the Antarctic continent and oceans causes cool summer and mild winter temperatures in southern Patagonia. Mean temperatures of austral summer (DJF) and winter (JJA) recorded at the local weather station at Laguna Potrok Aike are 13 °C and 2 °C, respectively, resulting in an annual mean temperature of 7.5 °C (Ohlendorf et al., 2013).

Whereas meteorological parameters such as wind speed, air temperature and relative humidity exhibit a clear seasonal variation pattern at Laguna Potrok Aike, $\delta^{18}O_{lw}$ values show relatively little inter-annual and intra-annual isotopic variations within a range between -3.4‰ and -3.9‰ and remain constant with increasing water depth, presumably due to groundwater recharge and strong wind-driven circulation in the whole water column (Mayr et al., 2007). $\delta^{18}O_{lw}$ values of lakes and ponds in the southern Patagonian steppe plot along a local evaporation line, regardless of depth, mixing, surface area and type, suggesting that isotope composition of the main source waters (precipitation and groundwater) are similar for all water bodies and evaporation is a main driver of the $\delta^{18}O_{lw}$ (Mayr et al., 2007).

Long-term isotopic data from the next GNIP (Global Network of Isotopes in Precipitation) station located on the leeward side of the southern Andes (south of 50°S) is available from Punta Arenas, located about 140 km southwest of Laguna Potrok Aike. For an observation period from 1990 to 2009, weighted monthly mean $\delta^{18}O$ values of precipitation at Punta Arenas

station are positively correlated with monthly mean air temperatures (R^2 = 0.89) and exhibit an isotopic range of about 5‰ (IAEA/WMO, 2014; Fig. 4.3).

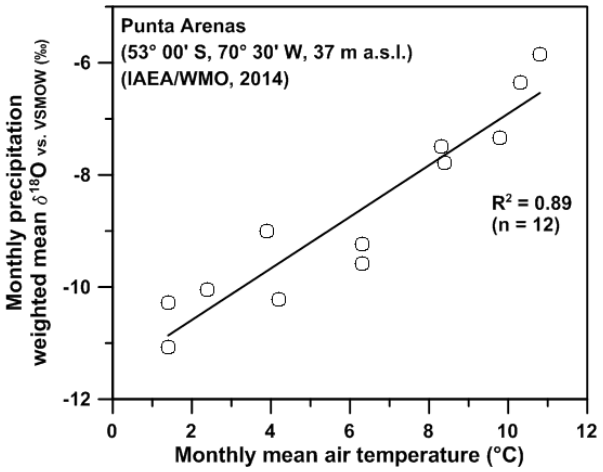


Figure 4.3. Relationship between monthly mean air temperature and weighted mean $\delta^{18}O$ of precipitation at GNIP station Punta Arenas (53° 00' S, 70° 30' W, 37 m a.s.l.) for the period from 1990 to 2009 (IAEA/WMO, 2014).

4.3. Material and methods

4.3.1. Material

In 2008 sediment cores were retrieved from two drilling sites in Laguna Potrok Aike within the framework of the PASADO project (Ohlendorf et al., 2011; Zolitschka et al., 2013; Fig. 4.1b). Sediment samples used in this study are from the composite profile 5022-2CP of site 2 which has a composite depth (cd) of 106 m, consisting of undisturbed pelagic sediments, volcanic tephra layers and mass movement sediments that resulted from lake internal sediment redistribution. The composite profile is divided into five lithological units based on the prevailing sedimentary structures and frequency of deposits of mass movement (Kliem et al., 2013b). Mass movement deposits and tephra layers were removed from the composite profile resulting in an event-corrected composite depth profile (cd-ec) of 45.8 m (Kliem et al., 2013b). The sediment section investigated in this study ranges between ca. 10 and 30 m (cd) or between 9.6 and 21.4 m (cd-ec) and consist of lithological unit B and C-1 (Fig. 3). Both unit B and C-1 mainly comprise pelagic laminated silts intercalated with thin fine sand and coarse silt layers originating from mass movement deposits. Pelagic silts are poorly laminated in unit C-1 which has a greenish and bluish gray color spectrum compared to dark and light gray laminations of unit B (Kliem et al., 2013b). A 0.2 m long sediment section between 20.2 and 20.4 m (cd) has

been newly identified as mass movement deposits and therefore removed from the event-corrected composite depth profile.

Well-preserved moss fragments occurred frequently in the sediments. There are mainly three species: *Drepanocladus perplicatus* (Amblystegiaceae), *Blindia inundata* (Seligeriaceae) and *Vittia pachyloma* (Amblystegiaceae) (cf. Fig. 2 in Zhu et al., 2014). These moss species were all reported as submerged aquatic species (Ochyra and Lightowlers, 1988; Hedenäs, 1997; Frahm, 2001). *D. perplicatus* fragments were dominant in most sediment samples. Mainly shoots and individual leaves were found in the sediments. Some shoots were preserved with attached leaves, but in many cases leaf laminae were completely eroded before sedimentation and only costae remained on the central axis of the shoot.

4.3.2. Age-depth model

An age-depth model based mostly on AMS radiocarbon dating of aquatic mosses has been previously established for the entire composite profile 5022-2CP (Kliem et al., 2013b). To constrain this existing model in the investigated sediment section, 22 additional samples of bulk aquatic moss and other organic matter were selected from the undisturbed pelagic sediment sections and sent to the Poznan Radiocarbon Laboratory and the NSF-Arizona AMS Laboratory for AMS ^{14}C determination (cf. Table 4.1 for detailed sample information). The age-depth model used in the present study (Fig. 4.4) was constructed with the software *clam 2.2* (Blaauw 2010), using the SHCal13 calibration curve (Hogg et al., 2013) and smoothed spline interpolation with a smoothing level of 0.5. The modeled depth range is from 9.4 to 26.5 m (cd-ec), including the sample Poz-8392 on the top and Poz-34236 on the bottom serving as connection points with the previous age-depth model by Kliem et al. (2013b). In total, 34 AMS ^{14}C dates from pelagic sediment sections were available for the modeled depth range (Table 4.1, Fig. 4.4).

There is a strong scatter between calibrated ages and event-corrected composite depth, particularly between 10 – 13.5 m cd-ec (Fig. 4.4). In order to obtain a reliable age-depth model, only the youngest ages were included in the age-depth model under the assumption that older than expected ^{14}C ages are the result of admixture of reworked old organic matter to the young counterparts. The main difference between the present and the previous age-depth model by Kliem et al. (2013b) is in the depth range between 12 and 15 m (cd-ec) where the calibrated ages derived from the present age-depth model are up to 1700 years younger than in the

previous one (Fig. 4.4). We argue that the present age-model based on more AMS ^{14}C dates tends to be more reliable in this depth range based on a 1.5 m thick sediment section consisting of a multi-layered volcanic tephra bed at the depth from 16.8 - 18.2 m (cd) corresponding to the event-corrected composite depth of 14.7 m (cd-ec) (Wastegård et al., 2013). Chemical analyses indicated that this volcanic tephra is the R_1 tephra derived from volcano Reclús (Wastegård et al., 2013). Based on high-resolution dating of 1 mm peat layers immediately beneath the Reclús tephra layer at two sites at the Strait of Magellan, McCulloch et al. (2005) have provided a weighted pooled mean age of 12,638 ± 60 ^{14}C years BP for the Reclús R_1 tephra. We recalibrated this ^{14}C age with CALIB 7.0 using SHCal13 (Hogg et al., 2013) and obtained a 2-sigma range of calibrated ages between 14,559 and 15,210 cal. BP (Fig. 4.4). Stern (2008) and Sagredo et al. (2011) reported nearly the same ages. According to the new age-depth model, the depth of 14.7 m (cd-ec) has an age of 15,102 cal. BP well within the reported age range of the Reclús R_1 tephra, whereas the previous model gives a considerably older age of 16,034 cal. BP (Kliem et al., 2013b). The higher reliability of the present age-depth model is validated by the consistency with the independently dated tephra ages.

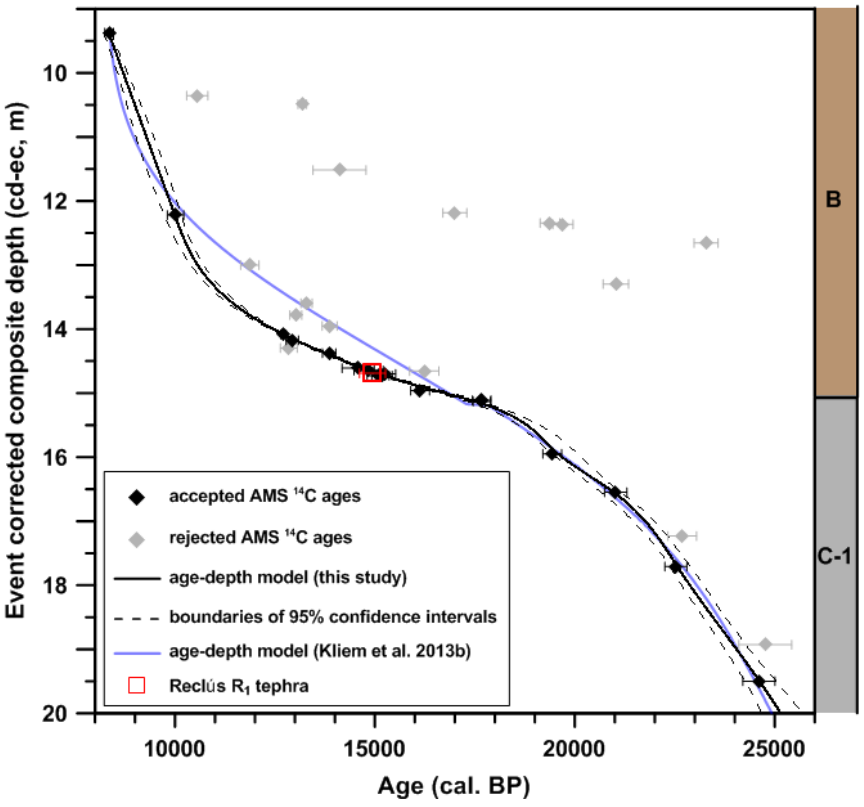


Figure 4.4. Age-depth model for the sediment section between 9 and 20 m event-corrected composite depth (cd-ec) from the composite profile 5022-2CP of Laguna Potrok Aike (cf. Table 1 for details). The age-depth model used in the present study is shown as a black line which is constructed by clam 2.2 applying a smooth spline with a smoothing level of 0.5 (Blaauw 2010). Dashed lines represent the upper and lower boundary of 95% confidence intervals. The accepted AMS ^{14}C ages are shown as black diamonds and the rejected ones in grey. Error bars represent the range of calibrated ages at 95% confidence intervals. The

previous age-depth model by Kliem et al. (2013b) is given as a blue line. The red open square represents the depth of the Reclús R_1 tephra. Its ^{14}C age from McCulloch et al. (2005) is recalibrated by CALIB 7.0 using SHCal13 (Hogg et al., 2013). Error bars are given for 2 sigma age range. Two lithological units (cf. text for detail) occurring in the investigating depth range are shown on the right.

Table 4.1. AMS ^{14}C ages for the modeled event-corrected sediment depth in the range of 9.37 - 26.48 m (cd-ec) for 5022-2CP of Laguna Potrok Aike. All ^{14}C ages derive from samples collected in pelagic sediment sections. Ranges of calibrated ages (at 95% confidence intervals, 2s) are the output of age-modeling software *clam 2.2* (Blaauw, 2010) applying the SHCal13 calibration curve (Hogg et al., 2013) and smoothed spline with a smoothing level of 0.5. Accepted ^{14}C ages are shown in bold.

Lab. No.*	Sediment depth (m cd)	Event corrected sediment depth (m cd-ec)	^{14}C Age (BP)	Error (±)	$\delta^{13}C$ (‰)	C-mass (mg)	Sample description	Range of calibrated ages (2s)	Median probability
Poz-8392[a]	**9.69**	**9.37**	**7580**	**50**	**-28.3**	**2.56**	**Stems of aquatic moss**	**8203 – 8421**	**8355**
Poz-48915	10.81	10.35	9390	90	-28.7	1.74	Bulk aquatic moss tissues	10,254 - 10,784	10,557
AA93659	10.95	10.49	11,379	57	-25.6	-	Bulk sediment	13,079 - 13,292	13,185
AA93660	12.22	11.52	12,200	200	-29.4	-	Wood, plant fragments	13,574 - 14,902	14,115
AA93661	12.99	12.18	14,042	70	-25.3	-	Bulk sediment	16,674 - 17,276	17,000
Poz-5985[a]	**13.04**	**12.22**	**8930**	**50**	**-18.9**	**2.28**	**Bone of Tuco Tuco**	**9780 - 10,188**	**10,016**
AA93662	14.06	12.34	16,101	84	-25.5	-	Wood, transparent shell fragments	19,122 - 19,612	19,378
Poz-48917	14.08	12.36	16,360	90	-29.3	1.18	Bulk aquatic moss tissues	19,476 - 19,980	19,704
Poz-49760	14.37	12.66	19,380	100	-27.3	1.77	Bulk aquatic moss tissues	22,983 - 23,581	23,284
Poz-8548[a]	14.78	13.00	10,240	60	8.4	3.61	Calcite fraction of bulk sample	11,611 - 12,067	11,872
Poz-48918	15.07	13.30	17,460	100	-28.5	3.14	Bulk aquatic moss tissues	20,717 - 21,355	21,026
Poz-49761	15.37	13.60	11,490	60	-25.1	1.50	Bulk aquatic moss tissues	13,147 - 13,428	13,291
Poz-8396[a]	15.55	13.78	11,200	60	-30.0	1.69	Stems of aquatic moss	12,831 - 13,130	13,023
Poz-48919	15.73	13.95	12,050	70	-31.6	1.41	Bulk aquatic moss tissues	13,712 - 14,089	13,868
Poz-49763	**15.87**	**14.08**	**10,840**	**60**	**-28.8**	**2.03**	**Bulk aquatic moss tissues**	**12,654 - 12,790**	**12,711**
Poz-48920	**15.95**	**14.18**	**11,120**	**70**	**-33.1**	**2.97**	**Bulk aquatic moss tissues**	**12,771 - 13,081**	**12,935**
AA93664	16.07	14.30	10,980	140	-29.7	-	Wood, seeds, plant fragments	12,663 - 13,082	12,847
Poz-49764	**16.15**	**14.38**	**12,040**	**60**	**-27.4**	**1.70**	**Bulk aquatic moss tissues**	**13,719 - 14,054**	**13,856**
Poz-8397[a]	**16.40**	**14.61**	**12,490**	**70**	**-31.2**	**1.60**	**Stems of aquatic moss**	**14,198 - 15,001**	**14,583**
Poz-49765	**16.42**	**14.65**	**12,590**	**60**	**-27.4**	**1.52**	**Bulk aquatic moss tissues**	**14,409 - 15,139**	**14,844**
Poz-5072[a]	**16.48**	**14.70**	**12,850**	**70**	**-25.8**	**2.64**	**Stems of aquatic moss**	**15,068 - 15,575**	**15,267**
Poz-49022	**18.28**	**14.73**	**12,720**	**70**	**-29.2**	**2.43**	**Bulk aquatic moss tissues**	**14,753 - 15,304**	**15,082**
AA93666	**18.28**	**14.73**	**12,783**	**64**	**-27.3**	**-**	**Plant fragments (large in quality)**	**14,906 - 15,415**	**15,179**
Poz-48922	18.40	14.85	13,530	70	-27.6	1.82	Bulk aquatic moss tissues	14,409 - 15,139	16,235
Poz-5073[a]	**18.51**	**14.96**	**13,450**	**70**	**-28.7**	**2.69**	**Stems of aquatic moss**	**15,881 - 16,354**	**16,132**
Poz-48923	**18.67**	**15.11**	**14,540**	**80**	**-29.3**	**1.58**	**Bulk aquatic moss tissues**	**17,450 - 17,913**	**17,671**
Poz-37017[b]	**18.69**	**15.13**	**14,540**	**70**	**-27.6**	**1.56**	**Stems of aquatic moss**	**17,465 - 17,900**	**17,672**
Poz-48925	**21.13**	**15.94**	**16,150**	**80**	**-24.0**	**1.30**	**Bulk aquatic moss tissues**	**19,190 - 19,662**	**19,435**
Poz-37022[b]	**22.09**	**16.54**	**17,460**	**80**	**-29.2**	**1.63**	**Stems of aquatic moss**	**20,760 - 21,317**	**21,023**
AA93669	22.57	17.23	18,850	170	-26.3	-	Bulk sediment	22,363 - 23,080	22,686
Poz-37007[b]	**23.25**	**17.70**	**18,700**	**120**	**-39.9**	**0.91**	**Stems of aquatic moss**	**22,304 - 22,852**	**22,527**
AA93670	25.01	18.93	20,600	270	-26.0	-	Bulk sediment	24,118 - 25,442	24,762
Poz-37020[b]	**27.20**	**19.50**	**20,490**	**120**	**-28.0**	**1.11**	**Stems of aquatic moss**	**24,242 - 25,045**	**24,604**
Poz-34236[bc]	**36.38**	**26.48**	**25,110**	**180**	**-25.0**	**1.45**	**Stems of aquatic moss**	**28,713 - 29,531**	**29,108**

[*] Poz: Poznan Radiocarbon Laboratory; AA: NSF-Arizona AMS Laboratory.

[a] Haberzettl et al. (2007).

[b] Kliem et al. (2013b).

[c] not shown in Fig. 4.4, but serving as connection point with previous age-depth model by Kliem et al. (2013b).

According to the new age-depth model the investigated sediment section covers the last glacial-interglacial transition from 26,000 to 8500 cal. BP. The temporal boundary between lithological units B and C-1 is around 17,600 cal. BP.

4.3.3. Laboratory Methods

Isolation of moss remains

To acquire as much moss remains as possible, ca. 10 cm^3 of sediments from every sample was screened. Each freeze-dried sediment sample was moistened with deionized water, placed on a magnetic stirrer and stirred for 2 h to disaggregate the material. Subsequently, the sample was carefully screened through a 200 µm sieve to obtain the coarse plant-debris fraction. The sieve fraction (> 200 µm) consists mainly of subfossil plant fragments such as shoots and leaves of mosses and remains of vascular plants, which were usually well preserved. Moss shoots were handpicked from the coarse sieve fraction under a binocular. To gain species-specific moss samples, we tried to pick only shoots of *D. perplicatus*. However, due to the similarity of the fragments of *D. perplicatus* and *V. pachyloma* and some not easily identifiable branches without leaves, an admixture of such moss fragments to the *D. perplicatus* samples cannot be ruled out. The remaining plant material in the coarse sieve fraction (>200 µm) could contain fragments of *B. inundata*, *V. pachyloma* and other unidentifiable mosses and individual leaves of *D. perplicatus* as well as remains of aquatic and possibly terrestrial vascular plants and is termed as 'residue' hereafter.

Each moss sample was first treated with a mixture of HCl and HF (10% respectively) and left for 16 h at room temperature to completely remove attached carbonates and minerogenic components. Samples were then rinsed with deionized water three times to remove reagents and remaining clastic matter and freeze-dried. The cleaned moss samples were weighed and homogenized by cutting the moss branches into fine segments with scissors to avoid loss of fine moss material compared to milling. Bulk OM of moss branches was first analysed for $\delta^{18}O$ and $\delta^{13}C$ values, before cellulose extraction was conducted. HCl-HF treatment of moss tissue prior to cellulose extraction has no effect on the $\delta^{18}O$ and $\delta^{13}C$ values of cellulose (Zhu et al., 2014).

Cellulose extraction

Cellulose was extracted from moss shoots and the residue fraction using the Cuprammonium solution (CUAM) method that has shown high reliability in yielding clean and pure cellulose from freshwater sediments, peat mosses and aquatic plants (Wissel et al., 2008; Moschen et al., 2009; Zhu et al., 2014). This method produces pure cellulose by dissolving and re-precipitating cellulose from whole plant material. Samples were first bleached with $NaClO_2$ (7%) acidified with concentrated acetic acid (96%) in a water bath for 10 h at 60 °C. The residual material was washed two times with hot deionized water (~70 °C) to remove the reagents and freeze-dried. The dry sample was mixed with ca. 30 ml CUAM solution (15 g/L) while placed in a dark room and stirred on a magnetic stirrer for 6 h and left for further 10 h at room temperature to completely dissolve the cellulose. After separation of not dissolved non-cellulose material, the cellulose solution was carefully decanted into a centrifuge tube and treated with 3 ml H_2SO_4 (20%) for cellulose precipitation. The white precipitated cellulose was then rinsed three times with deionized water and freeze-dried.

Stable isotope measurements

For carbon isotope analyses, an amount of moss OM or cellulose equivalent to 100 µg of carbon was weighed into tin capsules. Samples were combusted at 1020 °C using an elemental analyser (Thermo Scientific Flash 2000) interfaced on-line with an isotope ratio mass spectrometer (Thermo Scientific Delta V Advantage). Carbon content was determined by peak integration of mass-to-charge ratio (m/z) 44, 45 and 46, and calibrated against elemental standards. For oxygen isotope analyses, an amount of moss OM or cellulose providing 125 µg of oxygen was weighed into silver capsules. Immediately prior to oxygen isotope analysis, samples were placed overnight (16 h) in a vacuum drier at 100 °C to avoid analytical bias by adsorbed air moisture. Vacuum-dried samples were then pyrolysed at 1450 °C in a high temperature pyrolysis analyzer (HTO, HEKAtech) and measured on-line with a coupled isotope ratio mass spectrometer (Micromass IsoPrime). Oxygen content was determined by peak integration of m/z 28, 29 and 30, and calibrated against elemental standards. Each sample was measured at least 2 times for both carbon and oxygen isotopes. Isotope ratios are expressed as δ-values in per mil (‰), where

$$\delta = (R_{sample}/R_{standard} - 1) \cdot 1000$$

with R_{sample} and $R_{standard}$ as isotope ratios ($^{13}C/^{12}C$, $^{18}O/^{16}O$) of samples and standards, respectively. Isotope values are reported on the VPDB scale for carbon and the VSMOW scale for oxygen. Laboratory standards were inserted between samples to monitor the performance of the instrument and for calibration purposes. The standards USGS24 (-16.05‰), IAEA-CH-6 (-10.45‰) and IAEA-CH-7 (-32.15‰) were used for calibration of carbon isotope ratios of laboratory standards and samples, respectively (Coplen et al., 2006). The benzoic acid standards IAEA-601 (23.14 ±0.19‰) and IAEA-602 (71.28 ±0.36‰) (Brand et al., 2009) were used for calibration of oxygen isotope ratios of laboratory standards and samples, respectively. The overall precision of replicate analyses was better than ±0.1‰ for carbon and ±0.3‰ for oxygen isotope ratios. Ratios of carbon and oxygen content (C/O) of moss OM and cellulose were calculated on a weight base.

4.3.4. Reconstructed lake water $\delta^{18}O$ values

Modern field calibration datasets published in Zhu et al. (2014) were used to reconstruct the $\delta^{18}O_{lw}$ values from both bulk OM ($\delta^{18}O_{OM}$) and cellulose ($\delta^{18}O_{cell}$) of submerged aquatic mosses as well as the residue fraction applying the equations:

$$\delta^{18}O_{lw} = 1.156\ (\pm 0.036)\ \delta^{18}O_{OM} - 32.2\ (\pm 0.8); \quad (4.1)$$

$$\delta^{18}O_{lw} = 1.028\ (\pm 0.021)\ \delta^{18}O_{cell} - 30.4\ (\pm 0.5). \quad (4.2)$$

The uncertainty of the prediction (standard error of the regression) is 0.4‰ for Eq. (4.1) and 0.3‰ for Eq. (4.2), respectively (Zhu et al., 2014). The application of both equations in the investigation period is primarily based on the assumption that biochemical oxygen isotope fractionation during cellulose synthesis is almost constant under different temperatures. However, Sternberg and Ellsworth (2011) proposed a temperature effect on cellulose oxygen isotope enrichment relative to source water especially at temperatures below 20 °C. Accordingly, isotopic enrichment would increase with decreased temperature and the mean of increased enrichment between 4 and 15 °C is about 2‰ (Sternberg and Ellsworth, 2011). This value is, however, given by summarizing various field studies under different analytical conditions and has not been further confirmed by the latest modern calibration dataset from sites in southern Patagonia (Mayr et al., 2013), which shows no apparent effect of host water temperature on the fractionation between aquatic cellulose and host waters.

Samples with sufficient moss cellulose are much less than those providing sufficient moss OM and residue cellulose. Thus the quality of reconstruction of $\delta^{18}O_{lw}$ values using moss OM and residue cellulose needs to be evaluated. For this reason, we have compared the $\delta^{18}O_{lw}$ values reconstructed from moss OM and residue cellulose with those from moss cellulose by using the approach suggested by Zhu et al. (2014).

The effect of ocean water $\delta^{18}O$ changes on the isotopic composition of meteoric water during the last glacial-interglacial transition had to be accounted for. Thus, reconstructed ocean water $\delta^{18}O$ values (Lea et al., 2002) were used to correct the effect of ocean water changes on the Laguna Potrok Aike lake water isotopic composition. The data of Lea et al. (2002) were interpolated with a cubic spline function and subtracted from the reconstructed $\delta^{18}O_{lw}$ values (Mayr et al., 2013). In the following, the reconstructed $\delta^{18}O_{lw}$ corrected for changes in ocean water $\delta^{18}O$ are denoted as $\delta^{18}O_{lw\text{-}corr}$.

4.4. Results

The dry weight of subfossil aquatic moss remains in sediment samples (~10 cm^3) varied from complete absence to more than 100 mg (Fig. 4.5). This large range expresses the variability of moss burial rate within the sedimentary record likely controlled by the abundance of moss habitats in the lake, vicinity of these habitats to the coring location, sedimentation rate and redistribution processes by lake internal currents. The occurrence of moss organic matter is more discontinuous in lithological unit C-1 than in unit B. Moreover, a trend of reduced moss remains in the sediments towards younger sections, particularly above 16 m (cd), was observed. The C/O ratios of subfossil bulk moss OM, moss cellulose and residue cellulose have mean values of 1.17 (±0.05, n = 362), 0.88 (±0.02, n = 144) and 0.90 (±0.02, n = 185), respectively. These values are consistent with the mean value of 1.17 determined for bulk OM of modern aquatic moss samples and the stoichiometrically expected C/O ratio of 0.90 for cellulose (Wissel et al., 2008; Zhu et al., 2014), which confirms the purity of extracted cellulose and good preservation of moss remains in Laguna Potrok Aike sediments.

The $\delta^{18}O$ values range from 22.1‰ to 25.4‰ for bulk moss OM, from 22.8‰ to 26.7‰ for moss cellulose and from 23.2‰ to 26.9‰ for residue cellulose, respectively (Fig. 4.6). The $\delta^{18}O$ values are generally more ^{18}O enriched for samples in lithological unit B than for those in unit C-1. The ^{18}O enrichment in unit B is more pronounced by up to 2.5‰ for both cellulose fractions than by around 1‰ for bulk moss OM. A $\delta^{18}O$ increase occurs in the transition

between the two lithological units within a composite depth range from 22 to 16 m (cd). Between 30 and 22 m (cd) and between 16 and 10 m (cd) no general trend is observed for the $\delta^{18}O$ values of all three fractions but short-term fluctuations of up to 2‰ occur (Fig. 4.6). The amount of moss material preserved in each sample had no effect on the observed $\delta^{18}O$ of moss OM (Fig. 4.7) and any bias due to material availability thus can be excluded. The $\delta^{18}O$ values of samples from mass movement deposits and volcanic tephra layers are similar to those from the pelagic sediment sections and, thus, confirm their same lake-internal origin. For further interpretations and reconstructions, the samples from mass movement deposits are excluded.

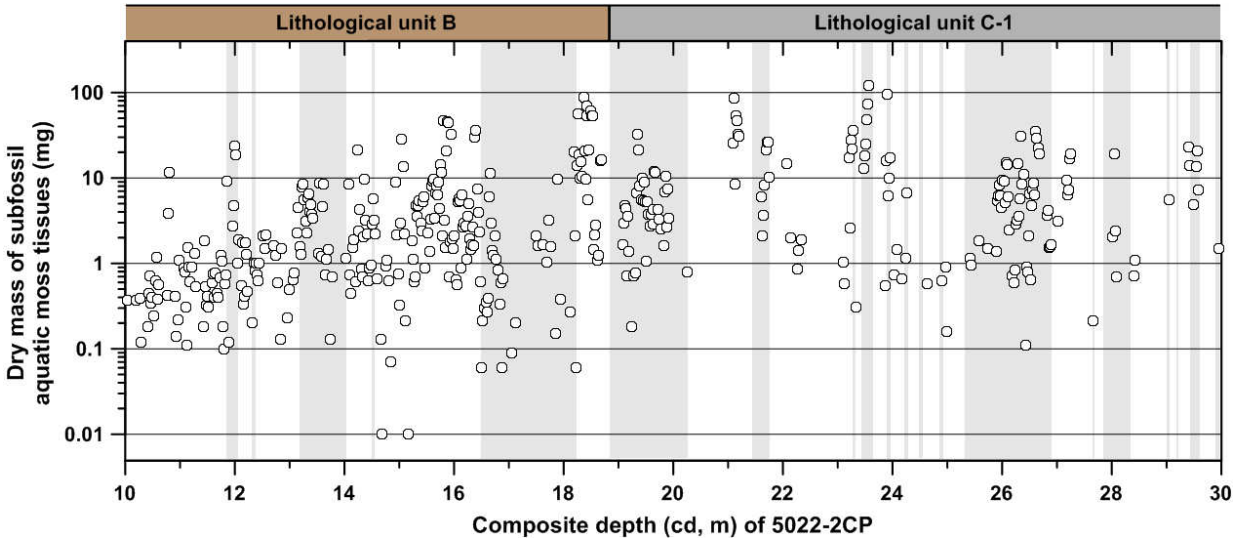


Figure 4.5. Weighed dry mass of subfossil aquatic moss remains handpicked from sediment samples within the investigated composite depth range of 5022-2CP of Laguna Potrok Aike. Vertical grey bars represent mass movement deposits and volcanic ash layers. Two lithological units (cf. text for detail) occurring in the investigating depth range are shown at the top of the figure. Note that the Y-axis is in log-scale.

Quality assessment shows that $\delta^{18}O_{lw\text{-}corr}$ values inferred from moss OM and residue cellulose are commonly parallel to the one-to-one moss cellulose line (Fig. 4.8) and, thus, confirm the validity of these two fractions for lake water inferences (Zhu et al., 2014). Nevertheless, some samples from lithological unit C-1 show around 1‰ more positive $\delta^{18}O_{lw\text{-}corr}$ values inferred from bulk moss OM compared to the moss cellulose reference line (1:1), while more positive $\delta^{18}O_{lw\text{-}corr}$ values inferred from residue cellulose are found for a couple of samples from lithological unit B. In terms of $\delta^{13}C$ values, bulk moss OM generally follows the moss cellulose reference line with an almost constant depletion. However, a marked bias towards more ^{13}C enriched values is observed for the samples of residue cellulose from lithological unit B, which indicates the presence of the remains of aquatic vascular plants in the residue fraction. According to Fig. 4.8 and Zhu et al. (2014), the observed positive $\delta^{13}C$ bias range of 2 - 4‰

suggests a 10 - 20% contribution of aquatic vascular plants to the residue fraction, which results, however, only in a positive $\delta^{18}O$ bias of less than 0.2‰ which is well within the analytical uncertainty. Therefore, it is reliable to use the residue cellulose for an auxiliary $\delta^{18}O_{lw}$ reconstruction in the present study.

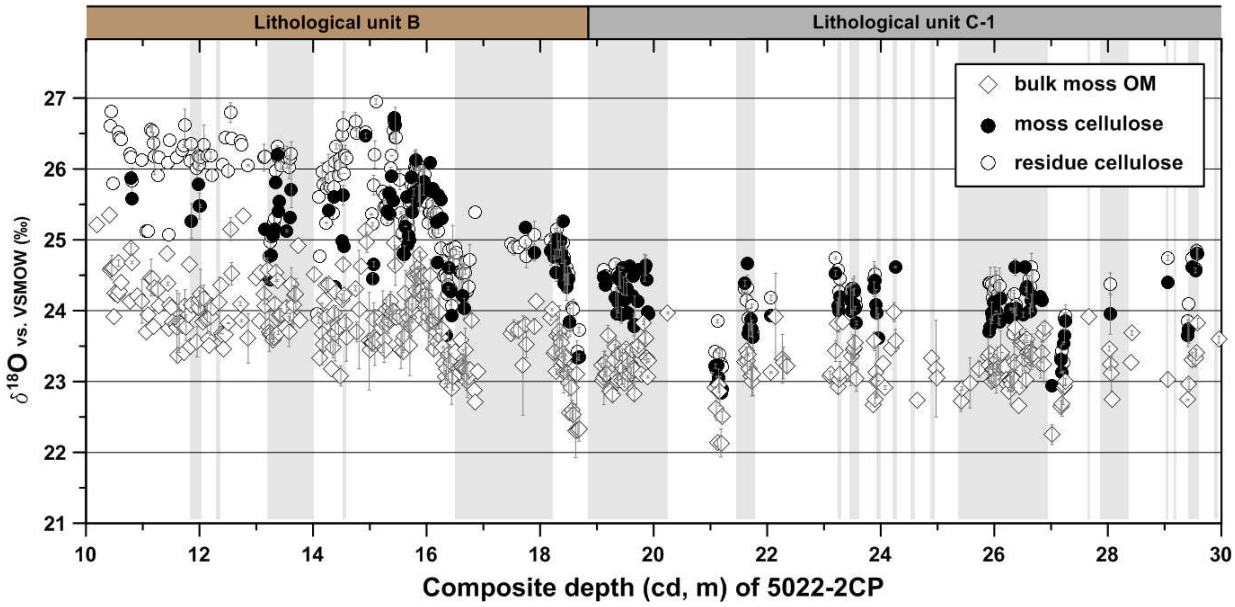


Figure 4.6. $\delta^{18}O$ values of all measured samples within the investigated composite depth range of 5022-2CP of Laguna Potrok Aike. Bulk aquatic moss organic matter (OM) is represented by open diamonds, aquatic moss cellulose by closed circles and residue cellulose by open circles. Standard deviations are shown as bars. Vertical grey bars represent mass movement sediment sections and volcanic ash layers. Two lithological units (cf. text for detail) occurring in the investigating depth range are shown at the top of the figure.

A composite $\delta^{18}O_{lw\text{-}corr}$ record based on aquatic moss shoots is constructed by the combination of bulk moss OM and moss cellulose applying moving average smoothing with a 500-years window (Fig. 4.9). The $\delta^{18}O_{lw\text{-}corr}$ record documents a mean $\delta^{18}O_{lw\text{-}corr}$ value of ca. -6.5‰ between 26,000 and 21,000 cal. BP (Fig. 4.9). Subsequently, a $\delta^{18}O_{lw\text{-}corr}$ decrease of ca. 1‰ occurred between 21,000 and 17,600 cal. BP and the minimum of the complete record of -7.5‰ was reached. From 17,600 till 12,800 cal. BP, $\delta^{18}O_{lw\text{-}corr}$ strongly increased by an amplitude of nearly 3‰ interrupted by a millennial period with declining values of up to ca. 0.7‰ beginning at around 15,600 cal. BP. Afterwards, the $\delta^{18}O_{lw\text{-}corr}$ values appeared to be subjected to millennial fluctuations and reached ultimately close to -3‰ in the early Holocene, similar with the present-day values (Fig. 4.9).

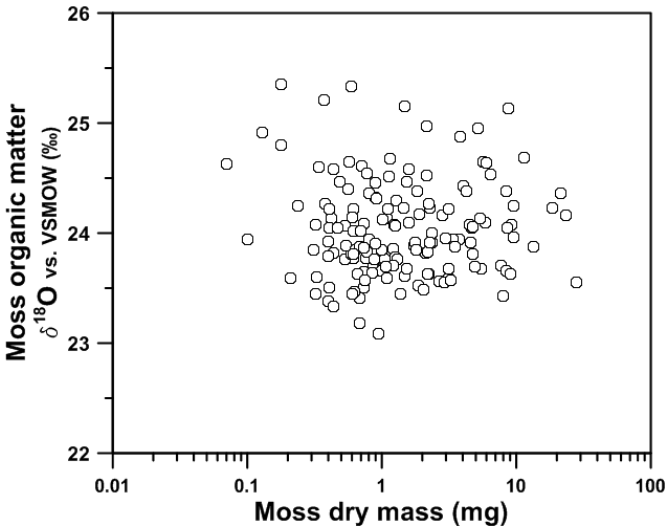


Figure 4.7. Relationship between dry mass of handpicked *Drepanocladus perplicatus* and $\delta^{18}O$ values of moss organic matter for samples within the composite depth between 10 and 16 m. Note that the X-axis is in log-scale.

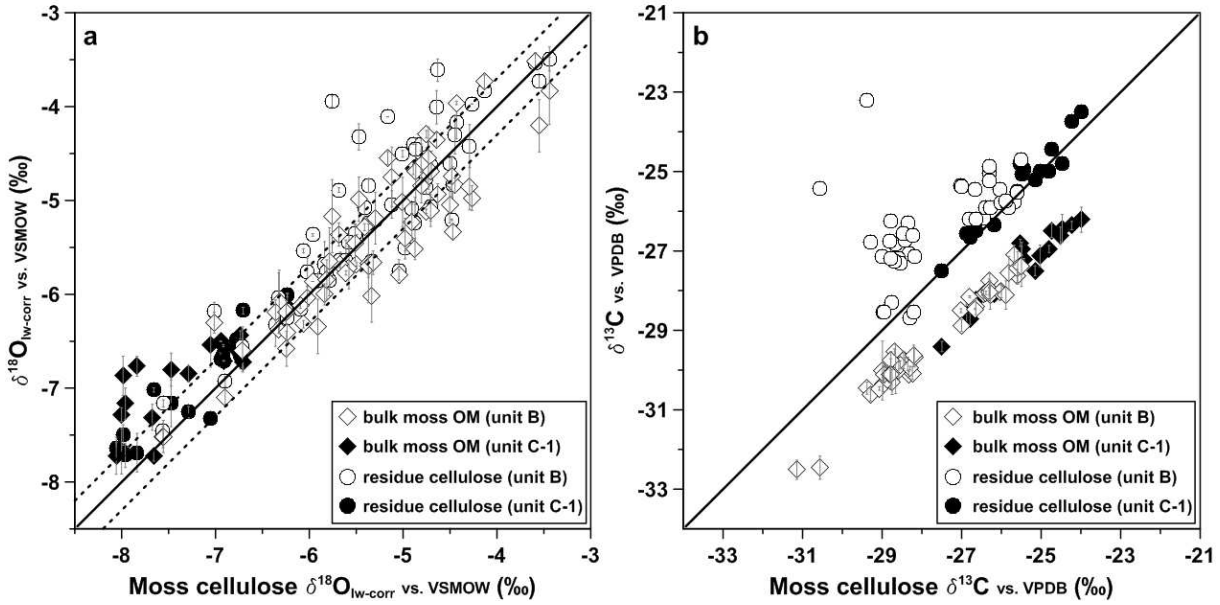


Figure 4.8. a) Reconstructed lake-water $\delta^{18}O$ ($\delta^{18}O_{lw\text{-}corr}$) from bulk aquatic moss organic matter (OM) (diamonds) and residue cellulose (circles) in relation to $\delta^{18}O_{lw\text{-}corr}$ values reconstructed from aquatic moss cellulose. Samples from the sediment sections of mass movement deposits and tephra layers are excluded. Samples from lithological unit B and C-1 are shown in open and closed symbols, respectively. One-to-one line of $\delta^{18}O_{lw}$ values reconstructed from aquatic moss cellulose is presented as a black line. **b)** Same as a), but for $\delta^{13}C$ values. Lower and upper limit of one-to-one line in a) are presented in dashed lines according to the standard error of regression for modern calibration data set (Zhu et al., 2014). Standard deviations of individual values are given as bars in a) and b).

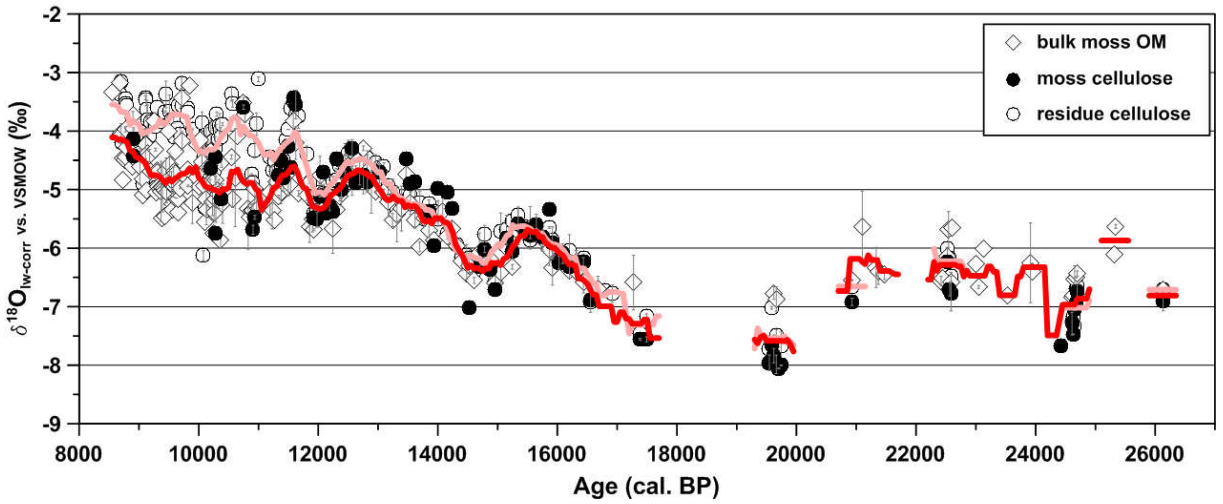


Figure 4.9. Isotopic record of reconstructed lake-water $\delta^{18}O$ ($\delta^{18}O_{lw\text{-}corr}$) from bulk aquatic moss organic matter (OM), aquatic moss cellulose and residue cellulose during the last Glacial-Interglacial transition period. Samples from the sediment sections of mass movement deposits and tephra layers are excluded. Color lines represent the moving average smoothing using a 500-years window (red: smoothing of average $\delta^{18}O_{lw\text{-}corr}$ of composite aquatic moss record combining moss OM with moss cellulose; pale red: smoothing of $\delta^{18}O_{lw\text{-}corr}$ of residue cellulose). Discontinuity prior to 17,600 cal. BP is caused by insufficient moss material.

4.5. Discussion

4.5.1. Factors controlling lake water $\delta^{18}O$ of Laguna Potrok Aike

Variations in $\delta^{18}O_{lw}$ are controlled by changes in the isotope composition of input waters (precipitation, surface inflow and groundwater inflow) and changes in the magnitude of subsequent evaporative ^{18}O enrichment (Edwards et al., 2004). It has been found that long-term temporal isotopic variation in precipitation at middle and high latitudes closely follows long-term changes in mean annual air temperature (Rozanski et al., 1992; Teranes and McKenzie, 2001; Darling et al., 2005). Under modern comparably stable conditions, seasonal or short-term variations of meteorological parameters and changes in $\delta^{18}O$ of precipitation ($\delta^{18}O_p$) do not have pronounced impacts on $\delta^{18}O_{lw}$ of Laguna Potrok Aike (Mayr et al., 2007). However, the highly significant positive correlation between monthly mean air temperature and weighted mean $\delta^{18}O_p$ at Punta Arenas, as shown in Fig. 4.3, indicates a potential influence of long-term local temperature changes on $\delta^{18}O_p$. Other than temperature change, $\delta^{18}O$ variations of precipitation can, however, also arise from changes in the direction of air masses bringing moisture to southern Patagonia. Precipitation brought from easterly directions is more enriched in heavy isotopes than those brought by westerly winds. The mean $\delta^{18}O_p$ of the former and the latter is -8‰ and -15‰, respectively (Mayr et al., 2007). Thus, within a longer period with increasing air temperature and more frequent easterlies, the $\delta^{18}O_p$ and, in turn, $\delta^{18}O$ of inflow

and $\delta^{18}O_{lw}$ could shift to more positive values. In addition, $\delta^{18}O_{lw}$ of lakes in semi-arid southern Patagonia are subjected to strong modification by evaporation, based on the fact that dry, extremely windy and highly evaporative conditions dominate the leeward side of the southern Andes (Garreaud et al., 2013). Today, the mean $\delta^{18}O$ of inflow (precipitation and groundwater) of Laguna Potrok Aike are around -13‰, while $\delta^{18}O_{lw}$ values have a range between -3‰ and -4‰ (Mayr et al., 2007) indicating high evaporative ^{18}O enrichment of more than 9‰ relative to meteoric waters.

In general, the degree of ^{18}O enrichment in through-flow lakes at a hydrological and isotopic steady state is a function of the hydrologic balance, i.e. the ratio of evaporation to inflow (E/I) and relative humidity (Gat, 2010). Accordingly, low relative humidity and high E/I, as exemplified by increased evaporation und reduced inflow, can cause strong ^{18}O enrichment of lake water. However, under non-steady state conditions a similar effect could also be induced by a marked increase of the lake water residence time as a result of reduced outflow rates. Presently, relative humidity at Laguna Potrok Aike has an annual average of about 0.65 (Ohlendorf et al., 2013) and the calculated E/I based on isotope modeling is around 0.6 (Mayr et al., 2007). Any substantial changes in factors controlling evaporation and relative humidity as well as lake water residence time and isotopic composition of meteoric water during the glacial and the last deglaciation would play a significant role in determining $\delta^{18}O_{lw}$ values of Laguna Potrok Aike.

4.5.2. $\delta^{18}O_{lw\text{-}corr}$ of the full Glacial (26,000 – 21,000 cal. BP)

Understanding the initial $\delta^{18}O_{lw\text{-}corr}$ under the full Glacial conditions is crucial for the interpretation of the entire record. The overall amplitude observed for $\delta^{18}O_{lw\text{-}corr}$ is about 3.5‰ (Fig. 4.9). This amplitude is smaller than probably expected for the last glacial-interglacial transition with dramatic changes in climatic conditions. $\delta^{18}O_{lw\text{-}corr}$ of the glacial period (26,000 – 21,000 cal. BP) seems to be unexpectedly enriched compared to the modern system under strong evaporation conditions (Mayr et al., 2007). Zhu et al. (2014) have shown that the $\delta^{18}O_{lw}$ values reconstructed from aquatic moss shoots are not affected by decomposition effects masking the original signal. To account for the glacial $\delta^{18}O_{lw\text{-}corr}$, which is more enriched than expected, two alternative scenarios with either (*i*) markedly ^{18}O depleted inflow or (*ii*) moderate change in $\delta^{18}O$ of inflow compared to modern inflow into Laguna Potrok Aike are conceivable.

(i) $\delta^{18}O$ of meteoric water and groundwater markedly lower than present

All estimates of regional temperatures in southern Patagonia indicate a pronounced decrease during the last Glacial. Alkenone derived sea-surface temperatures (SST) from marine sediment cores off the Chilean coast (Fig. 4.10f) indicate lower SSTs by ca. 6°C for the last Glacial relative to the present (Lamy et al., 2007; Caniupan et al., 2011). For the South American continent, lower air temperatures by 8-10°C during the LGM than today have been inferred from coupled ocean-atmosphere simulations (Rojas et al., 2009). Furthermore, Trombotto (2002) has suggested a lowering of the mean annual air temperature of at least 14°C in southern Patagonia during the LGM based on the presence of ice-wedge casts.

As discussed in section 4.5.1, $\delta^{18}O_p$ is positively correlated with surface air temperature. A mean spatial gradient of $\delta^{18}O_p$ with surface air temperature of 0.53‰ per °C (Gourcy et al., 2005) or 0.58‰ per °C (Rozanski et al., 1993) has been reported. On the temporal scale, an average $\delta^{18}O_p$-temperature coefficient of about 0.6‰ per °C is observed at mid- and high-latitudes (Rozanski et al., 1992). According to this relation, distinctly lowered temperatures would cause a strong ^{18}O depletion of precipitation in the order of 6‰ in southern Patagonia during the full Glacial compared to the present. If the groundwater flowing into Laguna Potrok Aike is mainly recharged by regional precipitation, the strong ^{18}O depletion of glacial precipitation would also have a direct impact on the $\delta^{18}O$ of inflow. Under these circumstances, $\delta^{18}O$ of surface and subsurface inflow into Laguna Potrok Aike during the full Glacial would be about -19‰ (present value: -13‰) assuming that the modern balance of precipitation from the Pacific and Atlantic was retained. This large ^{18}O depletion of inflow would result in an ^{18}O enrichment of about 12‰ between $\delta^{18}O_{lw\text{-}corr}$ (-6.5‰) recorded and $\delta^{18}O$ of inflow (-19‰) during the full Glacial compared to the modern magnitude of ^{18}O enrichment of about 9‰ (Mayr et al., 2007).

Today, climate in the south-eastern Patagonian steppe is characterized by strong westerly winds which are adiabatically warmed and dried while passing the Andes, leading to semi-arid and highly evaporative conditions in eastern Patagonia (Garreaud et al., 2013) that can explain the modern ^{18}O enrichment of lake water. Enrichment during the full Glacial might also have been caused by evaporation induced by a similar foehn-wind effect. It might have been strengthened by the thick Patagonian Ice Sheet covering the southern Andes which might have increased adiabatic warming and drying of subsiding air masses coming from westerly directions. This föhn-wind effect could be very pronounced in a cold and dry environment during the Glacial, which is corroborated by palynological studies of Laguna Potrok Aike sediments (Recasens et

al., 2012). At Lake Hoare in the modern McMurdo Dry Valley of Antarctica strong and dry regional föhn-winds heat adiabatically by about 20°C (from -30 to -10°C) upon their descent from the surrounding ice plateau, even in sunless austral winters (Clow et al., 1988). At a mean annual temperature of less than -15°C in the Dry Valley region, relative humidity averages to only 0.54 and the annual sublimation (ablation) rate of surface ice of lakes reaches about 300 mm (Clow et al., 1988; Chinn, 1993). In a similar way, strong and extremely dry downslope föhn-winds passing the ice-covered southern Andes could have resulted in higher-than-expected evaporation and sublimation rates during the Glacial. Thus, isotopic enrichment of lake water during the full Glacial could have been stronger than expected.

This interpretation is largely based on the predominance of the SHW at the latitude of Laguna Potrok Aike (52°S) during the Glacial. The Patagonian Ice Sheet covering the southern Andes from 38 to 56°S during the LGM (Glasser et al., 2008) implies the existence of westerly winds within this latitudinal belt, because a positive mass balance of modern glaciers in the southern Andes is favored by low summer temperature and high precipitation and the latter is, in turn, largely related to the westerly winds from the Pacific (Schneider et al., 2003). In fact, paleoclimate studies from sites between 30°S and 45°S in southwestern South America have implied much higher precipitation during the Glacial compared to the present (e.g. Heusser, 1989; Lamy et al., 1999; Moreno et al., 1999; Valero-Garcés et al., 2005).

(ii) Moderate change in $\delta^{18}O$ of source water compared to the present

If the SHW is located in a more equatorward position (Williams and Bryan, 2006), the balance between westerly and easterly winds would shift towards more easterly winds which could consequently dominate in southern Patagonia during the Glacial. Assuming almost 100% precipitation moisture from the Atlantic, $\delta^{18}O_p$ could be roughly estimated for about -14‰ (cf. discussion above). In this case, $\delta^{18}O$ of inflow into Laguna Potrok Aike would be more positive than the estimation in scenario (i) and the magnitude of ^{18}O enrichment would be smaller accordingly.

If the glacial temperature in southern Patagonia was lowered by more than 10°C (cf. discussion in scenario (i)), the local mean annual temperature at Laguna Potrok Aike would be lower than -3°C during the Glacial and the formation of permafrost would be fostered. The occurrence of a relict sand wedge dated to 35±3 ka in the Laguna Potrok Aike catchment area (Kliem et al., 2013a) indeed suggests permafrost conditions during the Glacial around the lake. Deep permafrost during the Glacial would have major impacts on the hydrological and isotopic water

balance of Laguna Potrok Aike. Groundwater recharge from meteoric water may then have been precluded due to impervious permafrost layers. Hence, any isotopic change in the precipitation may not have been transmitted into the groundwater. Decreased precipitation and then limited surface and subsurface inflows during the full Glacial would also generally make a smaller contribution to lake water budget than today. Thus, the expected large negative shift in $\delta^{18}O$ of inflow, as discussed in scenario (i), may not have occurred. In addition, deep permafrost could have largely prohibited the exchange between the groundwater and the lake water body (subsurface in- and outflow), thus converting Laguna Potrok Aike into a closed lake system with extremely prolonged lake water residence time under non-overflow conditions. Under these circumstances, even small evaporative isotopic enrichment effects could sum up to considerable cumulative ^{18}O enrichment of lake water.

In the absence of any further knowledge on key parameters determining the isotopic water balance of Laguna Potrok Aike, especially relative humidity and isotopic composition of atmospheric moisture and considering the occurrence of permafrost, it seems more likely that the $\delta^{18}O$ value of source water was not as negative as discussed in scenario (i) and that cumulative enrichment caused by prolonged lake water residence time had comparably strong impact on ^{18}O enrichment of lake water. The scenario (ii) is thus preferred to explain the observed glacial $\delta^{18}O_{lw\text{-}corr}$ values. Accordingly, the factor of SHW wind-driven evaporation might not be a determinant for lake water balance, in consistency with the hypothesis of an equatorward shift of 7-10° latitude of the SHW during the LGM (Toggweiler et al., 2006), supported by diminished opal flux and attenuated wind-driven upwelling in the Southern Ocean (Anderson et al., 2009) and low atmospheric CO_2 concentrations during the glacial period (Schmitt et al., 2012). However, the changes in strength and latitudinal position of the SHW during the LGM relative to today are still in an open debate, as a consequence of uncertainties in modelling results (Chavaillaz et al., 2013; Pollock and Bush, 2013; Rojas, 2013; Sime et al., 2013) and ambiguities in proxy interpretations (Kohfeld et al., 2013).

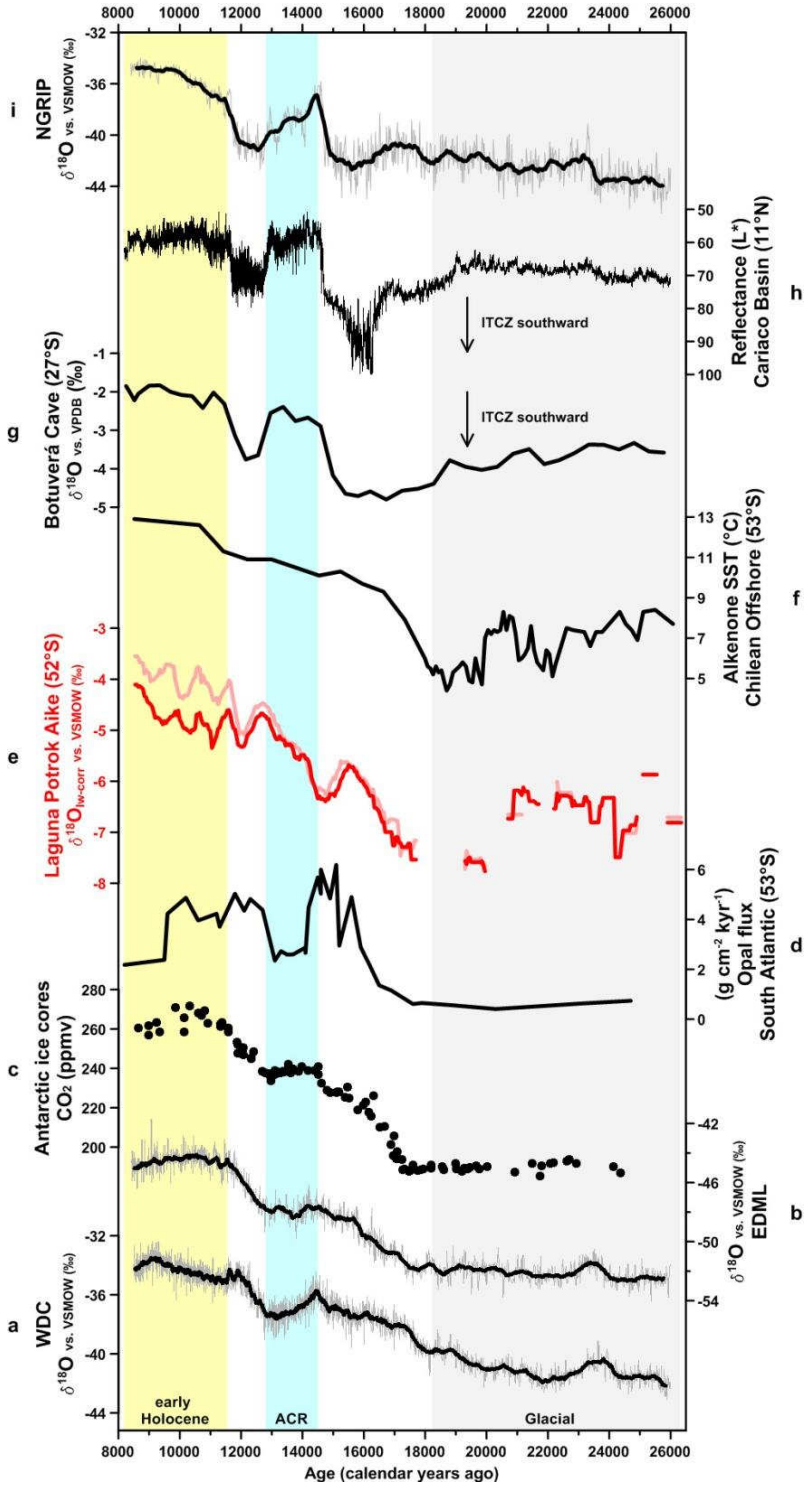


Figure 4.10. Reconstructed lake-water $\delta^{18}O$ of Laguna Potrok Aike in comparison to global proxy records. **a)** $\delta^{18}O$ record from the WDC in West Antarctica (WAIS Divide Project Members, 2013). **b)** $\delta^{18}O$ record from EDML of East Antarctica (EPICA Community Members, 2006). **c)** CO_2 concentration from Antarctic ice cores (Schmitt et al., 2012). **d)** Opal flux of TN057-13-4PC (53°S) in the Southern Atlantic (Anderson et al., 2009). **e)** Reconstructed lake-water $\delta^{18}O$ ($\delta^{18}O_{lw\text{-}corr}$) of Laguna Potrok Aike in this study, smoothed by a 500-years window (red: smoothing of average $\delta^{18}O_{lw\text{-}corr}$ of composite aquatic moss record combining moss cellulose with moss OM; pale red: smoothing of $\delta^{18}O_{lw\text{-}corr}$ of residue cellulose). Ocean water effect during the LGM and deglaciation has been corrected according to Lea et al. (2002). **f)** Alkenone derived SST record from the offshore core MD07-3128 (53°S) (Caniupán et al., 2011). **g)** $\delta^{18}O$ record of Botuverá Cave (27°S) in Southern Brazil (indicator of the ITCZ position) (Wang et al., 2007). **h)** Sediment total reflectance from Cariaco Basin (indicator of the ITCZ position) (Deplazes et al., 2013). **i)** $\delta^{18}O$ record of NGRIP on GICC05 time scale (Anderson et al., 2006; Rasmussen et al., 2006). ACR: Antarctic Cold Reversal.

4.5.3. Evolution of $\delta^{18}O_{lw\text{-}corr}$ and deglaciation history since 21,000 cal. BP

Between 21,000 and 19,500 cal. BP, $\delta^{18}O_{lw\text{-}corr}$ decreased from the main glacial level of about -6‰ towards a level of around -7.5‰ that was probably held until 17,600 cal. BP (Fig. 4.10e). This depletion by ca. 1.5‰ is large concerning the total amplitude of 3.5‰ for the entire record. Despite the discontinuous record for this time interval, the $\delta^{18}O_{lw\text{-}corr}$ of around -7.5‰ recorded around 19,000 and at 17,600 cal. BP implies less evaporative enrichment or more ^{18}O depleted surface inflow from ice or snow melt during this period. This is in line with the occurrence of exposed lacustrine sediments testifying an overflow situation for Laguna Potrok Aike at around 17 ka by OSL dating (Kliem et al., 2013a). The long-term SST cooling trend from ~25 to 19 kyr BP from a marine site (MD07-3128, 53°S) close to the Patagonian Ice Sheet has been interpreted as a locally enhanced SST cooling induced by the supply of large amounts of meltwater (Caniupán et al., 2011, Fig. 4.10f). The timing of a large SST cooling at around 21 kyr BP (Fig. 4.10f) is consistent with the beginning of the distinct depletion of $\delta^{18}O_{lw\text{-}corr}$ in Laguna Potrok Aike. About two millennia prior to the onset of the last deglaciation, the Intertropical Convergence Zone (ITCZ) also began to shift southward (Wang et al., 2007; Deplazes et al., 2013; Fig. 4.10g and h).

A marked and sustained two-step increase of $\delta^{18}O_{lw\text{-}corr}$ started from 17,600 cal. BP onwards (Fig. 4.10e) and lasted until 12,800 cal. BP with a millennial recession phase beginning at around 15,600 cal BP. The first increase lasted until 15,600 cal. BP and signifies the onset of the last deglaciation in the Patagonian steppe. This increase in $\delta^{18}O_{lw\text{-}corr}$ was not included in an earlier dataset (Mayr et al., 2013), but is clearly shown in our new data set, which has also an improved temporal resolution and lower analytical uncertainty. The initial rise of $\delta^{18}O_{lw\text{-}corr}$ from around 17,600 cal. BP occurred simultaneously with a rapid increase of lacustrine primary productivity in Laguna Potrok Aike reported by Hahn et al. (2013) and Zhu et al. (2013). This development at Laguna Potrok Aike is concurrent with increasing Antarctic temperatures (Fig. 4.10a and b), rising atmospheric CO_2 concentrations (Fig. 4.10c), an increased wind-driven upwelling in the Southern Ocean (Fig. 10d), warming off the coast of southern Chile (Fig. 4.10f) and a large southward displacement of the ITCZ (Fig. 4.10g and h). Moreover, glacier fluctuations in southern Patagonia also suggest rapid and widespread glacier retreat in the Andes around 18,300 - 17,500 cal. BP (e.g. McCulloch et al., 2005; Kilian et al., 2007; Sagredo et al., 2011), coinciding with deglacial warming.

Climatic warming alone has several effects on the isotopic water balance of Laguna Potrok Aike that altogether would certainly induce a cumulative rise in $\delta^{18}O_{lw}$ during the initial phase

of the last deglaciation. Firstly, increasing air temperature will cause an equivalent change in the isotopic composition of meteoric water towards more enriched isotopic values independent of its origin from the Pacific or Atlantic. For precipitation moisture from the Pacific, this effect could be reinforced by a diminishing isotopic rain shadow effect due to the receding Patagonian Ice Sheet. Secondly, rising air temperatures would result in a local moisture deficit and strengthen temperature-driven evaporation leading to enhanced ^{18}O enrichment of lake water. Thirdly, thawing permafrost would facilitate higher groundwater recharge from regional precipitation. The $\delta^{18}O$ of groundwater then would be closely coupled with $\delta^{18}O_p$ and affected by climate warming on the long-term scale. Considering the concept of E/I, the lake is in a non steady state condition during this phase induced by massive palaeogeographic and palaeoenvironmental changes, where, according to all considerations, increasing surface air temperature must be an important driver. It might be argued that the first deglacial rise in $\delta^{18}O_{lw\text{-}corr}$ lasting two millennia was mainly caused by rapid deglacial warming in southern Patagonia and the southern high latitudes (Pendall et al., 2001; Caniupán et al., 2011; Fig. 4.10a, b and f). Moreover, more ^{18}O enriched moisture from the Atlantic could be brought into southern Patagonia due to sea surface warming and a poleward retreating sea-ice front in the South Atlantic (Gersonde et al., 2005; Allen et al, 2011), as the westerly winds were probably weak. By constrast, according to Toggweiler et al. (2006) and Denton et al. (2010), the SHW shifted rapidly poleward at the onset of the last deglaciation. Such a rapid onset of strong westerly winds would induce strong evaporation from the water surface and also lead to strong evaporative isotopic enrichment that would explain the rising $\delta^{18}O_{lw\text{-}corr}$ as well. However, previous studies have related the massive abundance of pollen from the aquatic taxon *Myriophyllum* (Wille et al., 2007) and high lacustrine primary productivity (Hahn et al., 2013; Zhu et al., 2013) during the initial phase of the last deglaciation to relatively calm wind conditions favoring the flowering of *Myriophyllum* and algal blooms in warmer surface waters and seasonal stratification.

At around 15,600 cal. BP, the overall increase in $\delta^{18}O_{lw\text{-}corr}$ is reversed during a ca. 1000 years lasting phase with declining values. To some extent this period resembles the Antarctic Cold Reversal (ACR) with reduced opal flux in the Southern Ocean and a halt in the increase of atmospheric CO_2 concentrations (Fig. 4.10c and d), but occurs about 1000 years earlier. Since the independent tephra time marker Reclús R_1 occurring at the end of this phase strongly supports the reliability of the current age-depth model, the decrease in $\delta^{18}O_{lw\text{-}corr}$ began at least before 15,000 cal. BP and cannot be synchronized with the ACR. The decreasing $\delta^{18}O_{lw\text{-}corr}$ during this phase could probably be explained by increasing groundwater inflow into Laguna

Potrok Aike or by decreasing evaporation. Groundwater through-flow fostered by thawing permafrost and then supplied by ^{18}O depleted ice melt water from the Andes could have been increased, since 80% of the ice volume of the Patagonia Ice Sheet was suggested to be lost during the early phase of the last deglaciation (Hulton et al., 2002; Hubbard et al., 2005). Furthermore, large ice-dammed proglacial lakes existed about 100 km west of Laguna Potrok Aike during this phase (e.g. Sagredo et al., 2011; Solari et al., 2012) and probably provided an additional ^{18}O depleted water source. Alternatively, this period might also represent a switch in the dominant driver of the ^{18}O enrichment of lake water. Around that time the rapid climate warming during the initial phase of the last deglaciation is completed and the further rise in SST is much slower (Fig. 4.10f). Assuming that from now on the SHW progressively increased its influence on the hydrological balance of Laguna Potrok Aike, a decline in the ^{18}O enrichment of lake water could have occurred, as the increasing influence of the SHW during this period could not yet compensate for the lessening of temperature-driven evaporation. Only until the SHW exerted its full influence, strengthened wind-driven evaporation would result in large evaporative ^{18}O enrichment of lake water and increased $\delta^{18}O_{lw\text{-}corr}$ values. Thus, it might be argued that progressively enriched $\delta^{18}O_{lw\text{-}corr}$ of Laguna Potrok Aike from about 14,600 cal. BP (Fig. 4.10e) onward are mainly ascribed to intensified westerly wind and only to a lesser extent to the further slow temperature rise. This is consistent with a progressive increase in the intensity of the SHW over the period from the ACR until about 13,000 cal. BP and a maximum SHW strength at 52°S during the following millennia indicated by Mayr et al. (2013) for the period between 13.4 and 11.3 cal. kyr BP. For the period of the early Holocene, $\delta^{18}O_{lw\text{-}corr}$ values reconstructed from residue fraction are somewhat ^{18}O enriched by up to 1‰ than those inferred from aquatic moss shoots. This ^{18}O enrichment can possibly be attributed to the contamination of terrestrial plant tissues in the residue fraction. Nevertheless, increasing $\delta^{18}O_{lw\text{-}corr}$ since the onset of the early Holocene suggests an elevated E/I ratio, coinciding with the timing of the lowering lake level that reached a depth of -33m below the modern one shortly before 6790 cal. BP (Haberzettl et al., 2008; Anselmetti et al., 2009; Zolitschka et al. 2013).

Like the patterns of changes in the SHW during the LGM, for the period of the last deglaciation towards the early Holocene, the reconstructed development of the SHW based on the paleoclimatic sites in southern Patagonia remains controversial (cf. Kilian and Lamy, 2012; Villa-Martínez et al., 2012).

4.6. Conclusions

This study presents a high-resolution $\delta^{18}O_{lw}$ reconstruction for Laguna Potrok Aike located in semi-arid southern Patagonia throughout the last glacial-interglacial transition by using purified bulk OM and extracted cellulose of subfossil submerged aquatic mosses. These data provide a unique continental proxy record of the environmental development in the high southern latitudes during this period of fundamental climatic shifts. The temporal evolution of $\delta^{18}O_{lw\text{-}corr}$ of Laguna Potrok Aike is largely controlled by changes in $\delta^{18}O$ of the source water of lake, surface air temperature and evaporative ^{18}O enrichment.

Considering the occurrence of permafrost during the Glacial, the $\delta^{18}O_{lw\text{-}corr}$ record between 26,000 and 21,000 cal. BP is best explained by a main water supply from isolated groundwater whose $\delta^{18}O$ may not be as depleted as that of glacial meteoric water. Moreover, probably reduced interchange between in- and outflows and generally decreased inflows would have prolonged the lake water residence time. Under these circumstances, the higher than expected $\delta^{18}O_{lw\text{-}corr}$ during this period could be achieved despite possibly weakened evaporation under glacial conditions. Between 21,000 and 17,600 cal. BP, coinciding with the timing of a reconstructed lake level overflow of Laguna Potrok Aike, large ^{18}O depletion in $\delta^{18}O_{lw\text{-}corr}$ record is observed. Low $\delta^{18}O_{lw\text{-}corr}$ together with the overflow situation could be linked to an increased proportion of ^{18}O depleted ice or snow melt water reaching Laguna Potrok Aike via groundwater and surface inflows.

During the early phase of the last deglaciation from 17,600 to 15,600 cal. BP, the $\delta^{18}O_{lw\text{-}corr}$ showed a distinct increase. Considering the influence of strongly increased temperature during this phase with fundamental climatic shifts, this development of $\delta^{18}O_{lw\text{-}corr}$ can be interpreted as rapid climatic warming resulting in enhanced temperature-driven evaporation and cumulatively ^{18}O enriched meteoric water. Nevertheless, our data would also be in line with the hypothesis about a rapid poleward shift of the SHW (Toggweiler et al., 2006) causing increased opal flux in the Southern Ocean (Anderson et al., 2009) as well as elevated atmospheric CO_2 concentrations (Schmitt et al., 2012) immediately after the onset of the last deglaciation, given wind-driven evaporation as the sole driver of increasing $\delta^{18}O_{lw\text{-}corr}$.

The subsequent period from 15,600 to 14,600 cal. BP is characterized by declining $\delta^{18}O_{lw\text{-}corr}$ of the Patagonian steppe lake. This period is not equivalent to the ACR, because its onset preceded the ACR by at least 500 years according to the independent tephra time marker. It seems plausible to interpret this decline as the transition from a mainly temperature-driven

towards a wind-driven evaporative enrichment of $\delta^{18}O_{lw\text{-}corr}$. With the end of the strong temperature rise during the first two millennia and the onset of intensified SHW, $\delta^{18}O_{lw\text{-}corr}$ would be initially reduced due to the increased heat export from the continent and the import of depleted moisture from the Pacific.

After 14,600 cal. BP, $\delta^{18}O_{lw\text{-}corr}$ resumed its strong increase, indicating that at the latest from now on the intensifying SHW exerted its dominant control on the lake water balance of Laguna Potrok Aike by strengthened wind-driven evaporation. The SHW must have been established at the latitude of Laguna Potrok Aike (52°S) and increased in strength towards the early Holocene when the maximum was reached.

The overall development of the $\delta^{18}O_{lw\text{-}corr}$ during the last glacial-interglacial transition is consistent with lake level reconstructions describing an overflow situation prior to 17,000 cal. BP and lowering of lake level during the early Holocene, suggesting the development of a strongly evaporative steppe climate in the Laguna Potrok Aike region over the course of the last deglaciation.

Our interpretation of the $\delta^{18}O_{lw\text{-}corr}$ record of Laguna Potrok Aike provides a new view to the highly controversial topic regarding the patterns of changes in the SHW throughout the last glacial-interglacial transition and demonstrates that the understanding of SHW evolution in the high southern latitudes during this dynamic period is still far away from a consensus.

Acknowledgement

We are indebted to J-P. Frahm and L. Hedenäs for identification of aquatic mosses. This research used samples provided by the International Continental Scientific Drilling Program (ICDP) in the framework of the Potrok Aike Maar Lake Sediment Archive Drilling Project (PASADO). Funding for drilling was provided by the ICDP, the German Science Foundation (DFG), the Swiss National Funds (SNF), the Natural Sciences and Engineering Research Council of Canada (NSERC), the Swedish Vetenskapsrådet (VR) and the University of Bremen, Germany. The study was funded by grants of the DFG (LU786/7-1,2, MA4235/4-1,2) in the framework of the SPP1006 (ICDP). J. Zhu is very grateful to F. Lehmkuhl (RWTH Aachen University, Germany) for co-supervision of his PhD thesis.

Chapter 5

Synthesis

This thesis is placed within the framework of the Potrok Aike maar lake sediment archive drilling project (PASADO) and aims to explore late Quaternary environmental development of southern extra-Andean Patagonia by using an isotopic proxy approach. Stable isotope analyses of sedimentary organic material ($\delta^{13}C_{TOC}$ and $\delta^{15}N_{TN}$ for bulk sedimentary organic matter and $\delta^{18}O$ for subfossil aquatic moss remains) preserved in pelagic sediments of Laguna Potrok Aike are conducted to reconstruct the development of the lacustrine system and the southern Patagonian climate during the last glacial-interglacial transition period (26,000 – 8500 cal. BP), a period with fundamental climatic shifts.

The main findings of this thesis are summarized as follows:

1) Subfossil submerged aquatic mosses deposited in lacustrine sediments are useful proxy materials to reconstruct the past lake water $\delta^{18}O$ ($\delta^{18}O_{lw}$) based on a verified highly significant linear correlation between $\delta^{18}O$ of aquatic mosses (both moss cellulose and bulk moss organic matter) and their host waters. The large difference observed in the $\delta^{13}C$ of aquatic mosses and aquatic vascular plants is a good indicator for probable composition of the coarse aquatic plant debris, whose cellulose fraction can also be used to infer $\delta^{18}O_{lw}$ to some extent. Due to the observed isotopic discrepancy among different species, it is suggested that monospecific analysis of bulk moss organic matter should be preferred for the reconstruction of $\delta^{18}O_{lw}$. Indistinguishable bulk organic matter $\delta^{18}O$ values between shoots and leaves of submerged mosses imply that separation of different tissues is not necessary. C/O ratios of cellulose and bulk organic matter of subfossil moss remains can provide evidence for the purity of extracted cellulose and well-preserved moss material in the sediments. Based on oxygen isotope analyses of the handpicked subfossil submerged aquatic mosses preserved in Laguna Potrok Aike sediments, this thesis has generated a record of reconstructed $\delta^{18}O_{lw}$ ($\delta^{18}O_{lw\text{-}corr}$) for the last glacial-interglacial transition to assess changes in lake water balance and to identify the respective forcing factors.

2) Under full glacial conditions, from ca. 26,000 to 17,600 cal. BP, the lake had a very low primary productivity with a dominant organic matter source from lake algae (Fig. 5.1d, e and f). The narrow range of changes in $\delta^{15}N_{TN}$ may reflect little changes in the lacustrine nitrogen cycle during that time (Fig. 5.1g). The reconstructed glacial $\delta^{18}O_{lw\text{-}corr}$ was only about 3‰ lower than modern values and much less negative than expected (Fig. 5.1c). This could have resulted from the largely from meteoric waters isolated groundwater body owing to permafrost conditions. In addition, lake water residence time could be prolonged because of reduced interchanges between in- and outflows and generally decreased inflows. Under these circumstances, the higher than expected glacial $\delta^{18}O_{lw\text{-}corr}$ during this period could be achieved despite possibly weakened evaporation under glacial conditions. Large ^{18}O depletion in glacial $\delta^{18}O_{lw\text{-}corr}$ is observed for the period between 21,000 and 17,600 cal. BP, coinciding with the timing of a reconstructed lake level overflow of Laguna Potrok Aike. Low $\delta^{18}O_{lw\text{-}corr}$ together with the overflow situation could be linked to an increased proportion of ^{18}O depleted ice or snow melt water reaching Laguna Potrok Aike via groundwater and surface inflows.

3) At around 17,600 cal. BP, the lake underwent a rapid reorganization, demonstrated by increased lacustrine primary productivity (both aquatic macrophytes and algae) (Fig. 5.1d, e and f) and a distinct increase in $\delta^{18}O_{lw\text{-}corr}$ (Fig. 5.1g), in line with Antarctic warming and rising atmospheric CO_2 concentrations (Fig. 5.1a and b) as well as rapid glacier retreat in southern Patagonia. The main cause for this large shift of both primary productivity and lake water balance can be ascribed to rapid deglacial warming which could have resulted in partial thermal summer stratification and improved growing conditions for primary producers in the lake with increased nutrient supply from the catchment. Increased air temperature caused, on the one hand, strengthened temperature-driven evaporation resulting in the ^{18}O enrichment of lake water and, on the other hand, led also to cumulatively more ^{18}O enriched meteoric water. Due to thawing permafrost, the change in meteoric water isotopic composition could be transferred further into the groundwater and, subsequently, into the lake water.

4) The subsequent period from 15,600 to 14,600 cal. BP is characterized by declining $\delta^{18}O_{lw\text{-}corr}$. This period is not equivalent to the Antarctic Cold Reversal (ACR), because its onset preceded the ACR by at least 500 years according to the independent tephra time marker Reclús R_1. It seems plausible to interpret this decline as the transition from a mainly

temperature-driven towards a wind-driven evaporative ^{18}O enrichment of lake water. $\delta^{18}O_{lw\text{-}corr}$ would be initially reduced with the end of the strong temperature rise during the first two millennia of last deglaciation (17,600 – 15,600 cal. BP) and the onset of intensifying SHW. After 14,600 cal. BP, $\delta^{18}O_{lw\text{-}corr}$ resumed its strong increase, indicating that at the latest from now on the intensifying SHW exerted its dominant control on the lake water balance of Laguna Potrok Aike by strengthened wind-driven evaporation. Since then, the SHW must have been established at the latitude of Laguna Potrok Aike (52°S) and increased in strength towards the early Holocene. Since the onset of the early Holocene, the lacustrine system appeared to approach a new state with deteriorated growing conditions for all primary producers, reflected by lowered primary productivity towards a level comparable to that of the full Glacial. This development was likely caused by windier conditions and insufficient nutrient availability probably due to the low regeneration of nutrients in the lake after its exhaustion during the early phase with high primary productivity.

5) The aquatic primary productivity remained high during the last deglaciation. However, the deglacial variations of TOC, $\delta^{13}C_{TOC}$ and TOC/TN ratios are obviously larger than during the full Glacial, suggesting the instability of lake and environment during this transitional period. By using the updated age-depth model given in Chapter 4, the data profiles of $\delta^{13}C_{TOC}$, $\delta^{1}5N_{TN}$, TOC and TOC/TN ratio shift in the direction of more than 1000 years younger ages over the course of the last deglaciation compared to the previous ones shown in Chapter 2 (cf. Fig. 2.6 and 5.1). According to this, two large reductions in TOC have occurred within the periods 14,500 – 13,500 cal. BP and 12,400 – 11,800 cal. BP (Fig. 5.1e). However, both large declines in TOC may not be mainly a result of changes in lacustrine primary productivity, because of the independent change in $\delta^{13}C_{TOC}$ during both periods. A dilution effect could probably account for such large variations in TOC, because XRF data by Jouve et al. (2013) have shown relatively high Si contents in both periods, which are interpreted as an indicator of detrital input.

6) The overall reconstructed evolution of lacustrine primary productivity, nutrient supply and lake water balance of Laguna Potrok Aike during the last glacial-interglacial transition is in agreement with lake level reconstructions describing an overflow situation prior to 17,000 cal. BP and lowering of lake level during the early Holocene (Zolitschka et al., 2013), suggesting the development of a strongly evaporative steppe climate in the Laguna Potrok

Aike region over the course of the last deglaciation, along with the climatic shifts in Antarctica.

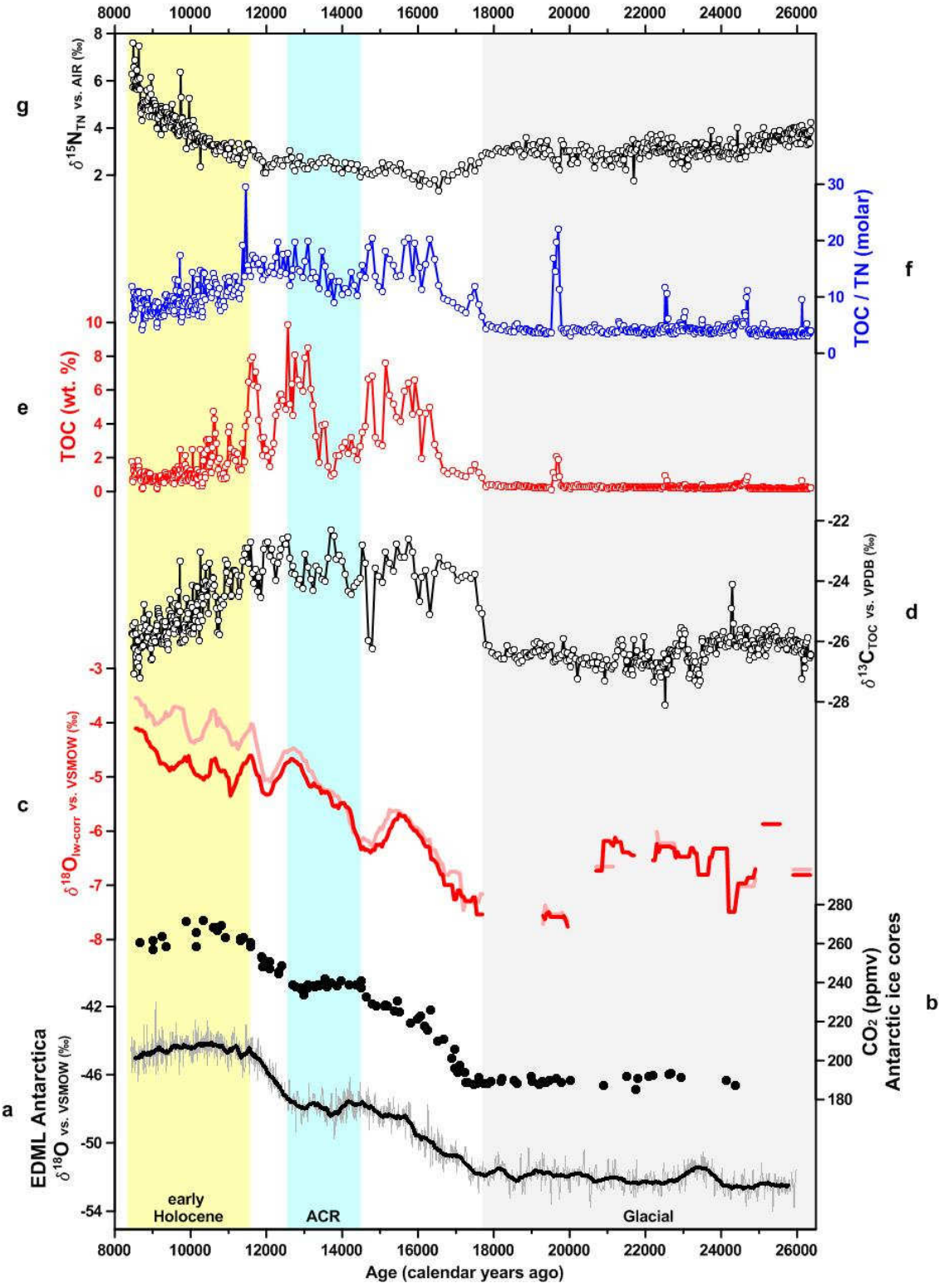


Figure 5.1. Proxy records of Laguna Potrok Aike in comparison with Antarctic records, plotted on the age-scale given in Chapter 4. **a)** $\delta^{18}O$ record from EDML of East Antarctica (EPICA Community Members, 2006). **b)** CO_2 concentration from Antarctic ice cores (Schmitt et al., 2012). **c)** Reconstructed lake-water $\delta^{18}O$ ($\delta^{18}O_{lw\text{-}corr}$) of Laguna Potrok Aike (Chapter 4), smoothed by a 500-years window (red: smoothing of average $\delta^{18}O_{lw\text{-}corr}$ values inferred from bulk aquatic moss organic matter

and aquatic moss cellulose; pale red: smoothing of $\delta^{18}O_{lw\text{-}corr}$ values inferred from residue cellulose). Ocean water effect during the LGM and deglaciation has been corrected according to Lea et al. (2002). **d)** $\delta^{13}C_{TOC}$ of bulk organic matter (<200µm) (Zhu et al., 2013). **e)** TOC content of bulk organic matter (<200µm) (Zhu et al., 2013). **f)** TOC/TN molar ratio of bulk organic matter (<200µm) (Zhu et al., 2013). **g)** $\delta^{15}N_{TN}$ of bulk organic matter (<200µm) (Zhu et al., 2013). ACR: Antarctic Cold Reversal.

Outlook

A preliminary study of glacial primary productivity in Laguna Potrok Aike has shown a probable climatic linkage between southern Patagonia and Antarctica during the full Glacial (Lücke et al., 2013). Despite their discontinuous appearence, the good availability of aquatic moss remains in glacial pelagic sediments allows a reconstruction of glacial $\delta^{18}O_{lw\text{-}corr}$ of Laguna Potrok Aike back to more than 50,000 years B.P. The extension of the $\delta^{18}O_{lw\text{-}corr}$ record would give us new insights into changes in the hydrological processes in southern extra-Andean Patagonia during the full Glacial and permit a better understanding of the connection between the lake response in southern Patagonia and the signals from Antarctica and the Southern Ocean. A reliable interpretation of glacial $\delta^{18}O_{lw\text{-}corr}$ and inter-site comparison could, however, only be achieved by a robust age-depth model of lake sediments and a better understanding of glacial conditions affecting lake hydrology, which could be constrained by multidisciplinary proxy studies of full Glacial sediments. In addition, even if numerous studies have shown that the fractionation of the oxygen isotopes between cellulose and host-water is independent of water temperature (cf. Wolfe et al., 2007), temperature effect on cellulose oxygen isotope enrichment relative to source water proposed by Sternberg and Ellsworth (2011) deserves careful laboratory studies to accomplish a robust isotopic proxy approach based on aquatic mosses.

References

Aagesen D. (2000) Crisis and conservation at the end of the world: sheep ranching in Argentine Patagonia. *Environmental Conservation* 27, 208-215.

Allen C. S., Pike J. and Pudsey C. J. (2011) Last glacial-interglacial sea-ice cover in the SW Atlantic and its potential role in global deglaciation. *Quaternary Science Reviews* 30, 2446-2458.

Anderson K. K., Svensson A., Johnsen S. J., Rasmussen S. O., Bigler M., Röthlisberger R., Ruth U., Siggaard-Anderson, M.-L., Steffensen J. P., Dahl-Jensen, D., Vinther B. M. and Clausen H. B. (2006) The Greenland Ice Core Chronology 2005, 15-42 ka. Part 1: constructing the time scale. *Quaternary Science Reviews* 25, 3246-3257.

Anderson R. F., Ali S., Bradtmiller L. I., Nielsen S. H. H., Fleisher, M. Q., Anderson B. E. and Burckle L. H. (2009) Wind-driven upwelling in the Southern Ocean and the deglacial rise in atmospheric CO_2. *Science* 323, 1443-1448.

Anselmetti F., Ariztegui D., De Batist M., Gebhardt C., Haberzettl T., Niessen F., Ohlendorf C. and Zolitschka B. (2009) Environmental history of southern Patagonia unravelled by the seismic stratigraphy of Laguna Potrok Aike. *Sedimentology* 56, 873-892.

Ariztegui D., Gilli A., Anselmetti F. S., Goñi R. A., Belardi J. B. and Espinosa S. (2010) Lake-level changes in central Patagonia (Argentina): crossing environmental thresholds for Lateglacial and Holocene human occupation. *Journal of Quaternary Science* 25, 1092-1099.

Bain J. T. and Proctor M. C. F. (1980) The requirement of aquatic bryophytes for free CO_2 as an inorganic carbon source: some experimental evidence. *New Phytologist* 86, 393-400.

Baruth B., Endlicher W. and Hoppe P. (1998) Climate and desertification processes in Patagonia. *Bamberger Geographische Schriften* 15, 307-320.

Batjes N. H. (1996) Total carbon and nitrogen in the soils of the world. *European Journal of Soil Science* 47, 151-163.

Benner R., Fogel M. L., Sprague E. K. and Hodson R. E. (1987) Depletion of ^{13}C in lignin and its implication for stable carbon isotope studies. *Nature* 329, 708-710.

Bertrand S., Sterken M., Vargas-Ramirez L., De Batist M., Vyverman W., Lepoint G. and Fagel N. (2010) Bulk organic geochemistry of sediments from Puyehue Lake and its watershed (Chile, 40°S): Implications for paleoenvironmental reconstructions. *Palaeogeography, Palaeoclimatology, Palaeoecology* 294, 56-71.

Beuning K. R. M., Kelts K., Russell J. and Wolfe B. B. (2002) Reassessment of Lake Victoria-Upper Nile River paleohydrology from oxygen isotope records of lake-sediment cellulose. *Geology* 30, 559-562.

Blaauw M. (2010) Methods and code for 'classical' age-modelling of radiocarbon sequences. *Quaternary Geochronology* 5, 512-518.

Blomqvist P., Pettersson A. and Hyenstrand P. (1994) Ammonium-nitrogen – a key regulatory factor causing dominance of non-nitrogen-fixing cyanobacteria in aquatic systems. *Archiv für Hydrobiologie* 132, 141-164.

Boettger T., Haupt M., Knöller K., Weise S., Waterhouse J., Rinne K., Loader N., Sonninen E., Jungner H., Masson-Delmotte V., Stievenard M., Guillemin M., Pierre M., Pazdur A., Leuenberger M., Filot M., Saurer M., Reynolds C., Helle G. and Schleser G. (2007) Wood cellulose preparation methods and mass spectrometric analyses of $\delta^{13}C$, $\delta^{18}O$, and nonexchangeable $\delta^{2}H$ values in cellulose, sugar, and starch: an interlaboratory comparison. *Analytical Chemistry* 79, 4603-4612.

Brand W. A., Coplen T. B., Aerts-Bijma A. T., Böhlke J. K., Gehre M., Geilmann H., Gröning M., Jansen H. G., Meijer H. A., Mroczkowski S. J., Qi H., Soergel K., Stuart-Williams H., Weise S. M. and Werner R. A. (2009) Comprehensive inter-laboratory calibration of reference materials for $\delta^{18}O$ versus VSMOW using various on-line high-temperature conversion techniques. *Rapid Communications in Mass Spectrometry* 23, 999-1019.

Burkhardt S., Riebesell U. and Zondervan I. (1999) Effects of growth rate, CO_2 concentration, and cell size on the stable carbon isotope fractionation in marine phytoplankton. *Geochimica et Cosmochimica Acta* 63, 3729-3741.

Caniupán M., Lamy F., Lange C. B., Kaiser J., Arz H., Kilian R., Baeza Urrea O., Aracena C., Hebbeln D., Kissel, C., Laj C., Mollenhauer G. and Tiedemann R. (2011) Millennial-scale sea surface temperature and Patagonia Ice Sheet changes off southernmost Chile (53°S) over the past ~60 kyr. *Paleoceanography* 26, PA3221, doi: 10.1029/2010PA0020 49.

Cerveny R. (1998) Present Climates of South America. In *Climates of the Southern Continents, Present, Past and Future* (eds. J. Hobbs, J. Lindesay and H. Bridgman). John Wiley & Sons, 107-135.

Chapligin B., Leng M., Webb E., Alexandre A., Dodd J., Ijiri A., Lücke A., Shemesh A., Abelmann A., Herzschuh U., Longstaffe F., Meyer H., Moschen R., Okazaki Y., Rees N., Sharp Z., Sloane H., Sonzogni C., Swann G., Sylvestre F., Tyler J. and Yam R. (2011) Inter-laboratory comparison of oxygen isotope compositions from biogenic silica. *Geochimica et Cosmochimica Acta* 75, 7242-7256.

Chavaillaz Y., Codron F. and Kageyama M. (2013) Southern westerlies in LGM and future (RCP4.5) climates. *Climate of the Past* 9, 517-524.

Chinn T. J. (1993) Physical hydrology of the Dry Valley lakes. In *Physical and Biogeochemical Processes in Antarctic lakes, Antarctic Research Series* (eds. G. W. J. Friedman and E. I. Friedman). American Geophysical Union, Washington DC, 1–51.

Clow G. D., McKay C. P., Simmons G. M. and Wharton R. A. (1988) Climatological observations and predicted sublimation rates at Lake Hoare, Antarctica. *Journal of Climate* 1, 715-728.

Cooper L. and DeNiro M. (1989) Oxygen-18 content of atmospheric oxygen does not affect the oxygen isotope relationship between environmental water and cellulose in a submerged aquatic plant, *Egeria densa* Planch. *Plant Physiology* 91, 536-541.

Coplen T. B., Brand W. A., Gehre M., Gröning M., Meijer H. A. J., Toman B. and Verkouteren R. M. (2006) New Guidelines for $\delta^{13}C$ Measurements. *Analytical Chemistry* 78, 2439-2441.

Coronato A., Ercolano B., Corbella H. and Tiberi, P. (2013) Glacial, fluvial and volcanic landscape evolution in the Laguna Potrok Aike maar area, Argentina. *Quaternary Science Reviews* 71, 13-26.

Daley T. J., Barber K. E., Street-Perrott F. A., Loader N. J., Marshall J. D., Crowley S. F. and Fisher E. H. (2010) Holocene climate variability revealed by oxygen isotope analysis of *Sphagnum* cellulose from Walton Moss, northern England. *Quaternary Science Reviews* 29, 1590-1601.

Darling W. G., Bath A. H., Gibson J. J. and Rozanski K. (2005) Isotopes in water. In *Isotopes in Palaeoenvironmental Research* (eds. M. J. Leng). Springer, Dordrecht, 1-66.

DeNiro M. J. and Epstein S. (1977) Mechanism of Carbon Isotope Fractionation Associated with Lipid Synthesis. *Science* 197, 261-263.

DeNiro M. J. and Epstein S. (1981) Isotopic composition of cellulose from aquatic organisms. *Geochimica et Cosmochimica Acta* 45, 1885-1894.

Denton G. H., Anderson R. F., Toggweiler J. R., Edwards R. L., Schaefer J. M. and Putnam A. E. (2010) The Last Glacial Termination. *Science* 328, 1652-1656.

Deplazes G., Lückge A., Peterson L. C., Timmermann A., Hamann Y., Hughen K. A., Röhl U., Laj C., Cane M. A., Sigman D. M. and Haug G. H. (2013) Links between tropical rainfall and north Atlantic climate during the last glacial period. *Nature Geoscience* 6, 213-217.

Dickson J. H. (1986) Chapter 30: Bryophyte analysis. In *Handbook of Holocene Paleoecology and Paleohydrology* (eds. B. E. Berglund). J. Wiley & Sons, New York, 622-643.

Dokulil M. and Teubner K. (2000) Cyanobacterial dominance in lakes. *Hydrobiologia* 438, 1-12.

Downing J., Watson S. and McCauley E. (2001) Predicting cyanobacteria dominance in lakes. *Canadian Journal of Fisheries and Aquatic Sciences* 58, 1905-1908.

Edwards T. W. D. and McAndrews J. H. (1989) Paleohydrology of a Canadian Shield lake inferred from ^{18}O in sediment cellulose. *Canadian Journal of Earth Sciences* 26, 1850-1859.

Edwards T. W. D., Wolfe B. B., Gibson J. J. and Hammarlund D. (2004) Use of water isotope traces in high latitude hydrology and paleohydrology. In *Long-term Environmental Change in Arctic and Antarctic lakes* (eds. R. Pienitz, M. S. V. Douglas and J. P. Smol), Springer, Dordrecht, 187-207.

El Bilali H. and Patterson R. T. (2012) Influence of cellulose oxygen isotope variability in sub-fossil *Sphagnum* and plant macrofossil components on the reliability of paleoclimate records at the Mer Bleue Bog, Ottawa, Ontario, Canada. *Organic Geochemistry* 43, 39-49.

EPICA community members (2006) One-to-one coupling of glacial climate variability in Greenland and Antarctica. *Nature* 444, 195-198.

Epstein S., Yapp C. J. and Hall J. H. (1976) The determination of the D/H ratio of non-exchangeable hydrogen in cellulose extracted from aquatic and land plants. *Earth and Planetary Science Letters* 30, 241-251.

Epstein S., Thompson P. and Yapp C. J. (1977) Oxygen and hydrogen isotopic ratios in plant cellulose. *Science* 198, 1209-1215.

Erickson M. and Miksche G. E. (1974) On the occurrence of lignin or polyphenols in some mosses and liverworts. *Phytochemistry* 13, 2295-2299.

Frahm J-P. (2001) Aquatic moss balls of *Blindia inundata* in Patagonia. *The Bryologist* 104, 502-503.

Freudenthal T., Wagner T., Wenzhöfer F., Zabel M. and Wefer G. (2001) Early diagenesis of organic matter from sediments of the eastern subtropical Atlantic: Evidence from stable nitrogen and carbon isotopes. *Geochimica Cosmochimica Acta* 65, 1795-1808.

Fry B. (2006) Stable isotope ecology. Springer, New York.

Garreaud R., Vuille M., Compagnucci R. and Marengo J. (2009) Present-day South American climate. *Palaeogeography, Palaeoclimatology, Palaeoecology* 281, 180-195.

Garreaud R., Lopez P., Minvielle M. and Rojas, M. (2013) Large-scale control on the Patagonian climate. *Journal of Climate* 26, 215-230.

Gat J.R. (2010) Isotope Hydrology: A study of the water cycle. Imperial College Press, London.

Gebhardt A. C., De Batist M., Niessen F., Anselmetti F. S., Ariztegui D., Haberzettl T., Kopsch C., Ohlendorf C. and Zolitschka B. (2011) Deciphering lake and maar geometries from seismic refraction and reflection surveys in Laguna Potrok Aike (southern Patagonia, Argentina). *Journal of Volcanology and Geothermal Research* 201, 357-363.

Gebhardt A. C., Ohlendorf C., Niessen F., De Batist M., Anselmetti F., Ariztegui D., Kliem P., Wastegård S. and Zolitschka B. (2012) Seismic evidence of up to 200 m lake-level change in Southern Patagonia since Marine Isotope Stage 4. *Sedimentology* 59, 1087-1100.

Gersonde R., Crosta X., Abelmann A. and Armand L. (2005) Sea-surface temperature and sea ice distribution of the Southern Ocean at the EPILOG Last Glacial Maximum – a circum-Antarctic view based on siliceous microfossil records. *Quaternary Science Reviews* 24, 869-896.

Glasser N.F., Jansson K.N., Harrison S. and Kleman J. (2008) The glacial geomorphology and Pleistocene history of South America between 38°S and 56°S. *Quaternary Science Reviews* 27, 365-390.

Glime J. M. (2007) *Bryophyte Ecology*. Volume 1. Physiological Ecology. E-book sponsored by Michigan Technological University and the International Association of Bryologists. Accessible at: http://www.bryoecol.mtu.edu, last access: 21 May 2014.

Goffinet B., Buck W. R. and Shaw A. J. (2008) Morphology, anatomy, and classification of the Bryophyta. In *Bryophyte Biology* (eds. B. Goffinet and A. J. Shaw). Cambridge University Press, Cambridge. 55-138.

Gourcy L. L., Groening M. and Aggarwal P. K. (2005) Stable oxygen and hydrogen isotopes. In *Isotopes in the water cycle: past, present and future of a developing science* (eds. P.K. Aggarwal, J. R. Gat and K. F. O. Froehlich). Springer, Dordrecht, 39-52.

Grimm E. (1987) CONISS: a fortran 77 program for stratigraphically constrained cluster analysis by the method of the incremental sum squares. *Computers and Geosciences* 13, 13-35.

Guilderson T., Burckle L., Hemming S. and Peltier W. (2000) Late Pleistocene sea level variations derived from the Argentine Shelf. *Geochemistry Geophysics Geosystems* 1, 1055, doi:10.1029/2000GC000098.

Haberzettl T., Corbella H., Fey M., Janssen S., Lücke A., Mayr C., Ohlendorf C., Schäbitz F., Schleser G., Wille M., Wulf S. and Zolitschka B. (2007) Lateglacial and Holocene wet-dry cycles in southern Patagonia: chronology, sedimentology and geochemistry of a lacustrine record from Laguna Potrok Aike, Argentina. *The Holocene* 17, 297-310.

Haberzettl T., Kück B., Wulf S., Anselmetti F., Ariztegui D., Corbella H., Fey M., Janssen S., Lücke A., Mayr C., Ohlendorf C., Schäbitz F., Schleser G. H., Wille M. and Zolitschka B. (2008) Hydrological variability in southeastern Patagonia and explosive volcanic activity in the southern Andean Cordillera during Oxygen Isotope Stage 3 and the Holocene inferred from lake sediments of Laguna Potrok Aike, Argentina. *Palaeogeography Palaeoclimatology Palaeoecology* 259, 213–229.

Hahn A., Kliem P., Ohlendorf C., Zolitschka B., Rosén P. and the PASADO Science Team (2013) Climate induced changes as registered in inorganic and organic sediment

components from Laguna Potrok Aike (Argentina) during the past 51 ka. *Quaternary Science Reviews* 71, 154-166.

Healey F. and Hendzel L. (1980) Physiological indicators of nutrient deficiency in lake phytoplankton. *Canadian Journal of Fisheries and Aquatic Sciences* 37, 442-453.

Hedenäs L. (1997) The *Drepanocladus* s. str. species with excurrent costae (Amblystegiaceae). *Nova Hedwigia* 64, 535-547.

Heegaard E., Birks H. J. B. and Telford R. J. (2005) Relationships between calibrated ages and depth in stratigraphical sequences: an estimation procedure by mixed-effect regression. *The Holocene* 15, 612-618.

Heikkilä M., Edwards T. W. D., Seppä H. and Sonninen E. (2010) Sediment isotope tracers from Lake Saarikko, Finland, and implications for Holocene hydroclimatology. *Quaternary Science Reviews* 29, 2146-2160.

Heusser C. J. (1989) Southern westerlies during the Last Glacial Maximum. *Quaternary Research* 31, 423-425.

Hodell D. and Schelske C. (1998) Production, sedimentation, and isotopic composition of organic matter in Lake Ontario. *Limnology Oceanography* 43, 200-214.

Hogg A, Hua Q., Blackwell P., Niu M., Buck C., Guilderson T., Heaton T., Palmer J., Reimer P., Reimer R., Turney C. and Zimmerman S. (2013) SHCal13 Southern Hemisphere Calibration, 0-50,000 years cal BP. *Radiocarbon* 55, 1889-1903.

Hollander D. and McKenzie J. (1991) CO_2 control on carbon-isotope fractionation during aqueous photosynthesis: A paleo-pCO_2 barometer. *Geology* 19, 929-932.

Hubbard A., Hein A. S., Kaplan M. R., Hulton N. R. J. and Glasser N. (2005) A modeling reconstruction of the last glacial maximum ice sheet and its deglaciation in the vincinity of the northern Patagonian icefeld, South America. *Geografiska Annaler* 87(A), 375-391.

Hulton N., Purves R., McCulloch R., Sugden D. and Bentley M. (2002) The Last Glacial Maximum and deglaciation in southern South America. *Quaternary Science Reviews* 21, 233-241.

IAEA/WMO (2014) Global Network of Isotopes in Precipitation. The GNIP Database. Accessible at: http://www.iaea.org/water, last access: 21 May 2014.

Imura S., Bando T., Seto K., Ohtani S., Kudoh S. and Kanda H. (2003) Distribution of aquatic mosses in the Sôya Coast region, East Antarctica. *Polar Bioscience* 16, 1-10.

Janssens J. A. (1990) Methods in Quaternary Ecology 11. Bryophytes. *Geoscience Canada* 17, 13-24.

Jones R., King L., Dent M., Maberly S. and Gibson E. (2004) Nitrogen stable isotope ratios in surface sediments, epilithon and macrophytes from upland lakes with differing nutrient status. *Freshwater Biology* 49, 382-391.

Jonsgard B. and Birks H. (1995) Late-glacial mosses and environmental reconstructions at Kråkenes, western Norway. *Lindbergia* 20, 64-82.

Jouve G., Francus P., Lamoureux S., Provencher-Nolet L., Hahn A., Haberzettl T., Fortin D. and Nuttin L. (2013) Microsedimentological characterization using image analysis and μ-XRF as indicators of sedimentary processes and climate changes during Lateglacial at Laguna Potrok Aike, Santa Cruz, Argentina. *Quaternary Science Reviews* 71, 191-204.

Jouzel J., Masson-Delmotte V., Cattani O., Dreyfus G., Falourd S., Hoffmann G., Minster B., Nouet J., Barnola J. M., Chappellaz J., Fischer H., Gallet J. C., Johnsen S., Leuenberger M., Loulergue L., Luethi D., Oerter H., Parrenin F., Raisbeck G., Raynaud D., Schilt A., Schwander J., Selmo E., Souchez R., Spahni R., Stauffer B., Steffensen J. P., Stenni B., Stocker T. F., Tison J. L., Werner M. and Wolff E. W. (2007) Orbital and millennial Antarctic climate variability over the past 800,000 years. *Science* 317, 793-796.

Kaplan M., Fogwill C., Sugden D., Hulton N., Kubik P. and Freeman S. (2008) Southern Patagonian glacial chronology for the Last Glacial period and implications for Southern Ocean climate. *Quaternary Science Reviews* 27, 284-294.

Kastner S., Ohlendorf C., Haberzettl T., Lücke A., Mayr C., Maidana N., Schäbitz F. and Zolitschka B. (2010) Southern hemispheric westerlies control the spatial distribution of modern sediments in Laguna Potrok Aike, Argentina. *Journal of Paleolimnology* 44, 887-902.

Keeley J. and Sandquist D. (1992) Carbon: freshwater plants. *Plant, Cell & Environment* 15, 1021-1035.

Kienast M., Higginson M. J., Mollenhauer G., Eglinton T. I., Chen M.-T. and Calvert S. E. (2005) On the sedimentological origin of down-core variations of bulk sedimentary nitrogen isotope ratios. *Paleoceanography* 20, PA2009, doi:10.1029/2004PA001081.

Kilian R., Schneider C., Koch J., Fesq-Martin M., Biester H., Casassa G., Arévalo M., Wendt G., Baeza O. and Behrmann J. (2007) Palaeoecological contraints on late Glacial and Holocene ice retreat in the Southern Andes (53°S). *Global and Planetary Change* 59, 49-66.

Kilian R. and Lamy F. (2012) A review of Glacial and Holocene paleoclimate records from southernmost Patagonia (49-55°S). *Quaternary Science Reviews* 53, 1-23.

Kliem P., Buylaert J. P., Hahn A., Mayr C., Murray A. S., Ohlendorf C., Veres D., Wastegård S., Zolitschka B. and the PASADO Science Team (2013a) Magnitude, geomorphologic response and climate links of lake level oscillations at Laguna Potrok Aike, Patagonian steppe (Argentina). *Quaternary Science Reviews* 71, 131-146.

Kliem P., Enters D., Hahn A., Ohlendorf C., Lisé-Pronovost A., St-Onge G., Wastegård S., Zolitschka B. and the PASADO Science Team (2013b) Lithology, radiocarbon chronology and sedimentological interpretation of the lacustrine record from Laguna Potrok Aike, southern Patagonia. *Quaternary Science Reviews* 71, 54-69.

Kohfeld K. E., Graham R. M., de Boer A. M., Sime L. C., Wolff, E. W., Le Quéré C. and Bopp L. (2013) Southern Hemisphere westerly wind changes during the Last Glacial Maximum: paleo-data synthesis. *Quaternary Science Reviews* 68, 76-95.

Lamy F., Hebbeln D. and Wefer G. (1999) High-resolution marine record of climatic change in mid-latitude Chile during the last 28,000 years based on terrigenous sediment parameters. *Quaternary Research* 51, 83-93.

Lamy F., Kaiser J., Arz H. W., Hebbeln D., Ninnemann U., Timm O., Timmermann A. and Toggweiler J. R. (2007) Modulation of the bipolar seesaw in the Southeast Pacific during Termination 1. *Earth and Planetary Science Letters* 259, 400-413.

Laws E., Popp B., Bidigare R., Kennicutt M. and Macko S. (1995) Dependence of phytoplankton carbon isotopic composition on growth rate and CO_2aq: Theoretical considerations and experimental results. *Geochimica et Cosmochimica Acta* 59, 1131-1138.

Lea D. W., Martin P. A., Pak D. K. and Spero H. J. (2002) Reconstructing a 350ky history of sea level using planktonic Mg/Ca and oxygen isotope records from a Cocos Ridge core. *Quaternary Science Reviews* 21, 283-293.

Lehmann M., Bernasconi S., Barbieri A. and McKenzie J. (2002) Preservation of organic matter and alternation of its carbon and nitrogen isotope composition during simulated and in situ early sedimentary diagenesis. *Geochimica et Cosmochimica Acta* 66, 3573-3584.

Lehmann M., Bernasconi S., Barbieri A., Simona M. and McKenzie J. (2004a) Interannual variation of the isotopic composition of sedimenting organic carbon and nitrogen in Lake Lugano: a long-term sediment trap study. *Limnology and Oceanography* 49, 839-849.

Lehmann M., Bernasconi S., McKenzie J., Barbieri A., Simona M. and Veronesi M. (2004b) Seasonal variation of the $\delta^{13}C$ and $\delta^{15}N$ of particulate and dissolved carbon and nitrogen in Lake Lugano: constraints on biogeochemical cycling in a eutrophic lake. *Limnology and Oceanography* 49, 415-429.

Leng M. J. and Marshall J. D. (2004) Palaeoclimate interpretation of stable isotope data from lake sediment archives. *Quaternary Science Reviews* 23, 811-831.

Leuenberger M., Siegenthaler U. and Langway C. (1992) Carbon isotope composition of atmospheric CO_2 during the last ice age from an Antarctic ice core. *Nature* 357, 488-490.

Li S., Ochyra R., Wu P., Seppelt R. D., Cai M., Wang H. and Li C. (2009) *Drepanocladus longifolius* (Amblystegiaceae), an addition to the moss flora of King George Island, South Shetland Islands, with a review of Antarctic benthic mosses. *Polar Biology* 32, 1415-1425.

Light J. J. and Heywood R. B. (1973) Deep-water Mosses in Antarctic Lakes. *Nature* 242, 535-536.

Litt T., Schmincke H. and Kromer B. (2003) Environmental response to climatic and volcanic events in central Europe during the Weichselian Lateglacial. *Quaternary Science Reviews* 22, 7-22.

Loader N. J., McCarroll D., van der Knaap W. O., Robertson I. and Gagan, M. (2007) Characterizing carbon istopic variability in Sphagnum. *The Holocene* 17, 403-410.

Longton R. E. (1988) *Biology of Polar Bryophytes and Lichens*. Cambridge University Press, Cambridge.

Lücke A., Schleser G. H., Zolitschka B. and Negendank J. F. W. (2003) A Lateglacial and Holocene organic carbon isotope record of lacustrine palaeoproductivity and climatic change derived from varved lake sediments of Lake Holzmaar, Germany. *Quaternary Science Revews* 22, 569-580.

Lücke A. and Brauer A. (2004) Biogeochemical and micro-facial fingerprints of ecosystem response to rapid Late Glacial climatic changes in varved sediments of Meerfelder Maar (Germany). *Palaeogeography, Palaeoclimatology, Palaeoecology* 211, 139-155.

Lücke A., Wissel H., Mayr C., Oehlerich M., Ohlendorf C., Zolitschka B. and the PASADO Science Team (2010) Carbon and nitrogen isotope composition of core catcher samples from the ICDP deep drilling at Laguna Potrok Aike (Patagonia, Argentina). In *Potrok Aike Maar Lake Sediment Archive Drilling Project* (eds. B. Zolitschka). Terra Nostra, 48-51.

Lücke A., Zhu J., Müller D., Wissel H., Hahn A., Ohlendorf C., Zolitschka B. and PASADO Science Team (2013) Productivity phases in Glacial Patagonian steppe lake sediments as counterparts to Antarctic warm events. EGU General Assembly, Vienna, Austria, April 7 - 12, 2013, EGU2013-7876.

MacDonald G. M., Edwards T. W. D., Moser K. A., Pienitz R. and Smol J. P. (1993) Rapid response of treeline vegetation and lakes to past climate warming. *Nature* 361, 243-246.

Mancini M. V., Prieto A. R., Paez M. M. and Schäbitz F. (2008) Late Quaternary vegetation and climate of Patagonia. In *The Late Cenozoic of Patagonia and Tierra del Fuego* (eds. J. Rabassa). Developments in Quaternary Sciences 11, 351-367.

Markgraf V. and Huber U. (2010) Late and postglacial vegetation and fire history in Southern Patagonia and Tierra del Fuego. *Palaeogeography, Palaeoclimatology, Palaeoecology* 297, 351-366.

Masco M., Kofalt R. and Humano G. (2005) Flora del campo experimental Potrok Aike. In *Campo Experimental Potrok Aike – Resultado de 15 Años de Labor Técnica* (eds. L. Gonzales, R. Iglesias and A. Ciblis). INTA, 31-34.

Massaferro J., Recasens C., Larocque-Tobler I., Zolitschka B. and Maidana N. (2013) Major lake level fluctuations and climate changes for the past 16,000 years as reflected by diatoms and chironomids preserved in the sediment of Laguna Potrok Aike, southern Patagonia. *Quaternary Science Reviews* 71, 167-174.

Mayr C., Lücke A., Stichler W., Trimborn P., Ercolano B., Oliva G., Ohlendorf C., Soto J., Fey M., Haberzettl T., Janssen S., Schäbitz F., Schleser G., Wille M., Zolitschka B. (2007a) Precipitation origin and evaporation of lakes in semi-arid Patagonia (Argentina) inferred from stable isotopes ($\delta^{18}O$, $\delta^{2}H$). *Journal of Hydrology* 334, 53-63.

Mayr C., Wille M., Haberzettl T., Fey M., Janssen S., Lücke A., Ohlendorf C., Oliva G., Schäbitz F., Schleser G. H. and Zolitschka B. (2007b) Holocene variability of the Southern Hemisphere westerlies in Argentinean Patagonia (52°S). *Quaternary Science Reviews* 26, 579-584.

Mayr C., Lücke A., Maidana N., Wille M., Haberzettl T., Corbella H., Ohlendorf C., Schäbitz F., Fey M., Janssen S. and Zolitschka B. (2009) Isotopic and geochemical fingerprints of environmental changes during the last 16,000 years on lacustrineorganic matter from Laguna Potrok Aike (southern Patagonia, Argentina). *Journal of Paleolimnology* 42, 81-102.

Mayr C., Lücke A., Wagner S., Wissel H., Ohlendorf C., Haberzettl T., Oehlerich M., Schäbitz F., Wille M., Zhu J. and Zolitschka B. (2013) Intensified Southern Hemisphere Westerlies regulated atmospheric CO_2 during the last deglaciation. *Geology* 41, 831-834.

McCulloch R., Bentley M., Purves R., Hulton R., Sugden D. and Clapperton C. (2000) Climatic inferences from glacial and palaeoecological evidence at the last glacial termination, southern South America. *Journal of Quaternary Science* 15, 409-417.

McCulloch R. and Davies S. (2001) Late-glacial and Holocene palaeoenvironmental change in the central Strait of Magellan, southern Patagonia. *Palaeogeography, Palaeoclimatology, Palaeoecology* 173, 143-173.

McCulloch R., Fogwill C., Sugden D., Bentley M. and Kubik P. (2005) Chronology of the last glaciations in central Strait of Magellan and Bahía Inútil, southernmost South America. *Geografiska Annaler* 87(A), 289-312.

McKnight D., Howes B., Taylor C. and Goehringer D. (2000) Phytoplankton dynamics in a stably stratified Antarctic lake during winter darkness. *Journal of Phycology* 36, 852-861.

Melles M., Brigham-Grette J., Glushkova O. Y., Minyuk P. S., Nowaczyk N. R. and Hubberten H.-W. (2007) Sedimentary geochemistry of core PG1351 from Lake El'gygytgyn – a sensitive record of climate variability in the east Siberian Arctic during the past three glacial-interglacial cycles. *Journal of Paleolimnology* 37, 89-104.

Ménot-Combes G., Burns S. J. and Leuenberger M. (2002) Variations of $^{18}O/^{16}O$ in plants from temperate peat bogs (Switzerland): implications for paleoclimatic studies. *Earth and Planetary Science Letters* 202, 419-434.

Meyers P. (1994) Preservation of elemental and isotopic source identification of sedimentary organic matter. *Chemical Geology* 114, 289-302.

Meyers P. and Lallier-Vergès E. (1999) Lacustrine sedimentary organic matter records of Late Quaternary paleoclimates. *Journal of Paleolimnology* 21, 345-372.

Meyers P. and Teranes J. (2001) Sediment organic matter. In *Tracking Environmental Change using Lake Sediments, Physical and Geochemical Methods (vol.2)* (eds. W. Last and J. Smol). Kluwer Academic Publications, pp. 239-269.

Meyers P. (2003) Applications of organic geochemistry to paleolimnological reconstructions: a summary of examples from the Laurentian Great Lakes. *Organic Geochemistry* 34, 261-289.

Michener R. and Lajtha K. (2007) Stable isotopes in ecology and environmental science. Blackwell Publishing, 566 pp.

Monnin E., Indermühle A., Dällenbach A., Flückiger J., Stauffer B., Stocker T., Raynaud D. and Barnola J. (2001) Atmospheric CO_2 concentrations over the Last Glacial Termination. *Science* 291, 112-114.

Moreno P. I., Lowell T. V., Jacobson Jr. G. L. and Denton G. H. (1999) Abrupt vegetation and climate changes during the Last Glacial Maximum and last termination in the Chilean Lake District: A case study from Canal de la Puntilla (41°S). *Geografiska Annaler* 81(A), 285-311.

Moreno P. I., Francois J. P., Moy C. M. and Villa-Martínez R. (2010) Covariability of the Southern Westerlies and atmospheric CO2 during the Holocene. *Geology* 38, 727-730.

Moreno P. I., Villa-Martínez R., Cárdenas M. L. and Sagredo E. A. (2012) Deglacial changes of the southern margin of the southern westerly winds revealed by terrestrial records from SW Patagonia (52°S). *Quaternary Science Reviews* 41, 1-21.

Moschen R., Kühl N., Rehberger I. and Lücke A. (2009) Stable carbon and oxygen isotopes in sub-fossil Sphagnum: Assessment of their applicability for palaeoclimatology. *Chemical Geology* 259, 262-272.

Moschen R., Kühl N., Peters S., Vos H. and Lücke A. (2011) Temperature variability at Dürres Maar, Germany during the Migration Period and at High Medieval Times, inferred from stable carbon isotopes of *Sphagnum* cellulose. *Climate of the Past* 7, 1011-1026.

Müller P. (1977) C/N ratios in Pacific deep-sea sediments: effect of inorganic ammonium and organic nitrogen compounds sorbed by clays. *Geochimica et Cosmochimica Acta* 41, 765-776.

Ochyra R. and Lightowlers P. J. (1988) The South Georgian moss flora - Vittia. *British Antarctic Survey Bulletin* 80, 121–127.

O'Leary M. (1988) Carbon isotopes in photosynthesis. *BioScience* 38, 328-336.

Ohlendorf C., Gebhardt C., Hahn A., Kliem P., Zolitschka B. and the PASADO Science Team (2011) The PASADO core processing strategy – A proposed new protocol for sediment core treatment in multidisciplinary lake drilling projects. *Sedimentary Geology* 239, 104-115.

Ohlendorf C., Fey M., Gebhardt C., Haberzettl T., Lücke A., Mayr C., Schäbitz F., Wille M. and Zolitschka B. (2013) Mechanisms of lake-level change at Laguna Potrok Aike (Argentina) – insights from hydrological balance calculations. *Quaternary Science Reviews* 71, 27-45.

O'Leary M. (1988) Carbon isotopes in photosynthesis. *BioScience* 38, 328-336.

Osmond C., Valaane N., Haslam S., Uotila P. and Roksandic Z. (1981) Comparisons of $\delta^{13}C$ values in leaves of aquatic macrophytes from different habitats in Britain and Finland; some implications for photosynthetic processes in aquatic plants. *Oecologia* 50, 117-124.

Park R. and Epstein S. (1961) Metabolic fractionation of C^{13} & C^{12} in plants. *Plant Physiology* 36, 133-138.

Parplies J., Lücke A., Vos H., Mingram J., Stebich M., Radtke U., Han J., Schleser G. H. (2008) Late glacial environment and climate development in northeastern China derived from geochemical and isotopic investigations of the varved sediment record from Lake Sihailongwan (Jilin Province). *Journal of Paleolimnology* 40, 471-487.

Paruelo J., Beltrán A., Jobbágy E., Sala O. and Golluscio R. (1998) The climate of Patagonia: general patterns and controls on biotic processes. *Ecología Austral* 8, 85-101.

Pendall E., Markgraf V., White J. W. C. and Dreier M. (2001) Multiproxy record of Late Pleistocene-Holocene climate and vegetation changes from a peat bog in Patagonia. *Quaternary Research* 55, 168-178.

Pollock E. W. and Bush A. B. G. (2013) Atmospheric simulations of southern South America's climate since the Last Glacial maximum. *Quaternary Science Reviews* 71, 219-228.

Price G. D., McKenzie J. E., Pilcher J. R. and Hoper S. T. (1997) Carbon-isotope variation in *Sphagnum* from hummock-hollow complexes: implications for Holocene climate reconstruction. *The Holocene* 7, 229-233.

Rasmussen, S. O., Andersen K. K., Svensson A. M., Steffensen J. P., Vinther B. M., Clausen H. B., Siggaard-Anderson M.-L., Johnsen S. J., Larsen L. B., Dahl-Jensen D., Bigler M., Röthlisberger R., Fischer H., Goto-Azuma K., Hansson M. E. and Ruth U. (2006) A new Greenland ice core chronology for the last glacial termination. *Journal of Geophysical Research* 111, D06102, doi: 10.1029/2005JD006079.

Recasens C., Ariztegui D., Gebhardt C., Gogorza C., Haberzettl T., Hahn A., Kliem P., Lisé-Pronovost A., Lücke A., Maidana N. I., Mayr C., Ohlendorf C., Schäbitz F., St-Onge G., Wille M., Zolitschka B. and the PASADO Science Team (2012) New insights into paleoenvironmental changes in Laguna Potrok Aike, Southern Patagonia, since the Late Pleistocene: the PASADO multiproxy record. *The Holocene* 22, 1323-1335.

Rojas M., Moreno P., Kageyama M., Crucifix M., Hewitt C., Abe-Ouchi A., Ohgaito R., Brady E.C. and Hope P. (2009) The Southern Westerlies during the last glacial maximum in PMIP2 simulations. *Climate Dynamics* 32, 525-548.

Rojas M. (2013) Sensitivity of Southern Hemisphere circulation to LGM and 4×CO2 climates. *Geophysical Research Letters* 40, 965-970.

Rozanski K., Araguás-Araguás L. and Gonfiantini R. (1992) Relation between long-term trends of oxygen-18 isotope composition of precipitation and climate. *Science* 258, 981-985.

Rozanski K., Araguás-Araguás L. and Gonfiantini R. (1993) Isotopic Patterns in Modern Global precipitation. In *Climate Change in Continental Isotopic Records* (eds. P.K. Swart, K.L. Lohmann, J. McKenzie and S. Savin) Geophysical Monograph 78, American Geophysical Union, Washington DC, 1-37.

Sachs J., Anderson R. and Lehman S. (2001) Glacial Surface Temperatures of the Southeast Atlantic Ocean. *Science* 293, 2077-2079.

Sagredo E. A., Moreno P. I., Villa-Martínez R., Kaplan M. R., Kubik P. W. and Stern C. R. (2011) Fluctuations of the Última Esperanza ice lobe (52ºS), Chilean Patagonia, during the last glacial maximum and termination 1. *Geomorphology* 125, 92-108.

Sand-Jensen K., Riis T., Markager S. and Vincent W. F. (1999) Slow growth and decomposition of mosses in Arctic lakes. *Canadian Journal of Fisheries and Aquatic Sciences* 56, 388-393.

Sauer P. E., Miller G. H. and Overpeck J. T. (2001) Oxygen isotope ratios of organic matter in arctic lakes as a paleoclimate proxy: field and laboratory investigations. *Journal of Paleolimnology* 25, 43-64.

Schmidt H-L., Werner R. A. and Roßmann A. (2001) ^{18}O Pattern and biosynthesis of natural plant products. *Phytochemistry* 58, 9-32.

Schmitt J., Schneider R., Elsig J., Leuenberger D., Lourantou A., Chappellaz J., Köhler P., Joos F., Stocker T. F., Leuenberger M. and Fischer H. (2012) Carbon Isotope Constraints on the Deglacial CO_2 Rise from Ice Cores. *Science* 336, 711-714.

Schneider C., Glaser M., Kilian R., Santana A., Butorovic N. and Casassa G. (2003) Weather observations across the Southern Andes at 53°S. *Physical Geography* 24, 97-119.

Sime L. C., Kohfeld K. E., Le Quéré C., Wolff E. W., de Boer A. M., Graham R. M. and Bopp L. (2013) Southern Hemisphere westerly wind changes during the Last Glacial Maximum: model-data comparison. *Quaternary Science Reviews* 68, 104-120.

Solari M. A., Le Roux J. P., Hervé F., Airo A. and Calderón M. (2012) Evolution of the Great Tehuelche Paleolake in the Torres del Paine National Park of Chilean Patagonia during the Last Glacial Maximum and Holocene. *Andean Geology* 39, 1-21.

Spaulding S., Ward J. and Baron J. (1993) Winter phytoplankton dynamics in a sub-alpine lake, Colorado, USA. *Archiv für Hydrobiologie* 129, 179-198.

Stenni B., Buiron D., Frezzotti M., Albani S., Barbante C., Bard E., Barnola J. M., Baroni M., Baumgartner M., Bonazza M., Capron E., Castellano E., Chappellaz J., Delmonte B.,

Falourd S., Genoni L., Iacumin P., Jouzel J., Kipfstuhl S., Landais A., Lemieux-Dudon B., Maggi V., Masson-Delmotte V., Mazzola C., Minster B., Montagnat M., Mulvaney R., Narcisi B., Oerter H., Parrenin F., Petit J. R., Ritz C., Scarchilli C., Schilt A., Schüpbach S., Schwander J., Selmo E., Severi M., Stocker T. F. and Udisti R. (2011) Expression of the bipolar see-saw in Antarctic climate records during the last deglaciation. *Nature Geoscience* 4, 46-49.

Stern C. R. (2008) Holocene tephrochronology record of large explosive eruptions in southernmost Patagonian Andes. *Bulletin of Volcanology* 70, 435–454.

Sternberg L. S. L. (1989) Oxygen and hydrogen isotope ratios in plant cellulose: mechanisms and applications. In *Stable isotope in ecological research, Ecological studies 68* (eds. Rundel P. W., Ehleringer J. R. and Nagy K. A.), Springer, New York, 124–141.

Sternberg L. (2009) Oxygen stable isotope ratios of tree-ring cellulose: the next phase of understanding. *New Phytologist* 181, 553-562.

Sternberg L. and Ellsworth P. F. V. (2011) Divergent Biochemical Fractionation, Not Convergent Temperature, Explains Cellulose Oxygen Isotope Enrichment across Latitudes. *PLoS ONE* 6(11), e28040, doi:10.1371/journal.pone.0028040.

Sternberg L., Pinzon M. C., Anderson W. T. and Jahren A. H. (2006) Variation in oxygen isotope fractionation during cellulose synthesis: intramolecular and biosynthetic effects. *Plant, Cell & Environment* 29, 1881-1889.

Stine S. and Stine M. (1990) A record from Lake Cardiel of climate change in southern South America. *Nature* 345, 705-708.

Sugden D., Bentley M., Fogwill C., Hulton N., McCulloch R. and Purves R. (2005) Late-Glacial glacier events in southernmost South America: a blend of 'northern' and 'southern' hemispheric climatic signals? *Geografiska Annaler* 85(A), 273-288.

Talbot M. and Lærdal T. (2000) The Late Pleistocene – Holocene palaeolimnology of Lake Victoria, East Africa, based upon elemental and isotopic analyses of sedimentary organic matter. *Journal of Paleolimnology* 23, 141-164.

Talbot M. (2001) Nitrogen isotopes in Palaeolimnology. In *Tracking Environmental Change using Lake Sediments, Physical and Geochemical Methods (vol.2)* (eds. W. Last and J. Smol). Kluwer Academic Publishers, 401-439.

Teranes J. and Bernasconi S. (2000) The record of nitrate utilization and productivity limitation provided by $\delta^{15}N$ values in lake organic matter – A study of sediment trap and core sediments from Baldeggersee, Switzerland. *Limnology and Oceanography* 45, 801-813.

Teranes J. L. and McKenzie J. A. (2001) Lacustrine oxygen isotope record of 20^{th}-century climate change in central Europe: evaluation of climatic controls on oxygen isotopes in precipitation. *Journal of Paleolimnology* 26, 131-146.

Toggweiler J. R., Russell J. L. and Carson S. R. (2006) Midlatitude westerlies, atmospheric CO_2, and climate change during the ice ages. *Paleoceanography* 21, PA2005, doi: 10.102 9/2005PA001154.

Trombotto D. (2002) Inventory of fossil cryogenic forms and structures in Patagonia and the mountains of Argentina beyond the Andes. *South African Journal of Science* 98, 171-180.

Turetsky M. R., Crow S. E., Evans R. J., Vitt D. H. and Wieder R. K. (2008) Trade-offs in resource allocation among moss species control decomposition in boreal peatlands. *Journal of Ecology* 96, 1297-1305.

Valero-Garcés B., Jenny B., Rondanelli M., Delgado-Huertas A., Burns S., Veit H. and Moreno A. (2005) Palaeohydrology of Laguna de Tagua Tagua (34° 30'S) and moisture fluctuations in Central Chile for the last 46 000 yr. *Journal of Quaternary Science* 20, 625-641.

Van der Putten N., Stieperaere H., Verbruggen C. and Ochyra R. (2004) Holocene palaeoecology and climate history of South Georgia (sub-Antarctica) based on a macrofossil record of bryophytes and seeds. *The Holocene* 14, 382-392.

Veres D., Lallier-Vergès E., Wohlfarth B., Lacourse T., Kéravis D., Björck S., Preusser F., Andrieu-Ponel V. and Ampel L. (2009) Climate-driven changes in lake conditions during late MIS 3 and MIS 2: a high-resolution geochemical record from Les Echets, France. *Boreas* 38, 230-243.

Villa-Martínez R., Moreno P. I. and Valenzuela M. A. (2012) Deglacial and postglacial vegetation changes on the eastern slopes of the central Patagonian Andes (47°S). *Quaternary Science Reviews* 32, 86-99.

Vogel H., Wessels M., Albrecht C., Stich H.-B. and Wagner B. (2010) Spatial variability of recent sedimentation in Lake Ohrid (Albania/Macedonia). *Biogeosciences* 7, 3333-3342.

von Grafenstein U., Erlenkeuser H., Brauer A., Jouzel J. and Johnsen S. (1999) A mid-European decadal isotope-climate record from 15,500 to 5000 years BP. *Science* 284, 1654-1657.

Vuillemin A., Ariztegui D. and the PASADO Science Team (2013) Geomicrobiological investigations in subsaline maar lake sediments over the last 1500 years. *Quaternary Science Reviews* 71, 119-130.

Wagner C. and Adrian R. (2009) Cyanobacteria dominance: Quantifying the effects of climate change. *Limnology and Oceanography* 54, 2460-2468.

Wagner B. and Seppelt R. (2006) Deep-water occurrence of the moss *Bryum pseudotriquetrum* in Radok Lake, Amery Oasis, East Antarctica. *Polar Biology* 29, 791-795.

Wagner S., Widmann M., Jones J., Haberzettl T., Lücke A., Mayr C., Ohlendorf C., Schäbitz F. and Zolitschka B. (2007) Transient simulations, empirical reconstructions and forcing

mechanisms for the Mid-holocene hydrological climate in southern Patagonia. *Climate Dynamics* 29, 333-355.

WAIS Divide Project Members (2013) Onset of deglacial warming in West Antarctica driven by local orbital forcing. *Nature* 500, 440-446.

Wang X., Auler A. S., Edwards R. L., Cheng H., Ito E., Wang Y., Kong X. and Solheid M. (2007) Millennial-scale precipitation changes in southern Brazil over the past 90,000 years. *Geophysical Research Letters* 34, L23701, doi: 10.1029/2007GL031149.

Wastegård S., Veres D., Kliem P., Ohlendorf C., Zolitschka B. and the PASADO Science Team (2013) Towards a late Quaternary tephrochronological framework for the southernmost part of South America - the Laguna Potrok Aike tephra record. *Quaternary Science Reviews* 71, 81-90.

Watanabe T., Naraoka H., Nishimura M. and Kawai T. (2004) Biological and environmental changes in Lake Baikal during the late Quaternary inferred from carbon, nitrogen and sulfur isotopes. *Earth and Planetary Science Letters* 222, 285-299.

Weischet W. (1996) Regionale Klimatologie. Teil 1: Die neue Welt. Teubner, Stuttgart, 468pp.

White J. W. C., Ciais P., Figge R. A., Kenny R. and Markgraf V. (1994) A high-resolution record of atmospheric CO2 content from carbon isotopes in peat. *Nature* 367, 153-156.

Wille M., Maidana N., Schäbitz F., Fey M., Haberzettl T., Janssen S., Lücke A., Mayr C., Ohlendorf C., Schleser G. and Zolitschka B. (2007) Vegetation and climate dynamics in southern South America: the microfossil record of Laguna Potrok Aike, Santa Cruz, Argentina. *Review of Palaeobotany and Palynology* 146, 234-246.

Williams G. P. and Bryan K. (2006) Ice Age Winds: An Aquaplanet Model. *Journal of Climate* 19, 1706-1715.

Wissel H., Mayr C. and Lücke A. (2008) A new approach for the isolation of cellulose from aquatic plant tissue and freshwater sediments for stable isotope analysis. *Organic Geochemistry* 39, 1545-1561.

Wolfe B. B., Edwards T. W. D., Elgood R. J. and Beuning K. R. M. (2001) Carbon and oxygen isotope analysis of lake sediment cellulose: methods and applications. In *Tracking environmental change using lake sediments. Vol. 2: Physical and Geochemical Methods* (eds. W. Last and J. Smol). Kluwer Academic Publications, Dordrecht. pp. 373-400.

Wolfe B. B., Falcone M. D., Clogg-Wright K. P., Mongeon C. L., Yi Y., Brock B. E., Amour N. A. St., Mark W. A. and Edwards T. W. D. (2007) Progress in isotope paleohydrology using lake sediment cellulose. *Journal of Paleolimnology* 37, 221-231.

Yu Z. and Eicher U. (1998) Abrupt climate oscillations during the last deglaciation in central North America. *Science* 282, 2235-2238.

Zhu J., Lücke A., Wissel H., Müller D., Mayr C., Ohlendorf C., Zolitschka B. and the PASADO Science Team (2013) The last Glacial-Interglacial transition in Patagonia, Argentina: the stable isotope record of bulk sedimentary organic matter from Laguna Potrok Aike. *Quaternary Science Reviews* 71, 205-218.

Zhu J., Lücke A., Wissel H., Mayr C., Ohlendorf C. and Zolitschka B. (2014) Characterizing oxygen isotope variability and host water relation of modern and subfossil aquatic mosses. *Geochimica et Cosmochimica Acta* 130, 212-228.

Zolitschka B., Schäbitz F., Lücke A., Corbella H. and Ercolano B. (2006) Crater lakes of the Pali Aike Volcanic Field as key sites for paleoclimatic and paleoecological reconstructions in southern Patagonia, Argentina. *Journal of South American Earth Sciences* 21, 294-309.

Zolitschka B., Anselmetti F., Ariztegui D., Corbella H., Francus P., Ohlendorf C., Schäbitz F. and the PASADO Scientific Drilling Team (2009) The Laguna Potrok Aike Scientific Drilling Project PASADO (ICDP Expedition 5022). *Scientific Drilling* 8, 29-34.

Zolitschka B., Anselmetti F., Ariztegui D., Corbella H., Francus P., Lücke A., Maidana N., Ohlendorf C., Schäbitz F. and Wastegård S. (2013) Environment and climate of the last 51,000 years – new insights from the Potrok Aike maar lake Sediment Archive Drilling project (PASADO). *Quaternary Science Reviews* 71, 1-12.

Abstract

Southern Patagonia possesses a unique value for the assessment of the global paleoclimatic system, because this area is the only continental mass intersecting the core of the Southern Hemisphere Westerly winds (SHW), which controls large-scale ocean ventilation and carbon-cycle feedbacks and could have played a crucial role in driving the global deglacial warming during the last glacial termination. Paleoclimatic archives in southern Patagonia provide also terrestrial linkage to the sediment records from the Southern Ocean and the ice cores from Antarctica. Despite the great importance, continuous paleoclimatic records in southern Patagonia are usually only available for the period from the last deglaciation onwards, because most study sites are located in the Andean region, which was covered by the immense Patagonian Ice Sheet during the last Glacial.

This research gap is being bridged by interdisciplinary multiproxy investigations within the framework of the Potrok Aike maar lake sediment archive drilling project (PASADO). The project provides a lake sediment record reaching back more than 50,000 years taken from Laguna Potrok Aike, a deep maar lake located in semi-arid southern extra-Andean Patagonia (51°58' S, 70°23' W, 113 m a.s.l.). By using stable isotope analysis of sedimentary organic material, this thesis has investigated the PASADO sediment section ranging from 26,000 to 8500 cal. BP, covering the last glacial-interglacial transition, to provide paleoenvironmental evidences from southern extra-Andean Patagonia for a time period with dramatic climatic changes. The work presented in Chapter 2, employs stable isotope ($\delta^{13}C_{TOC}$, $\delta^{15}N_{TN}$) and elemental (TOC, TN) analyses of fine-grained (<200μm) bulk organic matter preserved in pelagic sediments to reconstruct the lacustrine primary productivity and nutrient supply during this glacial-interglacial transition. Furthermore, a unique proxy approach based on cellulose and bulk organic matter of handpicked aquatic moss remains is established to infer the past oxygen isotope composition of lake water ($\delta^{18}O_{lw}$) (Chapter 3). The validity of this approach is determined by the highly significant correlation between $\delta^{18}O$ of submerged aquatic mosses (both moss organic matter and extracted cellulose) and their host waters. Using this proxy approach, a high-resolution $\delta^{18}O_{lw}$ record is generated for the investigated period and interpreted in the context of the fundamental climatic shifts during the last glacial-interglacial transition to assess the evolution of the SHW (Chapter 4).

Between 26,000 and 17,600 cal. BP, lacustrine phytoplankton was presumably the predominant organic matter source in an aquatic environment with low primary productivity. Meanwhile, the

reconstructed glacial $\delta^{18}O_{lw}$ had a mean value of around -6.5‰ that was only ca. 3‰ lower than the modern values. This is less negative than expected in consideration of probably large ^{18}O depletion of meteoric water during the full Glacial. It is argued that the isolated groundwater resulted from permafrost conditions could have had much less negative $\delta^{18}O$ values than glacial precipitation and the less ^{18}O depleted source water and prolonged lake water residence time could have caused observed less negative glacial $\delta^{18}O_{lw}$. At the onset of the last deglaciation, abrupt and distinct shifts of carbon and nitrogen isotopic and elemental values indicate that the lacustrine system underwent a rapid reorganization, synchronous with the rapid glacier retreat in southern Patagonia, the Antarctic warming and the elevated atmospheric CO_2 concentrations. Over the course of the last deglaciation, lacustrine primary productivity of both phytoplankton and aquatic macrophytes showed high levels despite large variations. The increased productivity can be attributed to improved growing conditions for primary producers because of deglacial warming in combination with sufficient nutrient availability and calm wind conditions. The reconstructed $\delta^{18}O_{lw}$ responded to the deglacial climatic shift with a significant two-step rise. Rapid deglacial warming is supposed to cause the ^{18}O enrichment of lake water by ca. 2‰ during the first rise between 17,600 and 15,600 cal. BP by increasing temperature-induced evaporation and more ^{18}O enriched precipitation. After a millennial period of receding values by up to 0.7‰, the reconstructed $\delta^{18}O_{lw}$ resumed pronounced increase since 14,600 cal. BP. This cumulative enrichment in ^{18}O of lake water could be interpreted as a response to the strengthened wind-driven evaporation, implying the intensification and establishment of the SHW at the latitude of Laguna Potrok Aike (52°C). During the early Holocene the lake approached a new state with reduced primary productivity probably induced by unfavorable growing conditions for primary producers in the lake like nutrient shortage after the preceding productive phase with high consumption as well as strengthened westerly winds. Since around 13,000 cal. BP, the SHW exerted its dominant influence on the lake water balance, reflected by reconstructed $\delta^{18}O_{lw}$ values close to the modern ones, indicating the establishment of a strongly evaporative steppe climate in the Laguna Potrok Aike region.

Zusammenfassung

Südpatagonien ist für paläoklimatische Studien in Bezug auf das globale Klimasystem von sehr großer Bedeutung. Klimatische Archive in Südpatagonien bilden das terrestrische Bindeglied an die Sedimentarchive aus den Süd-Ozeanen und die Eisbohrkerne aus der Antarktis. Außerdem ist Südpatagonien auch die einzige kontinentale Landmasse, die den Kern der südhemisphärischen Westwinde (SHW) schneidet. Die SHW steuert die großräumige Ozeanzirkulation und den globalen Kohlenstoffkreislauf, und kann auch eine entscheidende Rolle beim Antrieb der letzten deglazialen Erwärmung gespielt haben. Trotz der besonderen Bedeutung beschränken sich die kontinuierlichen Paläoklimaarchive in Südpatagonien üblicherweise auf den Zeitraum seit dem Ende der letzten Vereisung, weil sich die meisten Untersuchungsstellen in der Andenregion befinden, die während des letzten Glazials vom patagonischen Inlandeis bedeckt war.

Diese Forschungslücke wird zunehmend überbrückt von den interdisziplinären Multiproxy-Untersuchungen im Rahmen des Projekts „Potrok Aike Maar lake sediment archive drilling project“ (PASADO). Dieses Projekt macht das Sedimentarchiv der Laguna Potrok Aike, einem tiefen Maarsee im semi-ariden Südpatagonien (51°58' S, 70°23' W, 113 m ü.M.), für den Zeitraum der letzten 50,000 Jahre verfügbar. Die vorliegende, in das PASADO Projekt eingebundene Arbeit untersucht den Sedimentabschnitt, der den Zeitraum von 26,000 bis 8500 cal. BP umfasst, unter Einsatz von stabilen Isotopen von sedimentärem organischem Material. Kapitel 2 befasst sich mit den stabilen Isotopen ($\delta^{13}C_{TOC}$, $\delta^{15}N_{TN}$) und den Elementgehalten (TOC, TN) von feinkörnigen (<200µm) organischen Sedimenten, um die lakustrine Primärproduktivität zu rekonstruieren und Hinweise auf Nährstoffverfügbarkeit im See zu geben. Zudem ist ein neuer Proxy-Ansatz in Kapitel 3 aufgebaut, wobei die handverlesenen Makroreste von Wassermoosen und extrahierter Moose-Zellulose benutzt werden, um die Zusammensetzung der Sauerstoffisotopie des Seewassers ($\delta^{18}O_{lw}$) für den untersuchten Zeitraum zu rekonstruieren. Dieser Proxy-Ansatz gründet sich auf der hochsignifikanten linearen Korrelation zwischen dem $\delta^{18}O$ von aquatischen Moosen und ihrem Umgebungswasser. Mit diesem Ansatz wurde in Kapitel 4 eine hoch-auflösende Zeitreihe von $\delta^{18}O_{lw}$ für den untersuchten Zeitraum entwickelt und im Kontext der SHW Entwicklung im Verlauf des dramatischen globalen klimatischen Wechsels seit der letzten Eiszeit interpretiert.

Zwischen 26,000 und 17,600 cal. BP war Phytoplankton die vorherrschende organische Substanz in einem aquatischen System mit geringer Primärproduktivität. Das rekonstruierte

glaziale $\delta^{18}O_{lw}$ hatte einen Mittelwert von ca. -6.5‰, der nur 3‰ niedriger als der heute beobachtete Wert war. Unter Berücksichtigung der wahrscheinlich großen ^{18}O-Abreicherung der glazialen Niederschläge (~6‰), war damit das Niveau des glazialen $\delta^{18}O_{lw}$ weniger negativ als erwartet. Diese unerwartete ^{18}O-Anreicherung des Seewassers kann damit erklärt werden, dass das Grundwasser als eine Hauptquelle des Wasserzuflusses für den See wegen des Permafrostes während des Glazials vom Oberflächenwasser isoliert war und folglich eine weniger negative $\delta^{18}O$ Signatur als die glazialen Niederschläge hatte. Die mit Permafrost einhergehende verlängerte Verweilzeit des Wassers im See könnte auch zur weiteren ^{18}O-Anreicherung des Seewassers beigetragen haben. Das Ende der letzten Eiszeit ist gekenzeichnet durch die schlagartigen Verschiebungen der Isotopenverhältnisse und der Elementgehalte. Das lakustrische System erlebte eine schnelle Neugestaltung, zeitgleich mit dem raschen Rückzug der Vergletscherung in Südpatagonien, der Erwärmung in der Antarktis und der abrupten Erhöhung der atmosphärischen CO_2 Konzentration. Der Verlauf der letzten Deglaziation (Spätglazial) war trotz großer Variationen der lakustrischen Primärproduktivität von Phytoplankton und Makrophyten insgesamt von einer hohen Produktivität gekennzeichnet. Die erhöhte Produktivität lässt sich durch verbesserte Wachstumsbedingungen aufgrund der zunehmenden Erwärmung zusammen mit einer ausreichenden Nährstoffversorgung und wahrscheinlich ruhigen Windverhältnissen erklären. Das rekonstruierte $\delta^{18}O_{lw}$ reagiert auf den deglazialen Klimawandel mit einem zweistufigen Anstieg. Eine Kombination von zunehmender temperaturbedingter Evaporation und mehr ^{18}O angereicherten Niederschlägen führte zum ersten Anstieg um ca. 2‰ während des Zeitraums von 17,600 bis 15,600 cal. BP. Nach einer tausendjährigen Phase, in der das rekonstruierte $\delta^{18}O_{lw}$ um bis zu 0.7‰ zurückging, setzte sich der ausgeprägte Anstieg seit 14,600 cal. BP weiter fort, was jetzt als eine Folge von verstärkter windbedingte Evaporation interpretiert werden kann. Seit 13,000 cal. BP hat die SHW einen beherrschenden Einfluss auf den Wasserhaushalt der Laguna Potrok Aike ausgeübt. Zum Beginn des Frühholozäns näherte sich der See einem neuen Zustand mit reduzierter Primärproduktivität, die wahrscheinlich durch ungünstige Wachstumsbedingungen wie verstärkte Windintensität und Nährstoffmangel nach der vorhergehenden Phase mit hoher Produktivität verursacht wurde. Im Allgemeinen spiegelt das Entwicklungsprofil des Wasserhaushalts und der Primärproduktivität in Laguna Potrok Aike die Bildung eines Steppenklimas mit starker Evaporation in Südpatagonien im Laufe der letzten Deglaziation wider.